7-12-2014

The Trapeziometacarpal Joint: Tissue Characterization and Surgical Techniques for Treatment of Osteoarthritis

Christina Salas

Christina Salas
Candidate

Biomedical Engineering
Department

This dissertation is approved, and it is acceptable in quality and form for publication:

Approved by the Dissertation Committee:

Mahmoud Reda Taha, PhD , Chairperson

Deana Mercer, MD

Heather Canavan, PhD

Elizabeth Dirk, PhD

The Trapeziometacarpal Joint: Tissue Characterization and Surgical Techniques for Treatment of Osteoarthritis

by

Christina Salas

B.S., Mechanical Engineering, California State University Chico, 2005
M.S., Mechanical Engineering, University of New Mexico, 2008

DISSERTATION

Submitted in Partial Fulfillment of the
Requirements for the Degree of

Doctor of Philosophy
Engineering

The University of New Mexico

Albuquerque, New Mexico

May, 2014

Dedication

This dissertation is dedicated to my family. Your love and support has helped me through many stressful days. Just knowing that you are proud of my accomplishments, motivated me to continue working hard to achieve my goal of becoming a PhD. I could not have done this without each and every one of you. This includes future baby Hansen-Salas.

Without the pressure of your arrival I would forever be a graduate student.

I love you all so much!

Acknowledgments

I would like to express my sincere gratitude to Dr. Mahmoud Reda Taha for his support and guidance and for helping me achieve my goals.

Special thanks to my committee members Dr. Heather Canavan, Dr. Deana Mercer, and Dr. Elizabeth Dirk. They have been wonderful mentors throughout the duration of this research. I would also like to thank Justin Brantley, Kimberly Fields, Evan Baldwin, Cory Carlston, Julie Bowers, James Love, James "Bone" Dexter, Amy Overby, Darryl Encino, Dr. Jorge Orbay, Patricia Siegel, Frederic Gallienne, Colleen Irvin, and Matthew Rush for assistance with various parts of this research.

Lastly, I would like to thank all my friends (near and far) who have provided emotional support that made it possible for me to complete this research.

Preface

The following publications have been co-authored by the PhD candidate during the course of study. This list includes peer-reviewed journal articles and conference proceedings that are published, in review, or in preparation.

Journal Articles - Published

1. Cheema T, **Salas C**, Morrell N, Lansing L, Reda Taha MM, Mercer D. Opening wedge trapezial osteotomy as possible treatment for early trapeziometacarpal osteoarthritis: A biomechanical investigation of radial subluxation, contact area, and contact pressure. J Hand Surg Am. 2012 Apr; 37(4): 699-705.

2. **Salas C**, Mercer D, DeCoster TA, Reda Taha MM. Experimental and probabilistic analysis of distal femoral periprosthetic fracture: a comparison of locking plate and intramedullary nail fixation. Part A: experimental investigation. Comput Methods Biomech Biomed Eng. 2011 Feb;14(2):157-164.

3. **Salas C**, Mercer D, DeCoster TA, Reda Taha MM. Experimental and probabilistic analysis of distal femoral periprosthetic fracture: a comparison of locking plate and intramedullary nail fixation. Part B: probabilistic investigation. Comput Methods Biomech Biomed Eng. 2011 Feb;14(2):175-182.

4. Dragomir-Daescu D, Op Den Buijs J, McEligot S, Dai Y, Entwistle R, **Salas C**, Melton LJ 3rd, Bennet K, Khosla S, Amin S. Robust QCT/FEA models of proximal femur stiffness and fracture load during a sideways fall on the hip. Ann Biomed

Eng., 2011; 39(2): 742-755.

5. Afifi A, Medoro A, **Salas C**, Reda Taha MM, Cheema T. A novel cadaver model investigating irreducible metacarpophalangeal joint dislocation, J Hand Surg Am, 2009; 34(8): 1506-1511.

Journal Articles - In Review

1. **Salas C**, Dragomir-Daescu D. QCT/FEA predictions of proximal femur strength and stiffness depend on CT settings. J Biomech.

2. Mercer D, **Salas C**, OMahoney G, Stewart D, McClellan W, Moneim M. Partial trapeziectomy with capsular interposition as treatment for thumb carpometacarpal osteoarthritis: A cadaveric and clinical study. J Hand Surg Br.

3. Dickens A, **Salas C**, Rise L, Reda Taha M, Gehlert R. Titanium mesh as a low-profile alternative for patella fracture fixation: A biomechanical study. J Orthop Res.

4. Hoopes D, **Salas C**, Reda Taha M, DeCoster TA. Finite element design and experimental testing of a novel triangular external fixator configuration for tibial shaft fracture treatment. Orthopaedics.

Journal Articles - In Preparation

1. **Salas C**, Baldwin E, Brantley J, Carlston C, Reda Taha M, Mercer D. High resolution motion analysis of the thumb carpometacarpal joint: Relative contribution of the joint ligaments to thumb stability. J Orthop Res.

2. **Salas C**, Baldwin E, Brantley J, Carlston C, Reda Taha M, Mercer D. Mechanical properties of the thumb carpometacarpal joint ligaments and their correlation to joint stability. J Biomech.

3. **Salas C**, Brantley J, Baldwin E, Carlston C, Reda Taha M, Mercer D. Patient-specific finite element models of the thumb carpometacarpal joint: The effects of ligamentous laxity on joint contact pressure and stability. Ann Biomed Eng.

4. **Salas C**, Brantley J, Clark J, Baldwin E, Evans S, Reda Taha MM, Mercer D. Patterns of failure in the distal radius following treatment for AO 23-A3.2 fractures using two-column volar plating. J Biomech.

5. Hoblet A, **Salas C**, Brantley J, Mikola E. Pullout strength and stiffness of a non-metallic suture anchoring system for repair of the central slip of the extensor mechanism at the proximal interphalangeal joint. J Hand Surg Am.

Conference Articles - Published

1. **Salas C**, DeCoster T, Mercer D, Firoozbakhsh K, Reda Taha MM. Examining damage accumulation in osteoporotic distal femur fracture repair. Society for Experimental Mechanics 2009 Annual Conference & Exposition on Experimental & Applied Mechanics, Albuquerque, NM

2. Neidigk S, **Salas C**, Soliman E, Mercer D, Reda Taha MM. Creep and relaxation of osteoporotic bone. Society for Experimental Mechanics 2009 Annual Conference & Exposition on Experimental & Applied Mechanics, Albuquerque, NM

The Trapeziometacarpal Joint: Tissue Characterization and Surgical Techniques for Treatment of Osteoarthritis

by

Christina Salas

B.S., Mechanical Engineering, California State University Chico, 2005
M.S., Mechanical Engineering, University of New Mexico, 2008

Ph.D., Engineering, University of New Mexico, 2014

Abstract

The trapeziometacarpal (TMC) joint is one of the most important joints in the human body. It provides the thumb with the ability to cross over the palm of the hand, thus enabling motions of pinch and grip essential in performing routine daily activities. In the case of repeated use of this joint, the articular cartilage may wear through a progressive joint disease known as osteoarthritis (OA). This disease is characterized by pain at the base of the thumb, decreased range of motion, thumb instability, and decreased grip and pinch strength leading to impairment in vocational activities, significantly affecting quality of life. Much of the research surrounding the TMC joint has focused on development of non-surgical and surgical options for treatment of early and late stage OA. Unfortunately, the extent of research on characterizing the biophysical properties of the TMC joint and surrounding tissue is limited.

The following research will seek to identify the ligamentous structures hypothesized to act as primary stabilizers of the TMC joint through advanced, high-resolution motion analyses. Mechanical properties of the primary ligamentous stabilizers will be obtained through uniaxial tensile testing of ligamentous tissue. This tissue will be further characterized through histology, staining for identification of the presence and orientation of essential proteins which may serve to support the argument for primary stabilizing tissue. Using results from the tissue characterization studies, two techniques are presented for the treatment of early and late stage TMC joint osteoarthris, which are designed to maintain and/or regain stability of this joint. The final section introduces a methodology for development of patient-specific computational finite element models of the hand and thumb. Input properties of these models are based on computed tomography data and outputs from the motion analysis and mechanical testing studies.

Contents

List of Figures

List of Figures

List of Tables

Glossary

Anterior	An anatomical term of location defining front of the body or "in front of".
Distal	An anatomical term of location defining a region furthest from the point of attachment to the body.
Dorsal	An anatomical term of location defining the back of the body, commonly used when referring to the hand.
Extensor retinaculum	A strong, fibrous band extending obliquely across the back of the wrist through which the extensor tendons of the digits pass.
Inferior	An anatomical term of location meaning "below" or "under".
Lateral	An anatomical term of location defining a region away from the midline of the body, toward the side.
Medial	An anatomical term of location defining a region toward the middle of the body, toward the midline.
Posterior	An anatomical term of location defining the rear of the body or "in back of".
Proximal	An anatomical term of location defining a region near where an appendage joins the body.

Superficial — In anatomy, it defines a region near the surface of the body or "closer to the surface of the body".

Superior — An anatomical term of location meaning "above" or "over".

Thenar muscles — Refers to a group of muscles (abductor pollicis brevis, flexor pollicis brevis, and opponens pollicis) on the palm of the hand at the base of the thumb.

Transverse carpal ligament — A strong, fibrous band that arches over the carpals of the wrist, forming the carpal tunnel through which the flexor tendons of the digits pass.

Volar — An anatomical term of location defining the front of the body, commonly used when referring to the hand.

Chapter 1

Introduction

1.1 Motivation

Gross anatomical studies have been succesful at identification of key structures of the trapeziometacarpal (TMC) joint, and have been highly influential in shaping surgical techniques for treatment of injury or disease of this joint. In the case of joint osteoarthritis (OA), two theories have been implicated as primary factors in the development and subsequent progression of OA: 1. joint hypermobility and subluxation due to ligamentous laxity, and 2. cartilage degradation due to incongruent contact mechanics. Unfortunately, the extent of research on biophysical characterization of this joint is limited, and little substantive data exists to support either of these theories.

Before we can draw conclusions regarding the role that each plays in the onset and progression of OA, we must first have a clear understanding of the dynamic behavior of the native joint when subjected to physiologic motions. To investigate joint hypermobility and/or ligamentous laxity as a factor in OA, we must understand the

healthy joint ligaments contributions to structural stability. To investigate incongruent contact mechanics as a factor in OA, we must define native joint contact mechanics.

1.2 Dissertation Contributions

This dissertation introduces six major contributions to the literature on the trapeziometacarpal (TMC) joint:

1. Absolute displacements of the trapezium and base of the first metacarpal (1st MC base) in healthy cadaveric specimens (native; free of pathologic disease or defects) when subject to thumb extension, lateral pinch, and four sizes of grip (1/2, 1, 1-1/2, and 2 inch), is characterized through high-resolution motion analyses. This provides baseline information on the motion of the healthy joint during daily physiologic activities.

2. Relative displacements of the trapezium and 1st MC base in unhealthy cadaveric specimens (subject to dissection of the dorsal radial (DRL), posterior oblique (POL), ulnar collateral (UCL), anterior oblique (AOL), or intermetacarpal (IML) ligament) during thumb extension, lateral pinch, and four sizes of grip is characterized through high-resolution motion analyses. This provides information on the relative contribution of each ligament to the stability of the TMC joint.

3. Uniaxial tensile testing provides data on the ultimate tensile strength, stiffness, ultimate tensile stress, and ultimate strain of the DRL, POL, UCL, and AOL. This information, in collaboration with results from motion analysis testing, is used to identify the primary and secondary sta-

bilizing ligament of the TMC joint.

4. Histological study of these ligaments is used to characterize the microstructural orientation of collagen fibers. This qualitative analysis is used to refute or support the importance of each ligament to stability of the joint.

5. Native joint contact area and pressure is characterized when the hand is subject to lateral pinch loading. This provides baseline information on contact mechanics of the healthy joint. This information is then used to determine the effects of a surgical technique for treatment of early TMC OA.

6. Mechanical test data from the motion analysis and tensile testing studies are used as input parameters to a patient-specific finite element model of the thumb. This model may be used for future analysis of the effects of surgical techniques, implants, or disease on the behavior of the thumb.

1.3 Structure of Dissertation

This dissertation is structured as follows: Chapter 2 describes the structure and function of the trapeziometacarpal (TMC) joint including bony structures, cartilage, and surrounding ligaments. Osteoarthritis of the joint is defined in detail and current non-surgical and surgical options for treatment of osteoarthritis of the TMC joint are explained. Chapter 3 outlines the experimental methods used in characterizing the TMC joint. The methodology for identifying primary stabilizing ligaments using

advanced motion analysis tools is described and results of this study are presented. This section is followed by uniaxial tensile mechanical characterization of the joint ligaments. Finally, histological analysis is presented and compared with mechanical test results. In Chapter 4, the scope of this dissertation shifts to present the development of two surgical techniques for treatment of osteoarthritis of the TMC joint. Contact mechanics of the native joint is presented and used to determine the effects of a technique for early OA treatment. Mechanical testing is used to compare a new surgical technique for late stage OA, which salvages the primary stabilizing ligaments, with the commonly used surgical treatment, which destroys all ligamentous attachments. In Chapter 5, the methodology for the development of patient-specific finite element models of the hand and wrist are presented. The dissertation is concluded with discussion of future studies on TMC tissue characterization and plans for studies on prevention and treatment of TMC OA.

Chapter 2

Literature Review

2.1 The Trapeziometacarpal Joint (TMC)

2.1.1 Structure and Function

The trapeziometacarpal (TMC) joint lies between the first metacarpal bone of the thumb and the trapezium carpal bone of the wrist. [1] (Figure 2.1) The proximal end of the first metacarpal bone articulates with the distal end of the trapezium in a biaxial manner due to reciprocally opposed saddle shaped articular surfaces. The saddle shape of the joint allows for flexion (toward index finger in the plane of the palm), extension (away from index finger in the plane of the palm), abduction (away from the index finger perpendicular to the plane of the palm), adduction (toward index finger perpendicular to the plane of the palm) and opposition (swinging the metacarpal across the palm of the hand toward the little finger) of the thumb. (Figure 2.2) Opposition is a unique feature which enables us to pinch and grip objects. The combined movement of these primary motions, coupled with loose capsular tissue, allows for circumduction or rotation of the thumb.

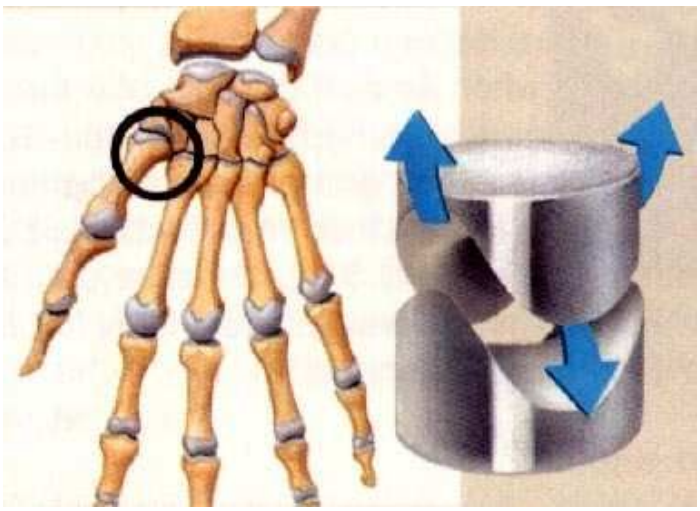

Figure 2.1: Skeletal drawing of the human hand identifying the trapeziometacarpal joint. This joint has a biaxial shape due to reciprocally opposed saddle surfaces similar to the inset on the right. [2]

The articular surface of the metacarpal and trapezium is covered with flexible, highly organized extracellular matrix known as hyaline cartilage. This tissue, commonly found on joint surfaces, is made up of specialized cells known as chondrocytes in a matrix composed of collagen and elastin fibers, proteoglycans, and high water content. [4, 5, 6] The water content, synovial fluid in the joint space, and smooth

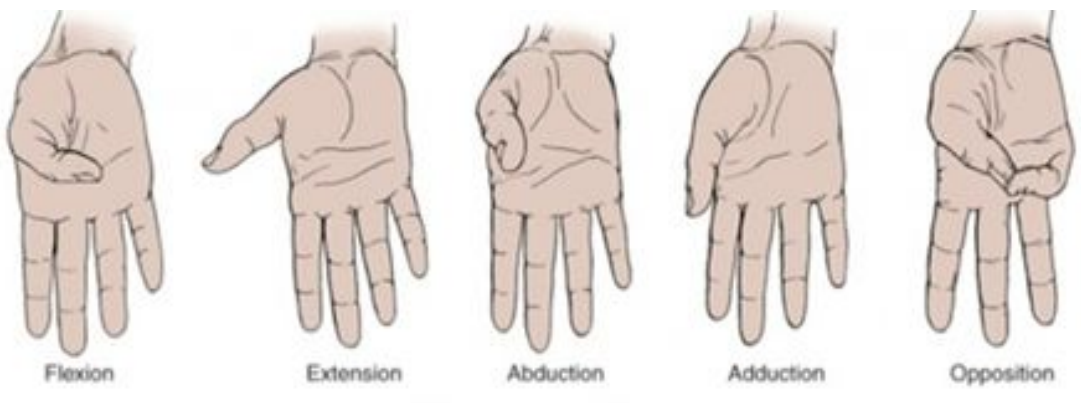

Figure 2.2: Representative image of the hand showing five possible anatomical thumb positions. [3]

surface of the tissue allows for reduced shear forces and permits smooth articulation of the bones.

The TMC joint is moderately stable due to the concave/convex nature of the first metacarpal and trapezium, but primary joint stability during thumb motion is attributed to the joint capsule and many ligaments attaching the metacarpal and trapezium to neighboring structures. Anatomical studies have identified as many as 16 ligaments providing stability to the trapezium and first metacarpal (Figure 2.3). [8] Muscles and tendons neighboring the TMC joint provide additional support (Figure 2.4) for restraint of the ligamentous system. [9]

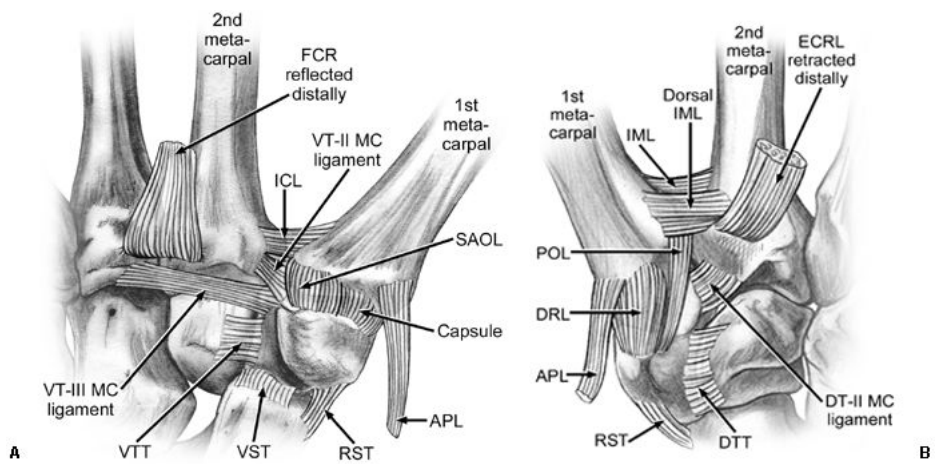

Figure 2.3: A. Volar and B. dorsal ligaments and tendons stabilizing the trapezium and first metacarpal. APL, abductor pollicis longus tendon; DRL, dorsoradial ligament; DT-II MC, dorsal trapezio-second metacarpal; DTT, dorsal trapeziotrapezoid ligament; ECRL, extensor carpi radialis longus tendon; FCR, flexor carpi radialis tendon; ICL, intercarpal ligament; IML, intermetacarpal ligament; POL, posterior oblique ligament; RST, radial scapotrapezial ligament; SAOL, superficial anterior oblique ligament also known as the anterior oblique ligament; VST, volar scaphotrapezial ligament; VT-II MC, volar trapezio-second metacarpal; VT-III MC, volar trapezio-third metacarpal; VTT, volar trapeziotrapezoidal ligament. The ulnar collateral ligament (UCL) lies between the 1st and 2nd metacarpals to the left of the SAOL in the left image but is not visible in this view. [7]

Figure 2.4: Palmar view of the hand showing proximal-medial trajectory of the deep and superficial thenar muscles (APB, FPB, OPP). The ADD has two heads directing the thumb transversely (medially) and obliquely (dorsally). [10]

2.2 The Role of Thumb Ligaments on the Stability of the TMC Joint

Many researchers have sought to identify the relative contributions that each of the TMC joint ligaments have in the stability of the TMC joint. Most have made inferences based on the physical structure or location/orientation of these ligaments. [11, 12, 13, 14, 8, 15, 16, 17, 18] Some have based their conclusions on histology and immunohistochemistry findings of sensory nerve endings in the ligaments. [19, 18] Few researchers have used mechanical test data to support their claims for ligamentous stability. [20, 21, 22, 23, 24]

The dorsal radial ligament (DRL) has been implicated as the primary stabilizer of the TMC joint most often in literature. This conclusion has been based on its high

ultimate tensile load prior to failure (205.5±60.2 N) [24], its ability to resist dorsal radial dislocation forces [20, 22, 23], its large thickness relative to other TMC joint ligaments [17, 18], and high content of sensory nerve endings [19, 18]. Early anatomic studies on the TMC joint implicated the deep anterior oblique ligament (dAOL) as the primary stabilizing structure due to its centrally placed anatomic location in the joint [13, 14]. The posterior oblique ligament (POL) has twice been implicated as a primary stabilizer due to its high strength [21] and high content of sensory nerve endings [19]. In 1981, Pagalidis suggested that the intermetacarpal ligament (IML) is the primary structure responsible for displacement of the first metacarpal. [12] Regardless of their reported findings on stability, most of these researchers believe that ligamentous instability plays a direct or indirect role in the development and progression of osteoarthritis.

2.3 Osteoarthritis (OA) of the TMC Joint

Normal thumb function can be disturbed when the thumb is subject to injury, autoimmune disease such as rheumatoid arthritis, or degenerative disease known as osteoarthritis (OA). When subjected to normal wear and tear over extended periods of time, the joint cartilage tissue begins to break down, leading to OA. (Figure 2.5) OA of the TMC joint is characterized by pain at the base of the thumb, decreased range of motion, tenderness and stiffness of the joint, thumb instability, and decreased grip and pinch strength. [25] OA is the most common form of arthritis, affecting one in four people over the age of 45. [26] It is most common in post-menopausal women in their fifth to seventh decade and can lead to impairment in vocational activities, hobbies, and activities of daily living, significantly affecting quality of life. [27]

The cause and subsequent progression of TMC OA has been the subject of debate

Figure 2.5: The normal and arthritic trapeziometacarpal joint. The arthritic joint shows breakdown of the articular cartilage with redness due to bone on bone contact. [28]

for many years. A clinical study by Eaton and Littler [11] suggests that hypermobility or instability due to ligamentous laxity leads to joint incongruity, which permits articular surface damage and the onset of OA. Pellegrini et al. [14] suggest that detachment or relaxation of the palmar beak ligament may play a role in the onset of OA. The Framingham study [29] found evidence that radial subluxation predisposes the TMC joint to OA in men. In a biomechanical study, Koff et al. [30] examined cartilage thickness maps of the TMC articular surfaces. They found that high stresses may exacerbate OA in these regions of the articular cartilage. Following over 50 years of debate, two factors are repeatedly implicated as the primary cause of TMC OA: 1. cartilage degradation due to incongruent contact mechanics, and 2. joint hypermobility and subluxation due to ligamentous laxity.

2.4 Current Treatment Options for TMC OA

2.4.1 Non-operative Treatment

In early stages of TMC OA, a doctor may recommend non-operative treatment options such as suggested modifications to daily activities, splinting, corticosteroid injections, laser therapy, and/or pain medication (Figure 2.6). [31, 32, 33, 34] Custom-made and pre-fabricated splinting is designed to improve pain by limiting joint range-of-motion. It has been shown that restricting motion of the diseased thumb may limit high joint contact forces, thus reducing pain to the patient. Corticosteroids (inflammation fighting medication) may be injected into the joint to decrease heat, redness, pain, and swelling due to OA. This medication does not limit range-of-motion like splinting, but repeated injections have been associated with nerve irritation, weakening of ligaments, and thinning of cartilage thus leading to greater pain once the corticosteroid affects wear off. [35] A less aggressive method of non-operative treatment is with the use of nonsteroidal anti-inflammatory drugs with or without prescription. These medications relieve pain by blocking cyclo-oxygenase enzymes (Cox-1 and Cox 2) which make tissue swelling and pain increasing prostaglandins. [36] As the disease progresses, these pain relievers manage the symptoms but fail to treat the underlying degenerative changes to the joint.

2.4.2 Surgical Techniques

In order to address these changes, surgical options are the only alternative. Many surgical treatments exist and are successful at modifying the biomechanical structure of the bone/joint. TMC fusion is characterized by internally fixing the metacarpal to the trapezium bone with staples, screws, or wire. [42, 43] (Figure 2.7) A disadvantage of TMC joint fusion is that it may predispose the affected patient to arthri-

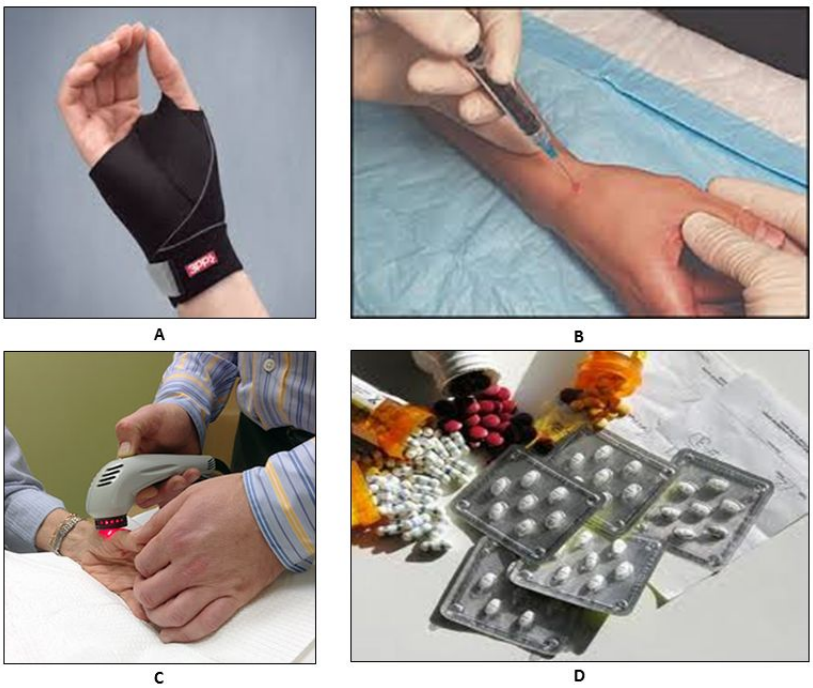

Figure 2.6: Non-operative treatment options for TMC OA include: A. Splinting [37], B. Corticosteroid injections [38], C. Laser therapy [39], and D. Pain medications.

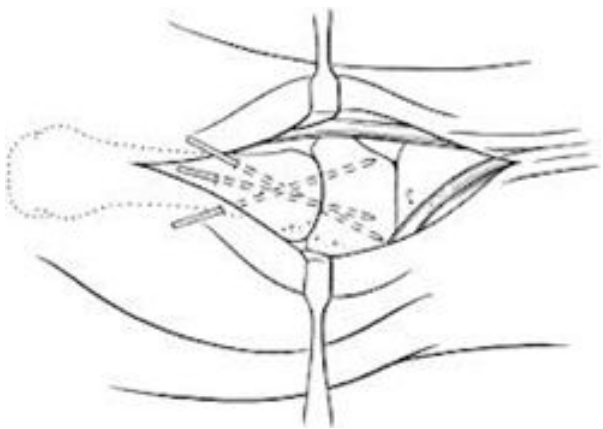

Figure 2.7: Fusion of the TMC joint is indicated for painful joint instability. Wire, screws, or staples are used to fix the trapezium to the metacarpal. In this figure, three Kirschner wires are placed through the metacarpal, across the joint space, and through the trapezium for stabilization. [40]

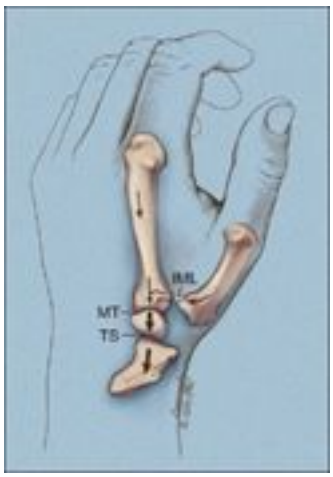

Figure 2.8: Total trapeziectomy is characterized by complete removal of the trapezium bone. MT - metacarpal/trapezoid joint; TS - trapezoid/scaphoid joint; IML - intermetacarpal ligament. [41]

tis of the neighboring joints. An alternative treatment which has been shown to maintain the mechanical strength of the thumb is known as resection arthroplasty. The most common type of resection arthroplasty is known as total trapeziectomy and is characterized by complete removal of the trapezium bone (Figure 2.8). [42] This method eliminates contact between the two arthritic joint surfaces but is associated with thumb shortening and greater thumb instability by removing primary ligamentous attachments. Implant arthroplasty, a third treatment, is characterized by the addition of an implant in/near the joint to prevent thumb shortening, increase mechanical strength, and decrease thumb laxity. One type of interpositional arthroplasty, developed by Kapandji and Heim, is known as opening-wedge trapezial osteotomy (OWTO) (Figure 2.9). [44] This technique uses a 10-15° wedge to change the tilt angle of the trapezium. It is hypothesized that alterations in the tilt angle may prevent dorsal-radial joint subluxation (dislocation).

The two most common treatments were designed to address the two pre-eminent theories (joint contact forces and ligament laxity) about the initiation and progres-

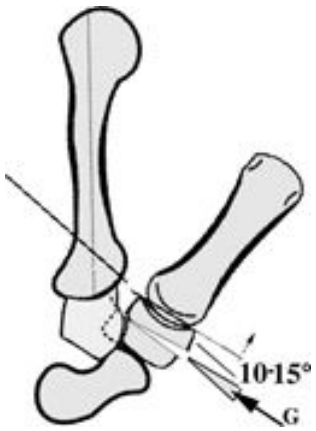

Figure 2.9: Opening wedge trapezial osteotomy is a form of interpositional arthroplasty. A wedge implant is placed dorsal-radially in the trapezium to change the tilt angle of the trapezium. [44]

sion of TMC OA: first metacarpal extension osteotomy (FMEO) [45, 46] is designed to increase joint stability by altering contact mechanics, and ligament reconstruction with tendon interposition (LRTI) [11, 47] is meant to decrease joint laxity. FMEO is a form of excisional arthroplasty where a 20-30° wedge is removed from the dorsal-radial surface of the metacarpal. The premise behind FMEO is similar to OWTO in that it alters the TMC joint mechanics by shifting the contact area of the TMC joint away from the deteriorating regions of the articular surface (Figure 2.10). In LRTI, the trapezium is removed in whole or in part and the palmar oblique ligament is reinforced with a portion of the flexor carpi radialis tendon (in some instances the abductor pollicis tendon is used) through a series of loops (Figure 2.11). The premise behind LRTI is that it will reduce hypermobility by limiting dorsal-radial migration and subluxation of the metacarpal on the trapezium.

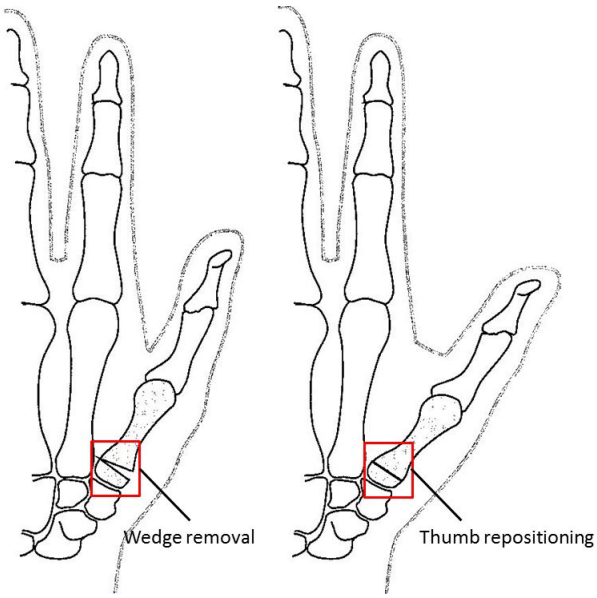

Figure 2.10: First metacarpal extension osteotomy is a form of excisional arthroplasty where a 20-30° wedge is removed from the metacarpal to change the contact angle of the metacarpal on the trapezium. [45]

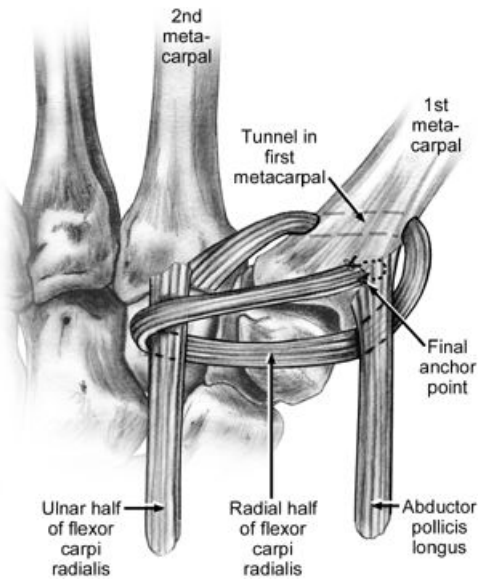

Figure 2.11: Ligament reconstruction with tendon interposition is characterized by a reinforcement of ligamentous attachments with neighboring tendons. [7]

Chapter 3

Characterizing the Trapeziometacarpal Joint: Experimental Study

3.1 Introduction

The following section presents the methodology and results of three experimental studies investigating the mechanical behavior and properties of ligamentous structures hypothesized to act as primary stabilizers of the trapeziometacarpal (TMC) joint. As described in the literature review section of this manuscript, as many as sixteen ligaments attach to the trapezium or at the base of the metacarpal and may provide stability to the TMC joint. Due to limited financial resources and time, this study focuses on five ligaments that have frequently been reported as *primary* stabilizing ligaments of this joint: the dorsal radial ligament (DRL), posterior oblique ligament (POL), anterior oblique ligament (AOL), ulnar collateral ligament (UCL), and the intermetacarpal ligament (IML). The DRL and POL are dorsal ligaments

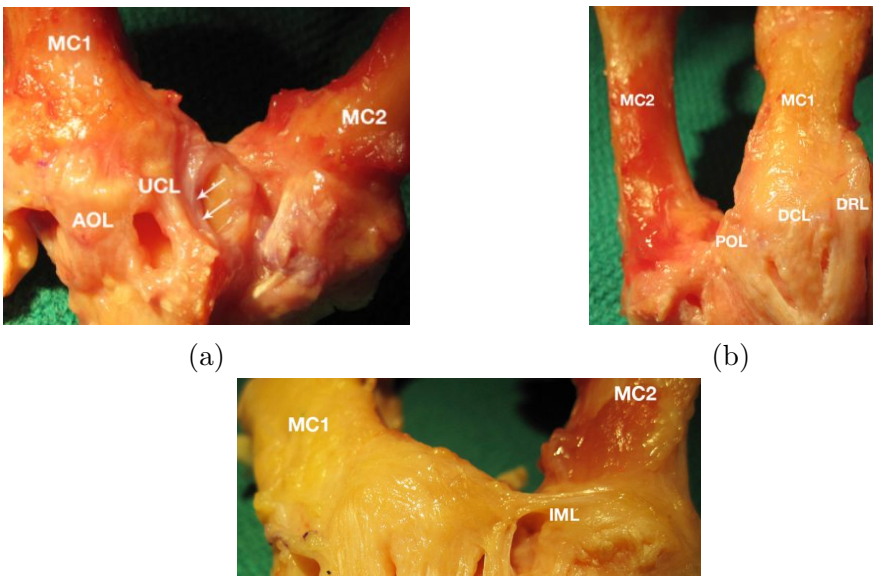

Figure 3.1: a. Volar and b. dorsal views of the TMC joint. The volar view shows the AOL and UCL ligaments. The dorsal view shows the POL and DRL ligaments. Note: This figure includes a third ligament defined as the dorsal central ligament (DCL). [18] This ligament was identified in only one of the specimens under investigation. For purposes of the present study, the DCL is considered part of the DRL. c. The position of the IML is shown in a dorsal view. MC1- first metacarpal, MC2- second metacarpal

with origin in the trapezium and insertion in the first metacarpal. (Figure 3.1b) The AOL is a volar ligament with origin in the trapezium and insertion in the first metacarpal. The UCL originates at the transverse carpal ligament and inserts in the first metacarpal. (Figure 3.1a) The IML originates in the second metacarpal and inserts in the first metacarpal. (Figure 3.1c) It should be noted that the AOL refers to the combined effects of the superficial and deep anterior oblique ligaments and the IML refers to the combined effects of the volar and dorsal intermetacarpal ligaments.

In Section 3.3, advanced, high resolution motion tracking is used to identify the primary stabilizers of the joint through serial sectioning of ligaments while the thumb

is positioned in extension, lateral pinch, and four diameters of grip motion. In Section 3.4, the six investigated ligaments are subject to mechanical testing to define ultimate failure load behavior. In Section 3.5, histology is completed on the five ligaments to characterize the presence and orientation of structural proteins. This data will be analyzed to determine whether correlation exists to mechanical test results.

3.2 Specimen Selection and Identification of Ligamentous Structures

Fifteen matched pairs of fresh-frozen cadaveric human hands and forearms were purchased from a whole-body anatomical donation center (Science Care®) (n=30). Serology reports for all specimens were evaluated and specimens were subject to fluoroscopic imaging (X-ray) to guarantee the specimens were free of pathologic joint defects or disease. One pair of specimens from a single donor were excluded from this study due to poor tissue quality effects from chemotherapy.

Prior to testing, a preliminary dissection was completed using specimens obtained from the University of New Mexico School of Medicine Anatomical Education Center. This anatomical dissection was completed in order to accurately identify the origin and insertion sites of the ligamentous tissue being investigated. Each ligament was excised at the insertion in the first metacarpal and marked using suture for identification (Figure 3.2). This method of identification was essential as the methodology for TMC ligament anatomical identification has not been well described in literature. The citation commonly used for identification of these ligaments is for general identification of wrist ligaments and describes looking for "longitudinal groupings of collagen fibers with an epiligamentous sheath surrounding them." [48, 49] The method of identification is made particularly difficult in the present study due to the

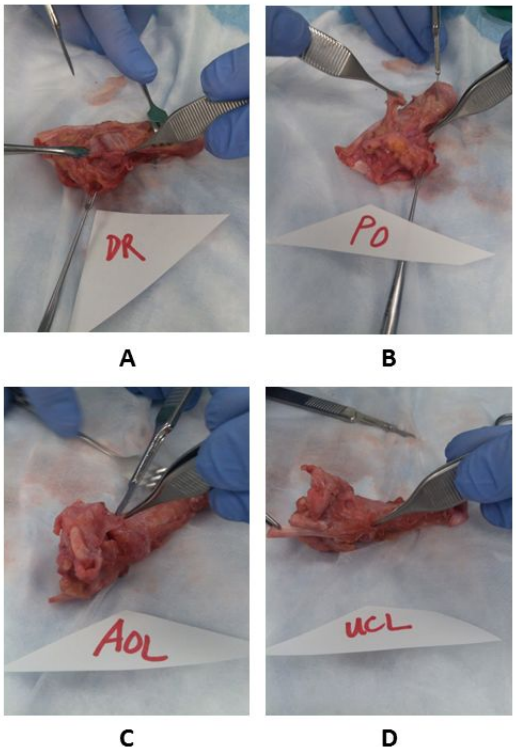

Figure 3.2: Ligament identified through preliminary anatomical dissection to determine their orientation and insertion points in the first metacarpal.

fact that ligamentous attachments must be severed at insertion sites through small incisions in the surrounding soft tissue, with the specimen remaining near intact.

3.3 High Resolution Motion Analysis to Identify the Primary TMC Joint Stabilizers

3.3.1 Specimen Preparation

A design of experiments methodology was used to determine the minimum number of specimens needed for investigating the individual and combined effects of all five

select ligaments (DRL, POL, AOL, UCL, and IML) on the stability of the TMC joint. This analysis yielded thirty-one necessary measures which could be analyzed with eleven individual specimens. In order to simplify test fixture fabrication, only right hands from the available specimens were used. Eleven specimens were randomly selected from the fourteen available right hands. The specimens selected for this study were kept frozen at -20°C, thawed twice for short periods before test day. The first thaw was for bone density measurements using X-ray and high-resolution computed tomography necessary for later numerical analyses. The second thaw was for specimen preparation including identification of an accessible site for ligament sectioning and identification of tendons necessary to produce thumb motions.

A single exposure site was created on the medial surface of the wrist just superficial to the TMC joint. This incision extended from 2mm proximal to the trapezium, distally along the first metacarpal at a distance of approximately 15mm from the TMC joint. (Figure 3.3) This length allowed for separation of the overlying tissue enough to gain exposure to the volar and dorsal ligaments of interest. Volarly, the thenar muscle bellies were raised off their attachment to the first metacarpal slightly, in order to gain access to the UCL from the exposure site. Raising these muscles off the surface of the metacarpal added slightly to instability of the joint. All specimens were dissected in the same manner prior to experimental testing so that any variability in stability could not be attributed to different joint exposure techniques.

Actions of lateral pinch and grip require movement of the thumb across the palm of the hand. Cooney and Chao reported that tendons applying force to the thumb during lateral pinch are the same as those applying force in grasp (grip) motion with a slightly lower magnitude of force. [50] These tendons are the flexor pollicis longus (FPL), abductor pollicis brevis (APB), adductor pollicis (ADD), and combined force from the flexor pollicis brevis and opponens pollicis (FPB/OPP). With assistance

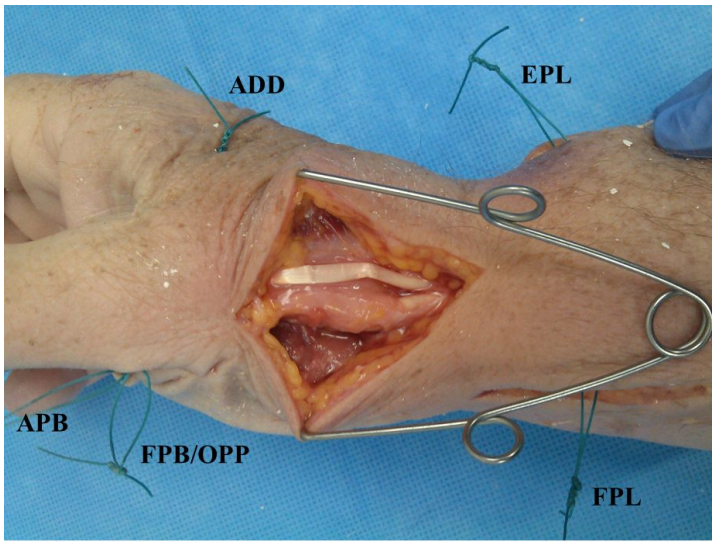

Figure 3.3: Anatomical dissection of a single specimen showing exposure of the TMC joint space and tagging of tendons used to produce thumb motion. APB - abductor pollicis brevis; ADD - adductor pollicis; EPL - extensor pollicis longus; FPL - flexor pollicis longus; FPB - flexor pollicis brevis; OPP - opponens pollicis.

from a trained orthopaedic hand surgeon, the APB, FPB/OPP, and ADD tendons were identified and suture tagged near the bone/tendon interface. The FPL was tagged just proximal to the transverse carpal ligament pulley system to guarantee the appropriate loading trajectory. To produce the motion of thumb extension (hitch-hikers thumb), the extensor pollicis longus (EPL) tendon was tagged just proximal to the extensor retinaculum. (Figure 3.3) High strength suture was later added to the suture tagged tendons for loading.

3.3.2 Test Fixture Fabrication

The test fixture developed for the motion analysis study is comprised of six essential components: the baseplate and overhang, dorsal blocking splint, medial wrist splint, diversion pulley for APB and FPB/OPP tendons, stand-alone magnetic diversion pulley for the ADD tendon, and end plate with eye bolts for uniform tendon load-

ing. The base of the fixture is fabricated from 1 inch thick 2024 bulk aluminum and has dimensions of 24 inches long by 8 inches wide. A 1/4 inch thick aluminum plate (3 inches long, 8 inches wide) is attached to the end of the base creating an L-shape. The base was designed in this manner so that the plate could be placed on the surface of a test table with the overhanging plate resisting lateral movement of the plate when subject to shear loads due to weighted tendons (Figure 3.4). A series of holes were drilled and tapped on the surface of the baseplate for attachment of dorsal blocking splint and diversion pulleys for APB and FPB/OPP tendons.

A forearm splint, known as a dorsal blocking splint (DBS), was created with the assistance of a trained physical therapist (Patricia Siegel, B.S., OTR/L, CHT). A DBS rests dorsally on the hand and positions the wrist at 20-30° of flexion, the 2nd-5th metacarpals are positioned at approximately 70° of flexion, and the fingers are fully extended (Figure 3.5) This splint, made from 1/16 inch thick heat moldable thermoplastic (Multiform Clear Elastic, Alimed®), was heated to 160°F and molded to the right hand of an average size specimen. A medially placed wrist splint was created

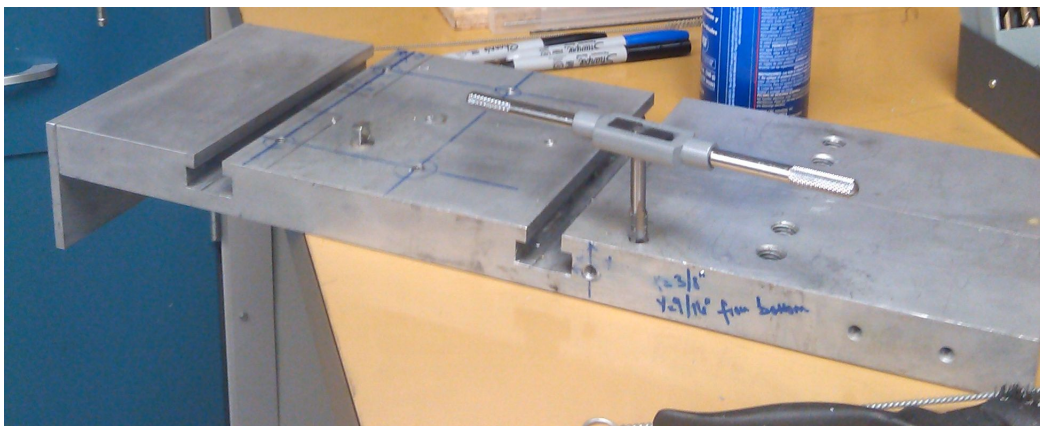

Figure 3.4: The baseplate of the experimental test fixture used for the motion analysis study. The figure shows a 1 inch thick base with 1/4 inch thick overhang to prevent slippage/shear of the plate when subject to tendon loading. Holes were drilled and tapped on the base plate surface for attachment of splint and diversion pulleys.

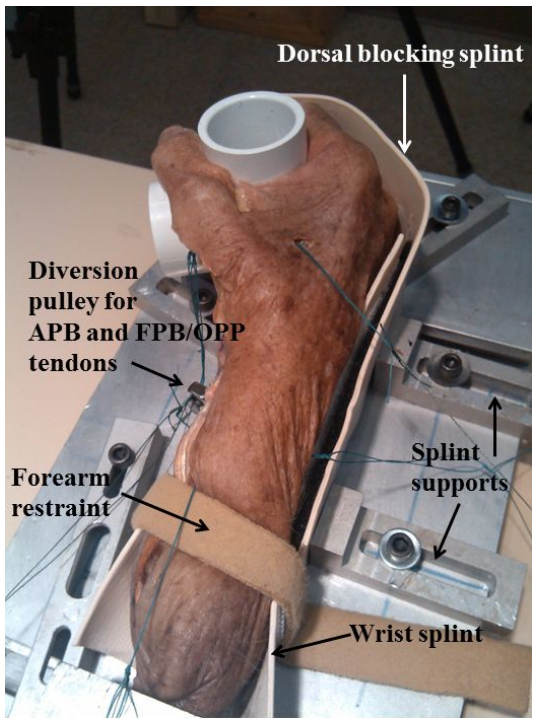

Figure 3.5: Top view of the baseplate with dorsal blocking splint and diversion pulley for APB and FPB/OPP tendons.

to keep the wrist from deviating radially. The two splints were attached dorsally with high strength velcro allowing for length adjustments for small and large hands. Three holes were drilled on the medial surface of the wrist splint for attachment to the baseplate. Three straps were added to restrain the forearm and hand. Metallic splint supports placed volarly and dorsally provide added stability.

The APB, FPB, and OPP thenar muscule trajectory lies along the proximal-medial direction (Figure 2.4). In order to achieve this loading trajectory, a small diversion pulley was placed on the baseplate along this trajectory in order to divert the high strength suture for appropriate loading (Figure 3.5). The ADD muscle is comprised of two components with trajectories acting transversely (medially) and obliquely in a proximal-dorsal direction. The distal attachment of this muscle is at the base of

the proximal phalanx. This is the site of suture attachment to the ADD. In order to achieve a trajectory matching that of the ADD muscle, a stand-alone magnetic diversion pulley is placed along this trajectory, approximately 18 inches from the site of suture attachment (Figure 3.6).

The final component of the motion analysis fixture is the end plate with eye bolts for directing the suture for loading. (Figure 3.7) This plate is made from 1 inch thick 6061 aluminum with a bolt pattern array for positioning of attachments. Length and width of the plate is 18 inches and 8 inches, respectively. Three eye bolts are positioned at the far end of the plate to direct suture attachments from the APB, FPB/OPP, ADD, and FPL tendons for loading. Resultant force vectors shown at

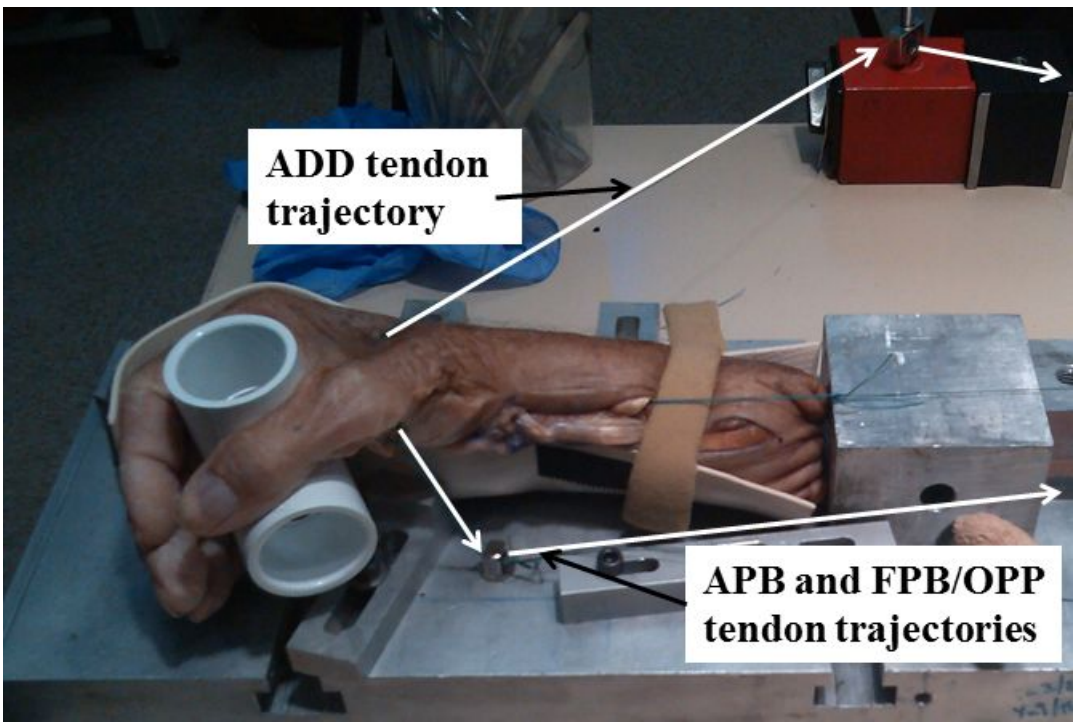

Figure 3.6: Oblique view of the motion tracking test fixture showing loading trajectories of the FPB/OPP tendons through the baseplate diversion pulley and ADD tendon through the stand-alone magnetic diversion pulley.

the bottom of the figure are equivalent in magnitude for the three suture attachments. All sutures are attached to a single loading block and a single distributed load is applied to all suture/tendon structures for pinch and grip motion. All motion analysis fixtures are positioned on top of a steel cabinet with casters for transport and positioning in the camera field of view. The cabinet was used for fixture storage between tests.

3.3.3 High Resolution Camera System

All testing for this study was completed in the Gait Analysis Laboratory in the Department of Orthopaedics, Division of Physical Therapy. This laboratory is equipped with a Vicon MX-T20 Series motion capture camera system and Vicon Nexus software. The Vicon motion capture system consists of ten cameras with infrared (IR)

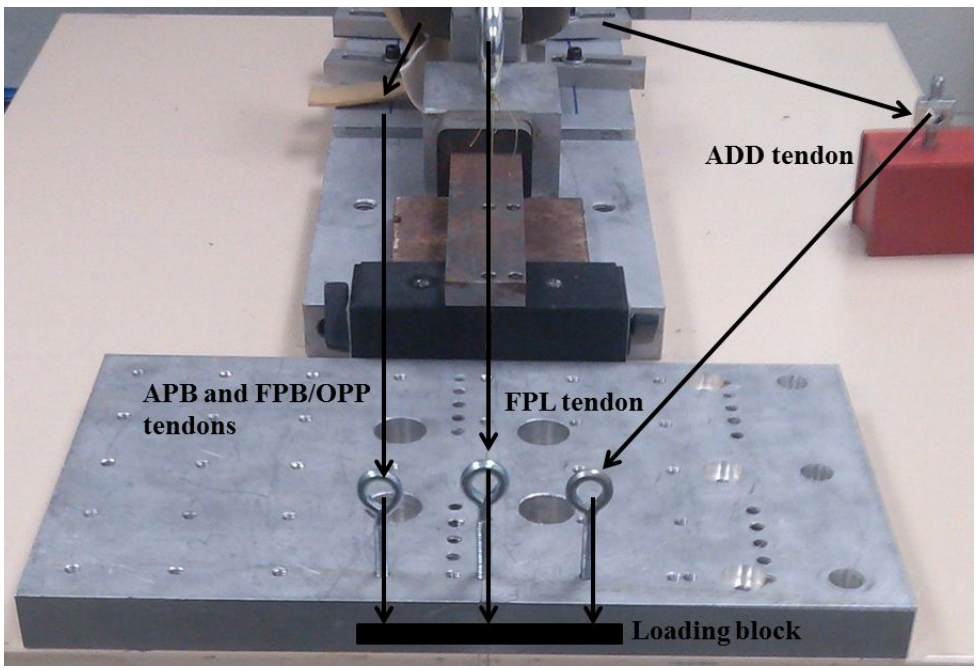

Figure 3.7: Aluminum endplate with three eyelets for diverting suture for distributed loading. This plate is positioned opposite the direction of the dorsal blocking splint.

optical filters and IR light emitting diodes (LEDs). IR radiation emitted by the LEDs is reflected off markers positioned on the subject of interest and captured by the cameras. Each camera has a resolution of 2 megapixels, a maximum frame rate of 690fps, and can record movements as small as 10,000th of a millimeter. Every pixel is used to gather information on each marker's center and radius for high accuracy. Six cameras were used in this study and positioned around the specimen test table to capture six degrees of motion of each marker set attached to the hand and wrist (Figure 3.8).

3.3.4 Marker Set Design and Placement

Motion analysis studies using IR cameras require a set of spherical reflective markers which are commonly placed on the skin of the subject of interest. These markers,

Figure 3.8: Vicon camera system positioned for testing. Six cameras were used to track the motion of all surface markers placed on the specimen.

attached with double-sided tape, may be positioned individually or fixed to a marker shell in clusters of three. For the present study, three sets of markers were used for analysis of thumb motion. All cluster shells were designed using a thin foam base with a centrally located screw extending vertically, at a height of approximately 2 cm from the base. One marker was placed on the surface of the screw and one was placed on either side of the screw. This configuration was necessary to prevent the three markers from being collinear, a requirement for motion analysis.

The first marker set (shell) was placed medially on the radius just proximal to the TMC joint. This marker set was used as a negative control to confirm that no motion was occurring in the radius during loading, indicative of an unstable restraint fixture. The second marker set (shell) was placed medially on the surface of the first metacarpal. This marker set was used to track the motion of the entire metacarpal during loading to guarantee that the path of the thumb was identical across specimens. The third marker set was comprised of three individual markers. The first marker of this set was placed on the surface of a sharp thumb tack which allowed for direct placement of this marker into the exposed bone of the trapezium. This marker provided information on absolute motion of the trapezium during loading. The second marker was placed on a tack which allowed for direct placement into the exposed bone at the base of the metacarpal. This marker provided information on absolute and relative motion of the metacarpal base. The last of this set was placed on the dorsal surface of the second metacarpal to provide a third point of reference for the trapezium and metacarpal base. The marker sets which were placed on the skin surface were sutured to the skin to prevent marker displacement. (Figure 3.9)

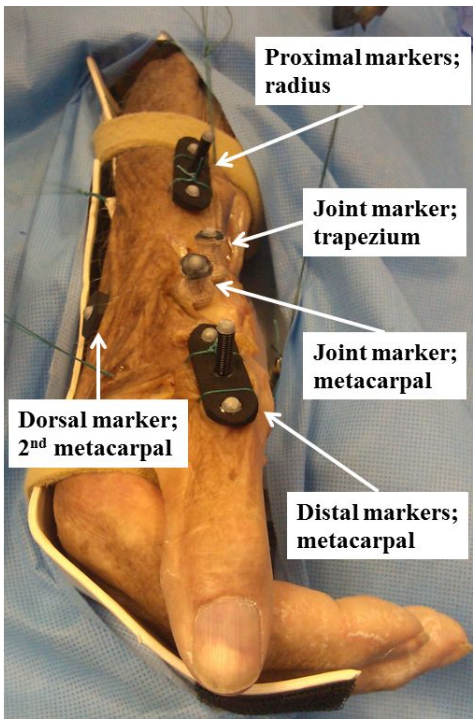

Figure 3.9: Representative test specimen with marker sets placed on the radius, first metacarpal, trapezium, base of the first metacarpal, and second metacarpal.

3.3.5 Methodology

As described in the Specimen Preparation section, a design of experiments model was used to determine that eleven specimens would be necessary to investigate the individual and combined effects of five ligaments on the stability of the TMC joint. Fresh frozen, cadaveric right hands were randomly selected and labeled from 1-11 for analysis. Each hand was sequentially placed in a test group where the ligaments to be investigated were assigned (Table 3.1).

The hands were positioned in the dorsal blocking splint of the test fixture and held with restraints. Camera marker sets were placed on each specimen as described above. Each specimen was subject to six distinct motions: thumb extension, lateral

Table 3.1: Assignment of specimens to ligament investigation groups. Each specimen was used to investigate at least two possible ligament combinations. The lettering defines the ligament(s) to be investigated and the order in which the ligaments were released.

Specimen ID	Ligaments Investigated*
1	D, DU, and DUIPA
2	U, UI, and UIP
3	I, ID, and IDU
4	P, PD, and PDU
5	A, AD, and ADU
6	UP, UPA, and UPAI
7	UA and UAI
8	PI, PID, and PIDU
9	IA, IAD, IADU
10	PA, PAD, PADU
11	API and APID

*D - dorsal radial; U - ulnar collateral; I - intermetacarpal; P - posterior oblique; A - anterior oblique

pinch, 0.5 inch grip, 1 inch grip, 1.5 inch grip, and 2 inch grip. Each of these motions were repeated three times before moving on to the next motion. The camera was triggered at the initiation of load and was stopped once the load was released. The following methodology was used for loading:

1. Load was applied to the EPL tendon at a magnitude of 1.5 kg-force, along the trajectory of the tendon and held for three seconds. This resulted in thumb extension (Figure 3.10). As load was released from the EPL, a counter load was applied to the ADD, APB, FPB/OPP, and FPL tendons at a magnitude of 3 kg-force. This load was held for three seconds then released. This produced the motion of lateral pinch (Figure 3.11).

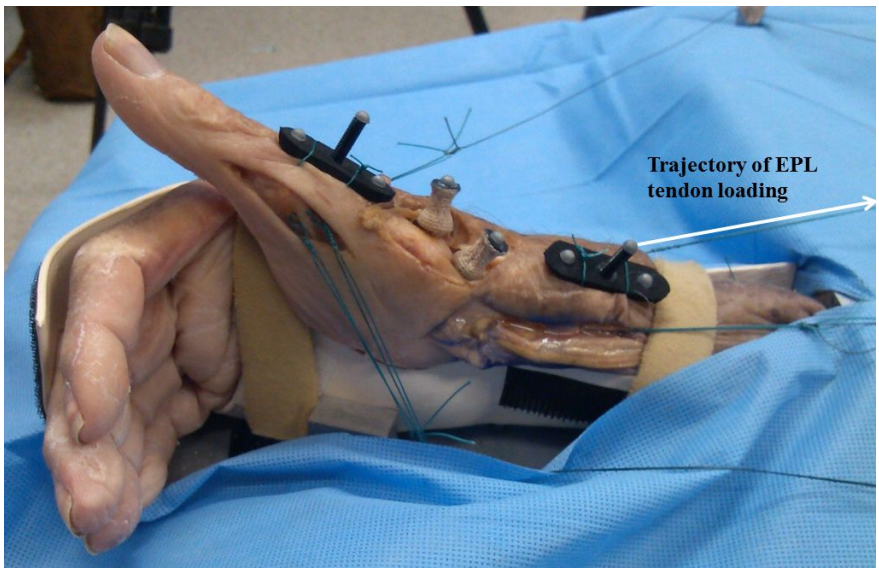

Figure 3.10: Specimen subject to EPL loading (1.5 kg-force) to produce a motion of thumb extension.

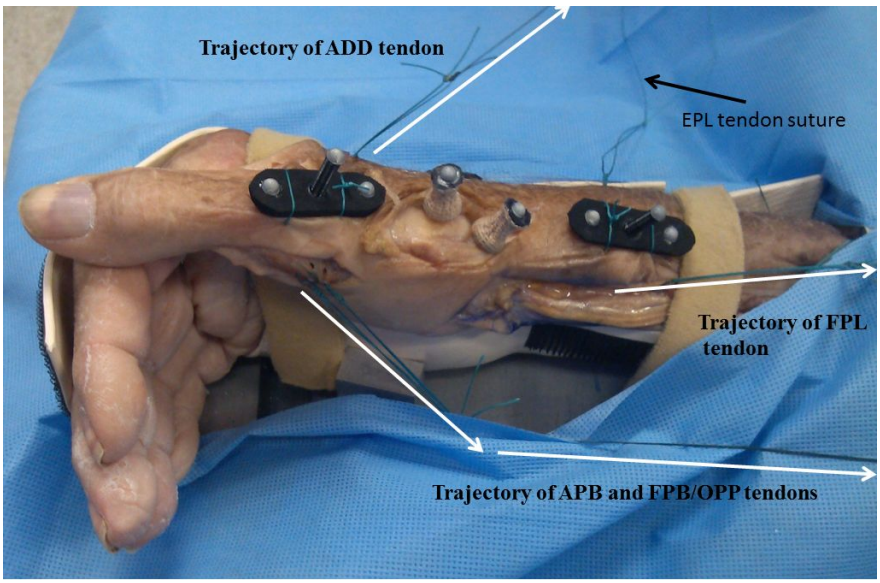

Figure 3.11: Specimen subject to combined ADD, APB, FPB/OPP, and FPL loading (3 kg-force) to produce a motion of lateral (key) pinch. Note that the suture tagged to the EPL tendon is relaxed under applied pinch load.

2. A 0.5 inch diameter L-shaped polymer pipe was placed between the thumb and fingers. The long end of the pipe was placed vertically downward, the short extended end was placed under the thumb to prevent significant opposition. Load was applied to the APB, ADD, FPB/OPP, and FPL tendons at a magnitude of 3kg-force, held for three seconds, and released (Figure 3.12a).

3. A 1 inch diameter L-shaped pipe was inserted between the thumb and fingers as above. Load was applied to the APB, ADD, FPB/OPP, and FPL tendons at a magnitude of 3kg-force, held for three seconds, and released (Figure 3.12b).

4. A 1.5 inch diameter L-shaped pipe was inserted between the thumb and fingers as above. Load was applied to the APB, ADD, FPB/OPP, and FPL tendons at a magnitude of 3kg-force, held for three seconds, and released (Figure 3.12c).

5. A 2 inch diameter L-shaped pipe was inserted between the thumb and fingers as above. Load was applied to the APB, ADD, FPB/OPP, and FPL tendons at a magnitude of 3kg-force, held for three seconds, and released (Figure 3.12d).

All specimens were subject to each motion prior to the start of ligament analysis to determine native thumb behavior. Following the native tests, each specimen was subject to sequential sectioning of the ligaments assigned to that specimen as defined in Table 3.1. Sectioning was performed by a trained orthopaedic surgeon using a number 15 scalpel by raising the ligament off the base of the first metacarpal. The specimens underwent all modes of extension, pinch, and grip following each ligament

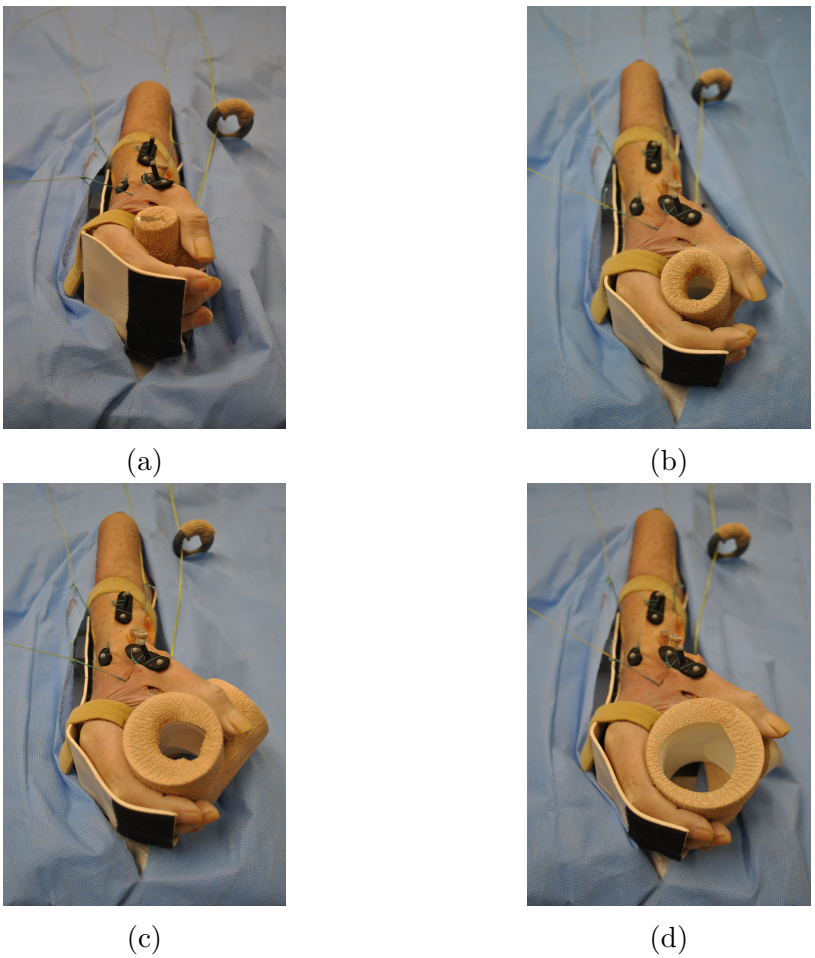

(a) (b) (c) (d)

Figure 3.12: Specimen subject to grip motions: (a) 0.5 inch grip; (b) 1 inch grip; (c) 1.5 inch grip; (d) 2 inch grip.

resection and motion capture data was collected.

The spatial positions of the radius, first and second metacarpals, and the trapezium were compiled using the Vicon Nexus system and exported to Matlab for analysis. The global coordinate system for this study is as follows: The y-axis defines distal/proximal motion (negative - distal toward fingers; positive - proximal toward body), the x-axis defines dorsal/volar motion (negative - dorsal/adduction; positive - volar/abduction), and the z-axis defines ulnar/radial motion (negative - down/ulnar;

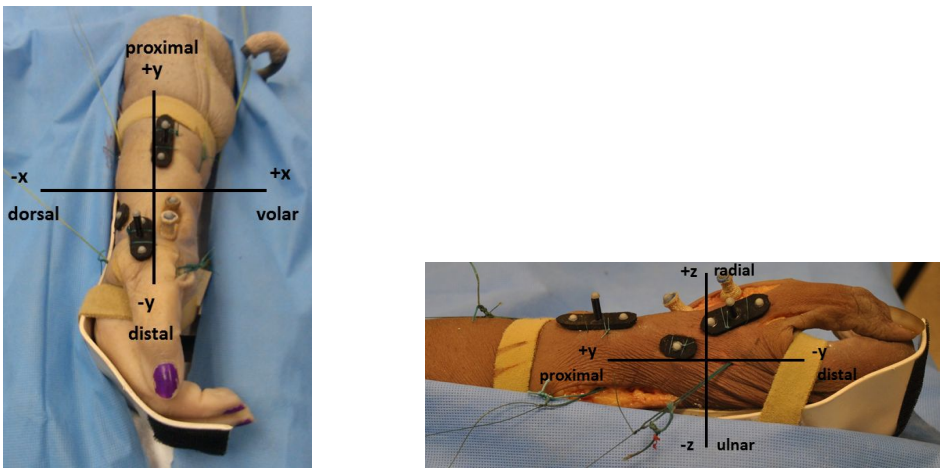

(a) (b)

Figure 3.13: Representative images of the hand showing direction of axes: (a) lateral view showing dorsal (-x)/volar (+x) and proximal (+y)/distal (-y) axes (b) posterior view showing proximal (+y)/distal (-y) and radial (+z)/ulnar (-z) axes.

positive - up/radial). (Figure 3.13) In the present study, absolute displacement of the trapezium and base of the first metacarpal was analyzed for native specimens (fully intact). Relative displacement of the trapezium and base of the first metacarpal was analyzed following single ligament sectioning.

3.3.6 Results

Native (fully intact) joint motion

Maximum displacement of the native trapezium when subject to combined extension and lateral pinch loads is shown in Appendix A in Table A.1. In extension, the trapezium displaced dorsally (neg x), proximally (pos y), and ulnarly (neg z) in 10 of 11 specimens, reaching maximum absolute displacement at maximum extension. The trapezium returned to its origin upon return to neutral position. In specimen 8, the trapezium displaced volarly (0.43 mm). In lateral pinch, the trapezium displaced dorsally, proximally, and ulnarly in 10 of 11 specimens. In specimen 10, the trapez-

ium displaced radially (0.06 mm). The two specimens that displaced differently than the others, moved less than 1mm.

Maximum displacement of the base of the first metacarpal (1st MC base) when subject to combined extension and pinch loads is shown in Appendix A in Table A.2. In extension, the 1st MC base displaced dorsally (neg x), proximally (pos y) and ulnarly (-z) in 10 of 11 specimens. In specimen 3, the 1st MC base dislaced radially (0.72 mm). In lateral pinch, the 1st MC base displaced dorsally in 6 of 11 specimens. In 10 of 11 specimens the 1st MC base displaced proximally. In 8 of 11 specimens the base displaced ulnarly. Those specimens that displaced radially moved less than 1mm. A representative plot of a single specimen when subject to combined extension and lateral pinch is shown in Figure 3.14.

A paired t-test was used to compare displacement of the trapezium with displacement

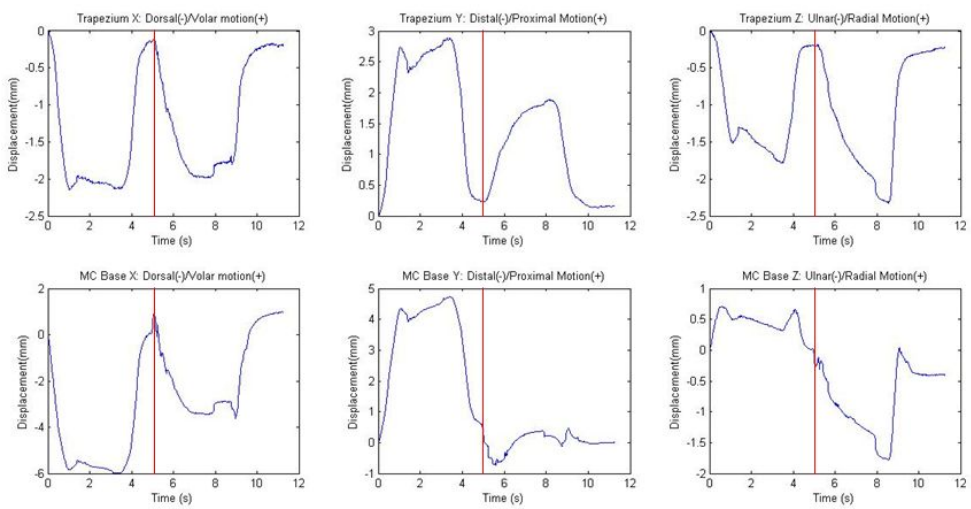

Figure 3.14: Representative plot showing motion of the trapezium and first metacarpal when subject to extension and lateral pinch loading. Note the transition from extension to pinch occurs at approximately 4.5 seconds denoted by vertical red lines.

of the 1st MC base when subject to extension and lateral pinch. A comparison of the means of maximum displacement during extension loads showed that 1st MC base dorsal ($p = 0.001$) and proximal ($p = 0.0005$) displacement is significantly greater than the trapezium, but no significant difference exists between the two bones in the radial/ulnar direction ($p=0.10$). The y-displacement data (proximal/distal) for specimen 2 was modified for pinch analysis because a review of this test showed that the specimen shifted proximally in the fixture during loading. This was confirmed by reviewing the y-displacement of the marker set on the distal radius (fixed). This marker set showed a 15 mm increase in proximal displacement when subject to pinch. Subtracting this 15 mm displacement from the y-displacement values of the trapezium and 1st MC base resulted in maximum displacements of 4.0188 mm and 2.0199 mm, respectively. A comparison of means of maximum displacement during pinch loads showed that 1st MC base dorsal ($p = 0.01$) and proximal ($p = 0.0001$) displacement is significantly lower than the trapezium, but no significant difference was found between the two bones in the radial/ulnar direction ($p=0.43$).

Maximum displacement for the native trapezium when subject to grip loads was consistent in both the x and y directions for all specimens at all grip sizes (1/2, 1, 1-1/2, 2). The trapezium displaced in the negative x-direction (dorsal) and in the positive y-direction (proximal). Motion in the z-direction moved from ulnar to radial displacement as grip size *increased*. 1/2 and 1 inch grip testing resulted in 1 of 11 specimens moving in the positive z-direction (radial). 1-1/2 inch grip testing resulted in 5 of 11 and 2 inch grip testing resulted in 6 of 11 specimens moving in the positive z-direction. Maximum displacement of the trapezium for all specimens and all grip sizes is shown in Appendix A in Table A.3.

A one-way analysis of variance (ANOVA) was completed to compare the means of maximum displacement of the trapezium across all grip sizes ($p=0.05$). No sig-

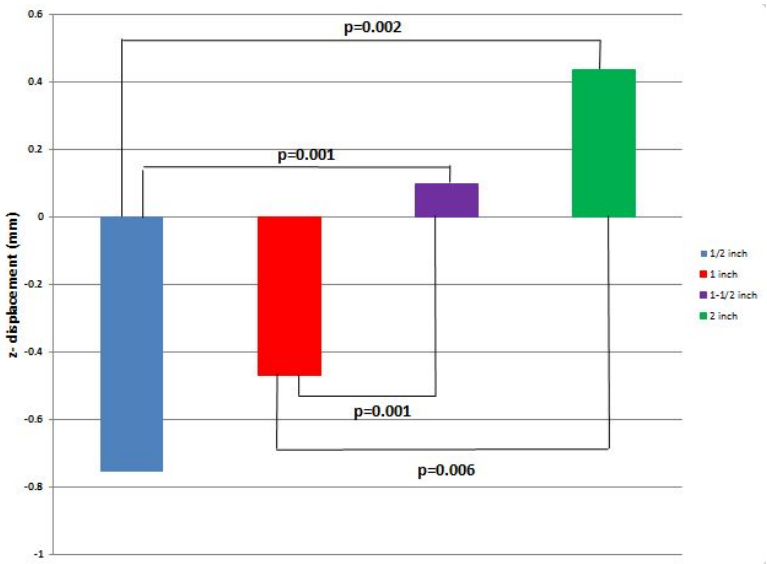

Figure 3.15: Column graph of mean displacement in the z-direction for the trapezium when subject to 1/2, 1, 1-1/2, and 2 inch grip. This graph shows significant differences between 1/2 and 1-1/2 inch, between 1/2 and 2 inch, between 1 and 1-1/2 inch, and between 1 and 2 inch grip sizes.

nificant difference was found between grip sizes for displacement in the x-direction (volar/dorsal) or y-direction (proximal/distal) ($p = 0.19$ and $p = 0.22$, respectively). A significant difference ($p = 0.04$) was found between grip sizes for displacement in the z-direction (ulnar/radial). A Bonferroni's post-hoc analysis was used for pairwise comparison with an adjusted p=0.0125. Ulnar displacement of the trapezium was significantly greater in 1/2 inch grip than 1-1/2 and 2 inch grip ($p = 0.001$ and $p = 0.002$, respectively) and significantly greater in 1 inch grip than 1-1/2 and 2 inch ($p = 0.001$ and $p = 0.006$, respectively). Means of 1-1/2 and 2 inch grip showed z-displacement was primarily in the radial direction. (Figure 3.15)

The pattern of motion for native testing when subject to grip loads was consistent for 1st MC base in the y-direction for all grip sizes. The 1st MC base moved in the positive y-direction (proximal). Motion in the x-direction trended toward dor-

sal displacement as grip size *increased*. 1/2 inch grip testing resulted in 7 of 11, 1 inch (10 of 11), 1-1/2 inch (9 of 11), and 2 inch (11 of 11) grip resulted in dorsal displacement. Motion in the z-direction moved from ulnar to radial displacement as grip size *increased*, similar to the motion of the trapezium (1/2 inch - 2 of 11; 1 inch - 4 of 11; 1-1/2 inch - 8 of 11; 2 inch - 9 of 11). Maximum displacement of the 1st MC base for all specimens and all grip sizes is shown in Appendix A in Table A.4.

A one-way ANOVA was completed to compare the means of maximum displacement of the 1st MC base across all grip sizes (p=0.05). No significant difference was found between grip sizes in the y-direction (proximal/distal) (p = 0.39). A significant difference was found between grip sizes in the x-direction (volar/dorsal) and z-direction (ulnar/radial) (p = 0.008 and p = 0.0004, respectively). A Bonferroni's post-hoc analysis was used for pairwise comparison with adjusted p=0.0125. This analysis found that the 1st MC base resulted in significantly less dorsal displacement when

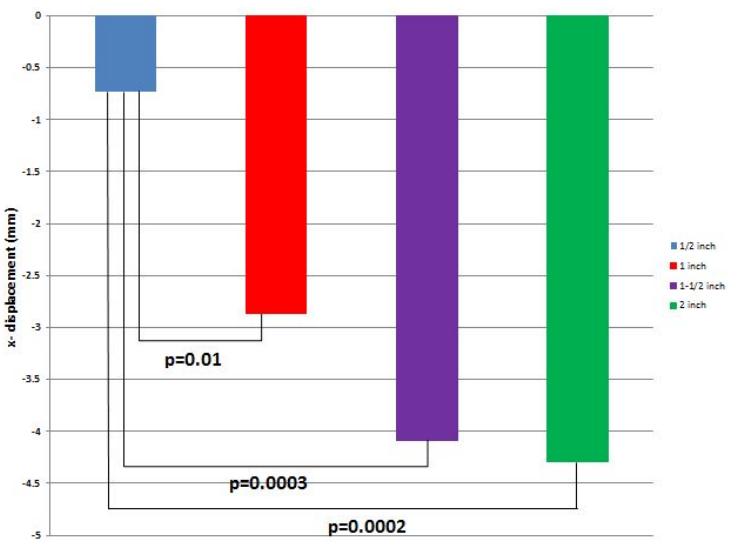

Figure 3.16: Column graph of mean displacement in the x-direction for the first metacarpal base when subject to 1/2, 1, 1-1/2, and 2 inch grip. This graph shows significantly less dorsal displacement in 1/2 inch than 1, 1-1/2, and 2 inch grip sizes.

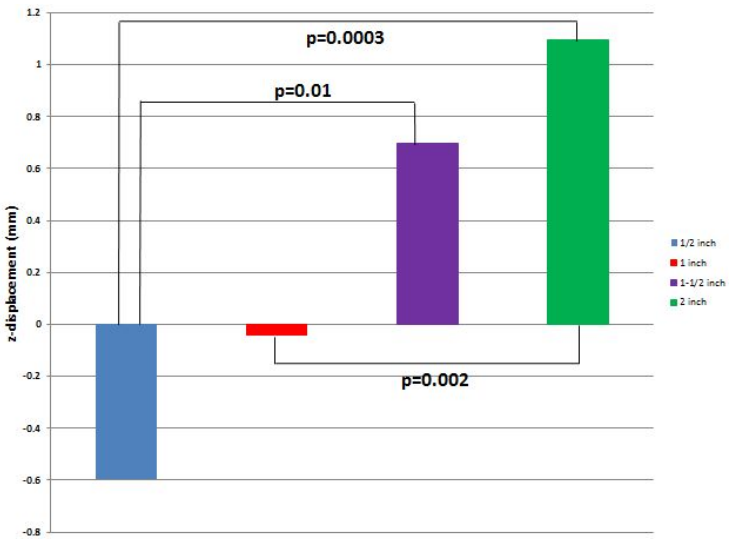

Figure 3.17: Column graph of mean displacement in the z-direction for the first metacarpal base when subject to 1/2, 1, 1-1/2, and 2 inch grip. This graph shows significant differences between 1/2 and 1-1/2 inch, between 1/2 and 2 inch, and between 1 and 2 inch grip sizes.

subject to 1/2 inch grip than 1, 1-1/2, and 2 inch grip ($p = 0.01$, $p = 0.0003$, and $p = 0.0002$, respectively). (Figure 3.16) 1st MC base ulnar displacement is significantly greater in 1/2 inch than 1-1/2 and 2 inch grip ($p = 0.01$ and $p = 0.0003$, respectively) and 1 inch grip is significantly greater than 2 inch grip ($p = 0.002$). (Figure 3.17) Means of 1-1/2 and 2 inch grip showed 1st MC base z-displacement was primarily in the radial direction. Representative plots showing trapezium and 1st MC base native bone displacement in x-, y-, and z-directions when subject to 1/2, 1, 1-1/2, and 2 inch grip is shown in Figure 3.18.

Effects of Ligament Sectioning on Joint Motion

The effects of ligament sectioning on maximum displacement of the trapezium and 1st MC base in x-, y-, and z-directions during extension, lateral pinch, and all sizes of grip loading was determined by comparison to native joint motion. As shown in Table 3.1, the first ligament sectioned from each specimen was used in this analysis.

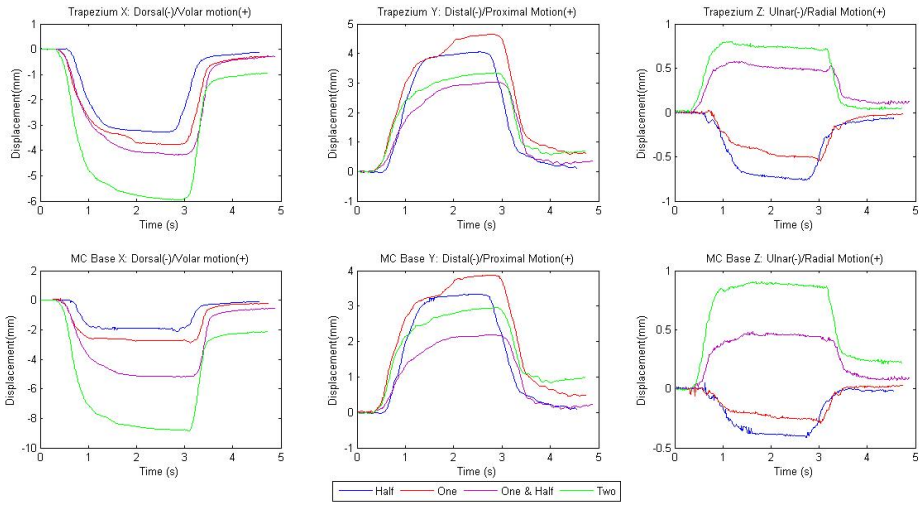

Figure 3.18: Representative plots showing trapezium and 1st MC base native bone displacement in x-, y-, and z-directions when subject to 1/2, 1, 1-1/2, and 2 inch grip.

The effects of AOL sectioning was determined using specimens 5, 7, and 11; UCL sectioning was determined using specimens 2 and 6; IML sectioning was determined using specimens 3 and 9; POL sectioning was determined using specimens 4, 8, and 10; and the effects of DRL sectioning was determined using specimen 1. Means of native joint displacement and joint displacement following ligament sectioning for all specimens in each group were used for comparison. Means of native joint displacement was subtracted from means of displacement following ligament sectioning in order to determine the effect of sectioning on joint motion. Note: Due to the small sample size used for analysis, it was not possible to obtain statistically significant results. Only clinically significant changes in displacement (defined as greater than 1mm difference) is reported.

Difference of means of maximum displacement (x, y, and z) of the trapezium when subject to extension and lateral pinch loads is shown in Appendix A in Table A.5. No significant effects on displacement of the trapezium during thumb extension are found for any ligaments sectioned. Analysis of the effects of ligament sectioning on

the trapezium when subject to lateral pinch show that sectioning the UCL resulted in decreased proximal displacement (-5.8363 mm); sectioning the IML resulted in decreased dorsal displacement (1.5679 mm), decreased proximal displacement (-2.1233 mm), and decreased ulnar displacement (1.3170 mm); and sectioning the DRL resulted in decreased proximal displacement (-2.6347 mm). Release of the IML had the greatest effect on the motion of the trapezium when subject to lateral pinch loads. (Figure 3.19)

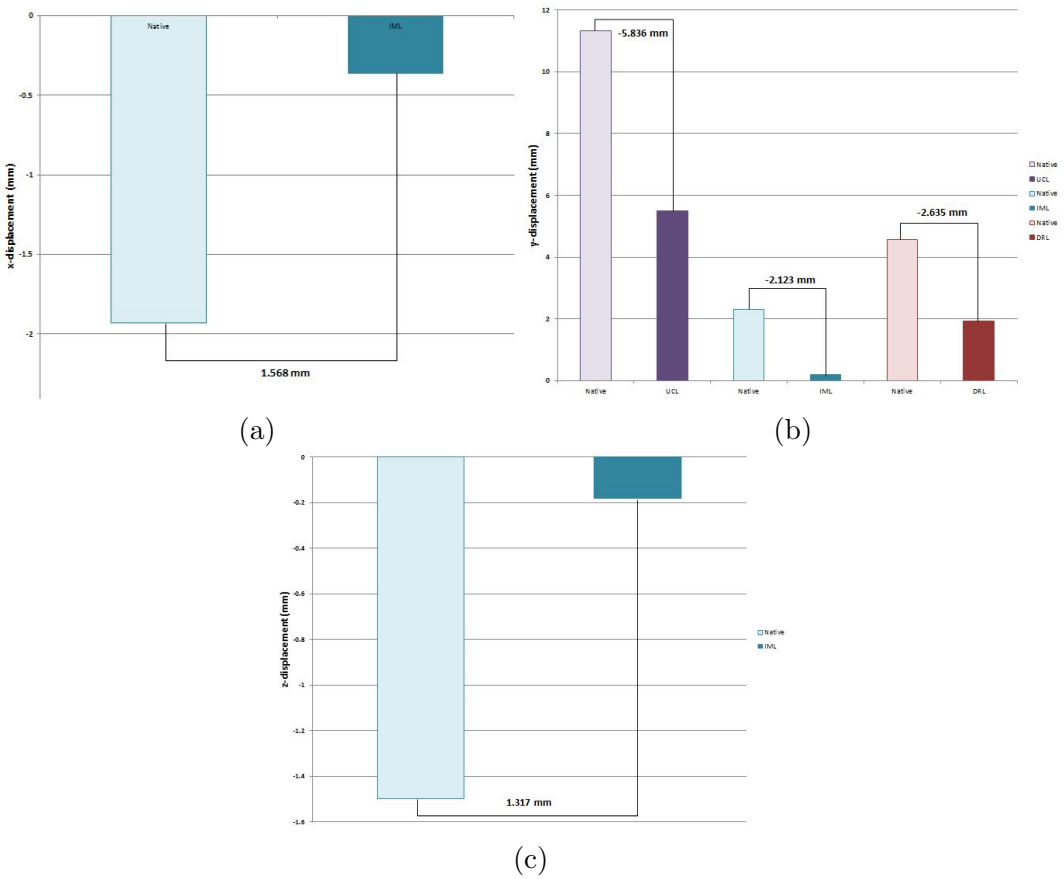

Figure 3.19: Relative displacement of the trapezium in the x-, y-, and z-directions when subject to lateral pinch. The figures show clinically significant differences in motion following sectioning of noted ligament.

Difference of means of maximum displacement (x, y, and z) of the 1st MC base when subject to extension and lateral pinch loads is shown in Appendix A in Table A.6. The effects of ligament sectioning on the 1st MC base when subject to thumb extension show that sectioning the AOL resulted in greater dorsal displacement and a shift from ulnar to radial displacement (-1.2830 mm and 1.4858 mm, respectively); sectioning the IML resulted in greater dorsal displacement and greater proximal displacement (-4.1510 mm and 3.4480 mm, respectively); sectioning the POL resulted in greater dorsal displacement, greater proximal displacement, and greater radial

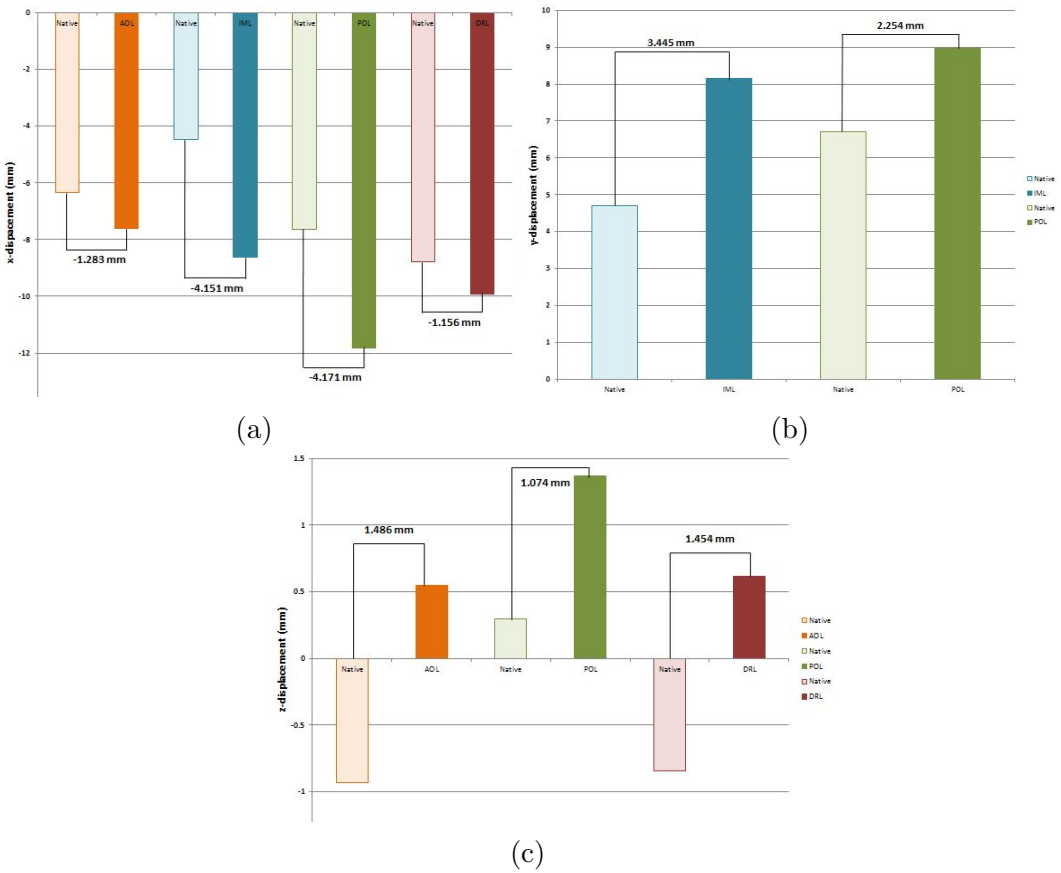

Figure 3.20: Relative displacement of the first metacarpal base in the x-, y-, and z-directions when subject to thumb extension. The figures show clinically significant differences in motion following sectioning of noted ligaments.

displacement (-4.1714mm, 2.2535 mm, and 1.0739 mm, respectively); and sectioning the DRL resulted in greater dorsal displacement and a shift from ulnar to radial displacement (-1.1560 mm and 1.4543 mm, respectively). (Figure 3.20) The POL and IML had the greatest effects on displacement of the 1st MC base when subject to thumb extension.

The effects of ligament sectioning on the 1st MC base when subject to lateral pinch loads show that sectioning the AOL resulted in decreased volar displacement and decreased distal displacement (-1.8039 mm and 1.5871 mm, respectively); sectioning the UCL resulted in increased volar displacement, a shift from distal to proximal displacement, and a shift from ulnar to radial displacement (1.8239 mm, 10.2698 mm, and 1.0200 mm, respectively); sectioning the IML resulted in decreased dorsal displacment and decreased proximal displacement (1.9661 mm and -1.2336 mm, respectively); sectioning the POL resulted in a shift from dorsal to volar displacement, a shift from proximal to distal displacement, and an increased in ulnar displacement (7.7635 mm, -2.1535 mm, and -2.5538 mm, respectively); and sectioning the DRL resulted in a shift from volar to dorsal displacement and reduced proximal displacement (-5.1198 mm and -1.2728 mm, respectively). (Figure 3.21) Release of the POL had the greatest effect on the motion of the 1st MC base when subject to lateral pinch.

Difference of means of maximum displacement of the trapezium when subject to grip loads and sectioning of the AOL, UCL, IML, POL, and DRL is shown in Appendix A in Table A.7. Analysis of the effects of ligament sectioning on the trapezium for each grip size show that for 1/2 inch grip, sectioning of the DRL caused increased dorsal displacement (-2.1414 mm) and sectioning of the IML caused increased proximal displacement (1.3733 mm). (Figure 3.22) For 1 inch grip, sectioning of the UCL caused increased dorsal displacement (-1.3511 mm). For 1-1/2 inch grip, sectioning of the POL and DRL caused increased dorsal displacement (-1.1860mm and -1.0172 mm,

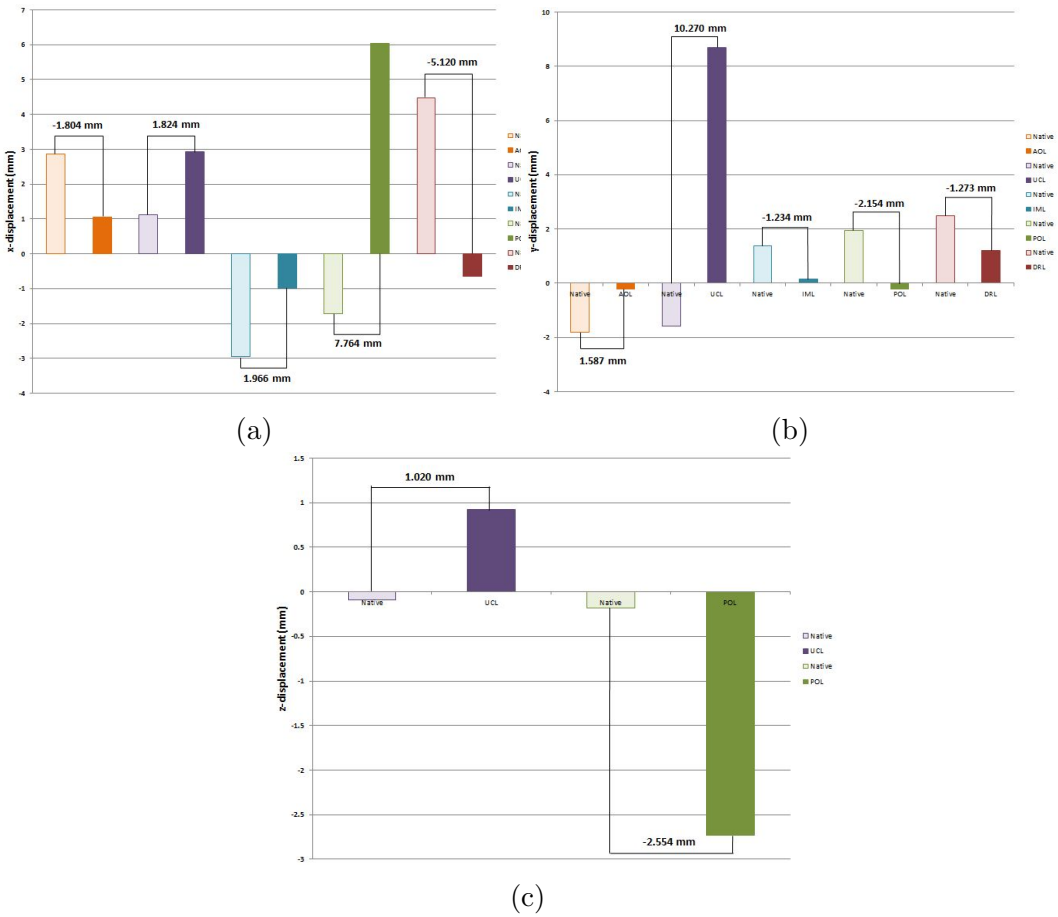

Figure 3.21: Relative displacement of the first metacarpal base in the x-, y-, and z-directions when subject to lateral pinch. The figures show clinically significant differences in motion following sectioning of noted ligaments.

respectively), but sectioning the IML caused decreased dorsal displacement (2.6728 mm). (Figure 3.23) For 2 inch grip, sectioning the POL caused increased dorsal displacement (-1.0949 mm). (Figure 3.24) Sectioning of the ligaments had the greatest effect on volar/dorsal (x-direction) displacement of the trapezium during grip loading.

Difference of means of maximum displacement of the 1st MC base when subject to grip loads and sectioning of the AOL, UCL, IML, POL, and DRL is shown in Appendix A in Table A.8. Analysis of the effects of ligament sectioning on the 1st

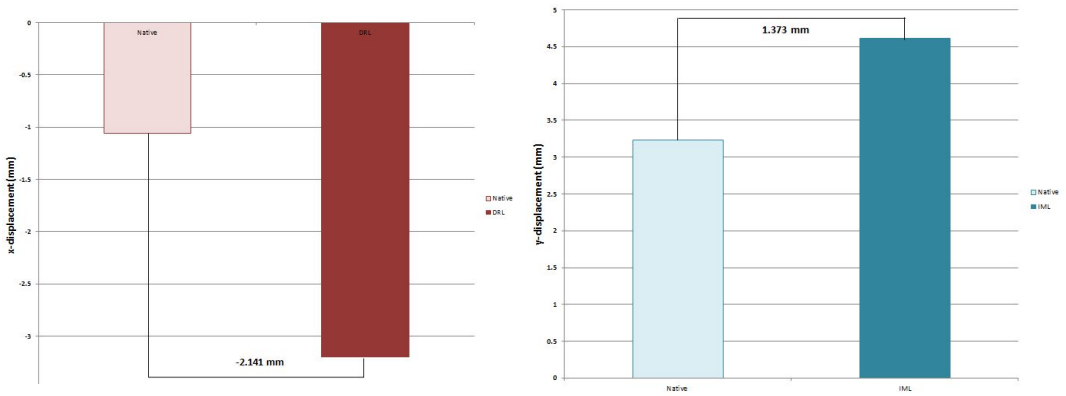

(a) (b)

Figure 3.22: Relative displacement of the trapezium in the x- and y-directions when subject to 1/2 inch grip. The figures show clinically significant differences in motion following sectioning of noted ligaments.

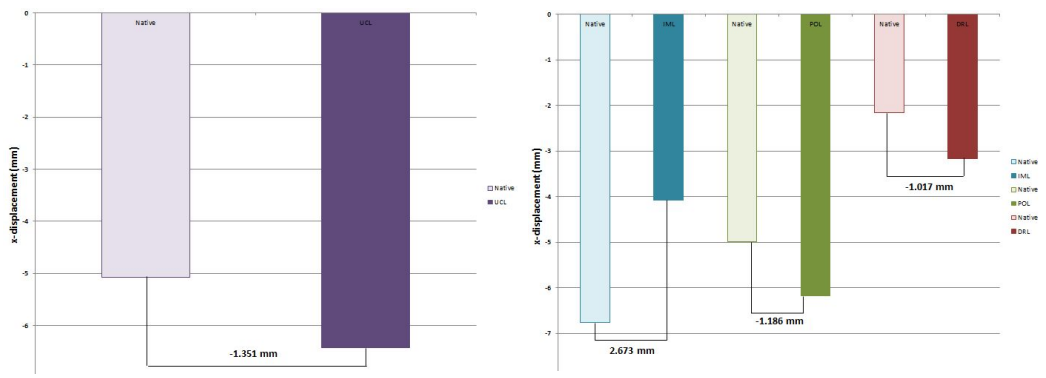

(a) (b)

Figure 3.23: Relative displacement of the trapezium in the x-direction when subject to a) 1 inch and b) 1-1/2 inch grip. The figures show clinically significant differences in motion following sectioning of noted ligaments.

MC base for each grip size show that for 1/2 inch grip, sectioning of the IML resulted in a change from dorsal to volar displacement (4.1325 mm), but sectioning of the DRL resulted in a change from volar to dorsal displacement (-5.6310 mm); sectioning of the IML and DRL resulted in increased proximal displacement (1.0724mm and 1.2580 mm, respectively). (Figure 3.25) For 1 inch grip, sectioning the AOL, IML,

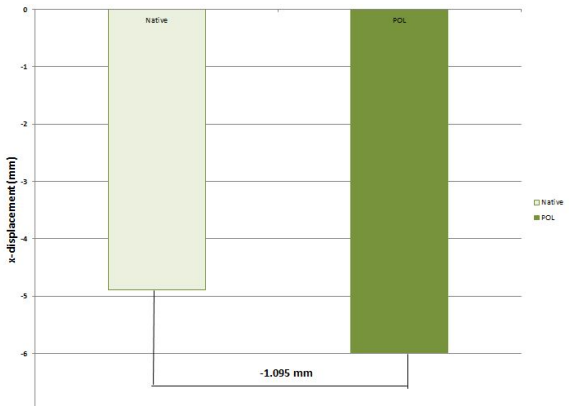

Figure 3.24: Relative displacement of the trapezium in the x-direction when subject to 2 inch grip. The figure shows clinically significant differences in motion following sectioning of noted ligaments.

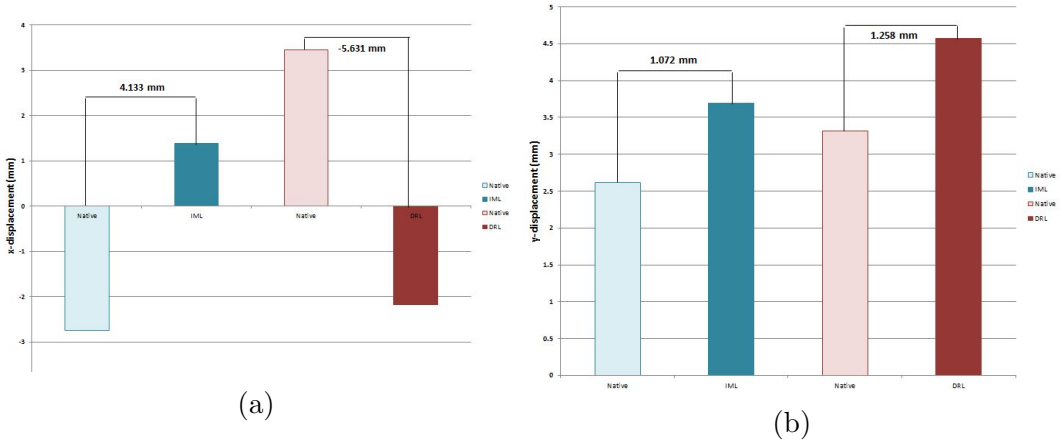

(a) (b)

Figure 3.25: Relative displacement of the first metacarpal base in the x- and y-directions when subject to 1/2 inch grip. The figures show clinically significant differences in motion following sectioning of noted ligaments.

and POL resulted in a change from dorsal to volar displacement (1.3510 mm, 1.9325 mm, and 2.6011 mm, respectively), but sectioning the DRL resulted in a change from dorsal to volar displacement (-5.5000 mm). For 1-1/2 inch grip, sectioning of the UCL and IML reduced the amount of dorsal displacement (1.2614 mm and 3.3940 mm, respectively), but sectioning the POL increased the amount of dorsal displace-

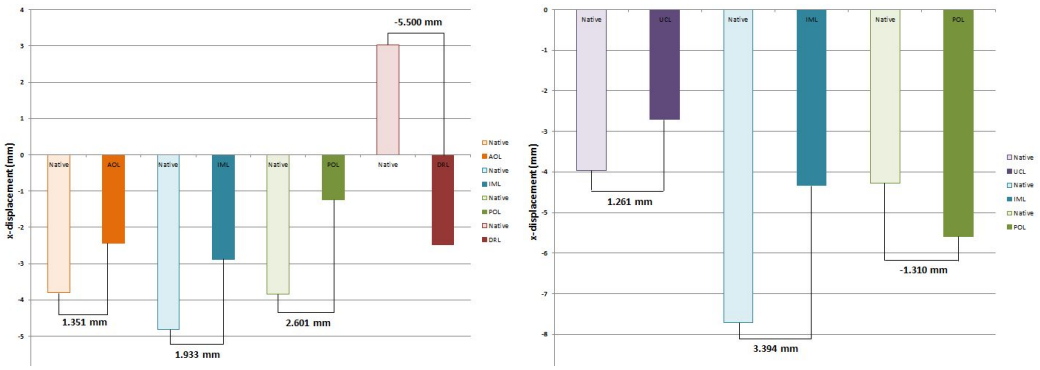

(a) (b)

Figure 3.26: Relative displacement of the first metacarpal base in the x-direction when subject to a) 1 inch and b) 1-1/2 inch grip. The figures show clinically significant differences in motion following sectioning of noted ligaments.

ment (-1.3100 mm). (Figure 3.26) For 2 inch grip, sectioning the POL resulted in an increase in dorsal displacement. (Figure 3.27) Sectioning of the ligaments had the greatest effect on volar/dorsal (x-direction) displacement of the 1st MC base during grip loading. A representative example of the effect of sectioning the AOL, UCL, IML, POL, and DRL ligament when subject to 1/2 inch grip is shown in Appendix B in Figures B.1, B.2, B.3, B.4, and B.5, respectively.

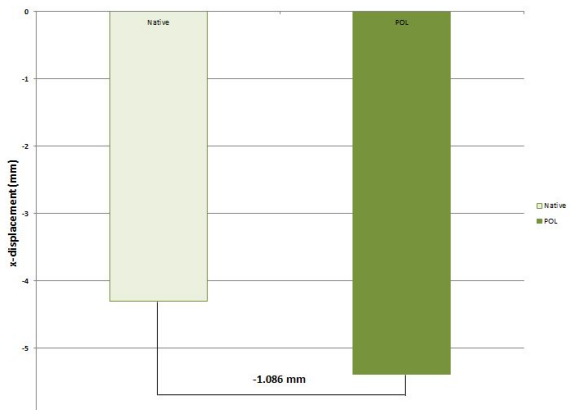

Figure 3.27: Relative displacement of the first metacarpal base in the x-direction when subject to 2 inch grip. The figure shows clinically significant differences in motion following sectioning of noted ligaments.

3.3.7 Discussion

Few studies have investigated the motion of the trapezium and first metacarpal base when subject to mechanical loading using high-resolution motion tracking markers. An early study by Strauch et al. [20] investigated the effects of sectioning the DRL, POL, AOL, and IML on the 1st MC base when an acute dorsal dislocation is applied to the thumb. Dorsal dislocation measurements of Kirschner wires placed in the trapezium and first metacarpal were taken with standard calipers. They found that the DRL provided the primary restraint to acute dorsal dislocation such as a fall on the thumb. In 1998, Van Brenk et al. [22] similarly investigated the effects of sectioning the DRL, POL, AOL, and IML when subject to acute dorsal radial loads. Dorsal radial displacement was measured using a linear variable transducer. They found that the DRL was essential in preventing dorsal radial subluxation. In 2003, Kuo et al. [51] investigated the feasibility of using surface markers for assessing motion of the TMC joint. They found that this method of motion analysis is most appropriate for measuring motion of the thumb relative to the carpal bones. In 2007, Colman et al. [23] used a three-dimensional magnetic tracking system to investigate the effects of sectioning the AOL and DRL on the 1st MC base when subject to opposition and lateral pinch. They found that the DRL was most important in preventing radioulnar translation. To our knowledge, no studies have used high-resolution optoelectronic tracking to investigate the native motion of the trapezium and 1st MC base when subject to thumb extension, lateral pinch, or grip. No studies have investigated the effects of sectioning the UCL when subject to these loads. None have studied the effects of sectioning the IML or POL when subject to lateral pinch. Additionally, no studies have investigated the effects of ligament sectioning on the trapezium and 1st MC base when subject to grip loads.

Some limitations exist in this phase of the study. First, a limited number of cadaveric

specimens was available for this study due to the high cost of cadaveric materials. While a minimum number of 11 specimens is sufficient to investigate the effects of ligament sectioning on the motion of the trapezium and first metacarpal base, only a few ligaments sectioned were repeated. A greater number of samples would be needed to establish statistical significance of the effects of sectioning each ligament. In the present study, a clinically significant measure (> 1 mm displacement) was used for analysis. Second, manual loading of the tendons was completed for all phases of this study. It is possible that a slight change in trajectory of the loaded tendons or a slight change in the magnitude of loading may effect the findings of this study. In future work, a fully automated fixture will be used for tendon loading to guarantee consistency in trajectory and magnitude of loading. Finally, in the present study, only translation of the trapezium and 1st MC base was analyzed. In future studies, we will investigate six degrees of freedom of movement for these bones.

3.3.8 Conclusions

Analysis of native joint motion showed that, in extension and lateral pinch, the trapezium and 1st MC base displace dorsally, proximally, and ulnarly. When subject to grip loads, the trapezium displaces dorsally and proximally, and shifts from ulnar (1/2 and 1 inch grip) to radial displacement (1-1/2 and 2 inch grip) as grip size increased. The 1st MC base displaced proximally for all grip sizes. As grip size increased, the 1st MC base displaced dorsally and radially. This finding is significant as most researchers believe that the 1st MC base displaces radially when subject to all pinch and grip loads. The present study reports that only in large grip motions does the 1st MC base displace radially.

Analysis of motion of the trapezium when subject to ligament sectioning is reported for thumb extension, lateral pinch, and grip loads. Ligament sectioning had no sig-

nificant effect on displacement during thumb extension. This may be due to the fact that loading of the trapezium is limited during this motion and any effects of sectioning would be negligible. In lateral pinch, the IML had the greatest effect on motion of the trapezium by reducing dorsal, proximal, and ulnar displacement. This is an interesting find since the IML is an extracapsular ligament that has no attachment to the trapezium. This finding may show that passive motion of the trapezium is greatly affected by active motion of the 1st MC base. This is supported by the result of native joint motion showing identical trajectories for the trapezium and 1st MC base when subject to lateral pinch. Sectioning of ligaments was found to have the greatest effect on volar/dorsal displacement of the trapezium when subject to grip loads. When gripping, the thumb is shifted volarly in proportion to the size of the object being held. When load is applied to the tendons, native joint motion has shown that thumb is directed dorsally. Results of this study found that sectioning of the dorsal ligaments (DRL or POL) allowed for increased dorsal displacement of the trapezium. This finding suggests that these ligaments are the primary restraint to dorsal displacement of the trapezium when subject to dorsally directed forces.

Analysis of motion of the 1st MC base when subject to ligament sectioning is reported for thumb extension, lateral pinch, and grip loads. A major finding of this study is that sectioning of the dorsal ligaments (POL and DRL) resulted in greater dorsal and radial displacement during thumb extension. This supports the theory that these ligaments are the primary restraint to dorsal displacement of the metacarpal during dorsally directed loads. [20, 22] In lateral pinch, sectioning the POL had the greatest effect on joint motion. Interestingly, sectioning the POL resulted in a shift from dorsal to volar displacement of the 1st MC base. This implies that the POL is the primary restraint to volar displacement during lateral pinch. Unfortunately, this result could not be compared to Colman et al. [23], as they did not investigate the effects of sectioning the POL when subject to lateral pinch loads. Like the trapez-

ium, sectioning of the ligaments had the greatest effect on volar/dorsal displacement of the 1st MC base. The results of grip loading support the theory the that the POL is a primary stabilizer, acting as a restraint to dorsal displacement and preventing significant volar displacement.

3.4 Tensile Mechanical Properties of TMC Joint Ligaments

3.4.1 Introduction

In the present study, the contralateral limbs of the specimens used in the motion analysis study were investigated to determine the mechanical properties of the four ligaments with origin and insertion on the trapezium and first metacarpal, respectively. The ultimate tensile load (UTL), ultimate tensile stress (UTS), ultimate strain, and stiffness of the dorsal radial ligament (DRL), ulnar collateral ligament (UCL), posterior oblique ligament (POL) and anterior oblique ligament (AOL) is reported. Morphometric analysis of the length, width, and thickness of each ligament is also reported and used for calculation of mechanical properties. This data may provide information on the relative contribution of each to the stability of the TMC joint. Results from this study are used with the findings from the motion analysis study of Section 3.3 to draw conclusions regarding the primary ligamentous stabilizers of the TMC joint. Results were also compared with results reported in literature [18, 24].

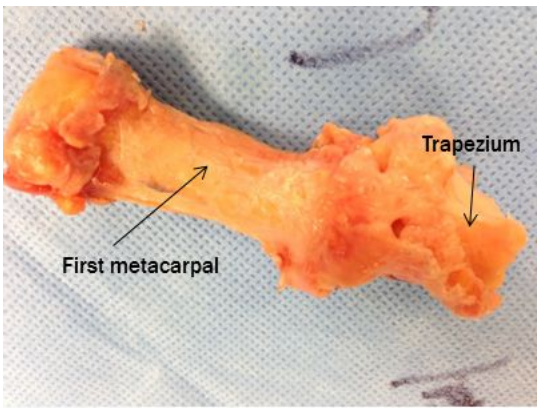

Figure 3.28: Trapeziometacarpal joint ligaments, trapezium, and first metacarpal dissected *en bloc* for morphometric analysis.

3.4.2 Morphometric analysis

The ligaments to be investigated, the trapezium, and the first metacarpal from each specimen were meticulously dissected *en bloc* from the eleven contralateral limbs of the specimens analyzed in the previously described motion analysis study. (Figure 3.28) These specimens were labeled and frozen at -20°C then thawed for 24 hours prior to use in the present study. Ligaments were identified by a trained hand surgeon as groupings of collagen fibers surrounded by an epiligamentous sheath. A digital caliper (0.1 mm accuracy) was used to measure the length, width, and thickness of each ligament when subject to passive tension. The cross-sectional area of each ligament was calculated using the equation for the area of an ellipse ($A = \pi ab$), where $a = 0.5 * \text{width}$ and $b = 0.5 * \text{thickness}$.

3.4.3 Fixture Design and Fabrication

The very small size and slippery surface of the TMC ligaments makes tensile testing of these ligaments using traditional tensile loading fixtures difficult. Immediately following morphometric analysis, the attachment to the first metacarpal was iden-

tified for each ligament and a micro-rotary tool was used to cut the bones around each ligament. Approximately 10mm of cortical bone proximal to the ligamentous attachment point. Ligamentous attachment to the trapezium was maintained. An appropriate tensile testing fixture for this study allows for direct gripping of the first metacarpal end of the ligament to the actuator of the load frame. Additionally, this fixture allows for fixation of the trapezium to the base of the load frame.

Ligament Attachment Fixture (LAF)

An important design criteria for the LAF is that the grips will be in direct contact with the first metacarpal bone/ligament complex. Therefore, this fixture should be designed to resist slippage or shear of the ligament out of the tensile grips. A number of techniques have been used to prevent slippage of ligaments and tendon from test grips, namely using serrated jaws, abrasive paper, and hydraulic or pneumatic clamps. [52, 53] These techniques, while reducing slippage, can create stress concentrations at the tissue/grip interface causing premature failure. [54] More recently, liquid nitrogren, dry ice, and thermoelectrically cooled tissue clamps have been used. [55, 56] These methods prevents slippage and tissue damage while maintaining adequate grip strength.

In order to achieve adequate shear resistance, the LAF was custom fabricated to hold dry ice (solid CO_2) with a fine grit gripping surface for added shear resistance. The body of the LAF is fabricated from 316L stainless steel with central sloped walls for grip fixture adjustment and two surrounding wells for holding the dry ice (Figure 3.29). Two pressure grips with fine grit sit on the angled surface to accommodate tissue ranging from 1mm to 20mm thick. A single pressure block is designed to fit stationary in the angled cavity and positioned near the top surface of the base. This block is attached to the grips through four springs attached to eight screws with horizontal through holes (not shown) in order to maintain position of the grips

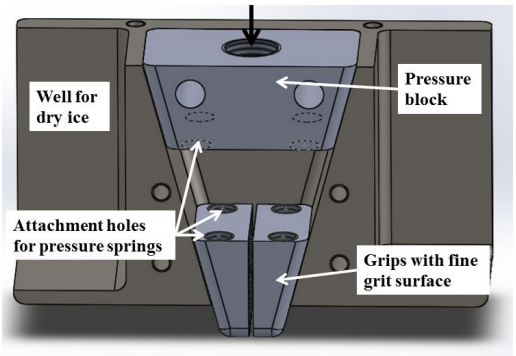

(a)

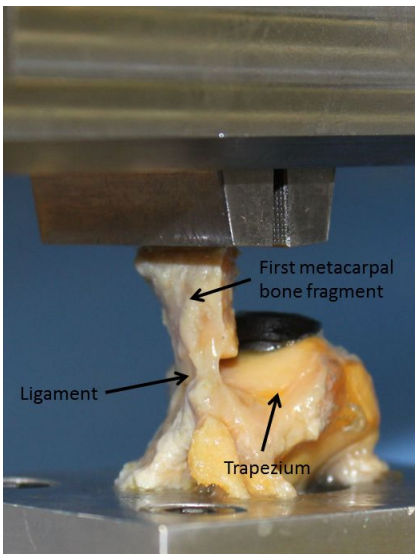

(b)

Figure 3.29: (a) Cross sectional view of ligament attachment fixture (LAF) showing grips and pressure device. (b) LAF gripping bone distal to the ligament under investigation.

within the enclosed base. A centrally placed tapped hole in the pressure block holds a set screw for manually adjusting the pressure of the grips on the soft tissue. A polyurethane box encloses the base to minimize dry ice sublimation.

Trapezial Attachment Fixture (TAF)

An important design consideration for the TAF is that all ligaments have maintained attachment to the trapezium, even those not immediately under investigation. Therefore, the TAF should not impinge upon the ligaments attached to the trapezium, and should allow for horizontal translation of the bone in order to line each of the ligaments with the vertical axis of the load frame actuator during testing.

In order to satisfy these design criteria, a TAF was custom fabricated using horizontally placed linear carriages and rails (Part 9184T51 and Part 9184T41, McMaster-Carr) positioned normal to one another to allow for full 2-dimensional translation of

the trapezium. A rail-to-load cell spacer plate was designed to attach the lower rail to the base of the load frame or frame mounted load cell. A circular pattern of 8mm through holes allow for frame/cell attachment. A linear pattern of 4mm tapped holes allows for lower rail attachment. A rail-to-rail spacer plate was designd to attach the lower carriage to the upper rail. A square pattern of 5mm through holes allows for lower carriage attachment. A linear pattern of 4mm tapped holes allows for upper rail attachment. A trapezium-to-carriage block was designed to attach the trapezium to the upper carriage. A square pattern of 5mm through holes allows for upper carriage attachment.(Figure 3.30) A 5mm radius hemisphere is placed centrally to hold the trapezium. A 4mm threaded hole placed in the center of the hemisphere allows for restraint of the trapezium along its short axis. (Figure 3.31)

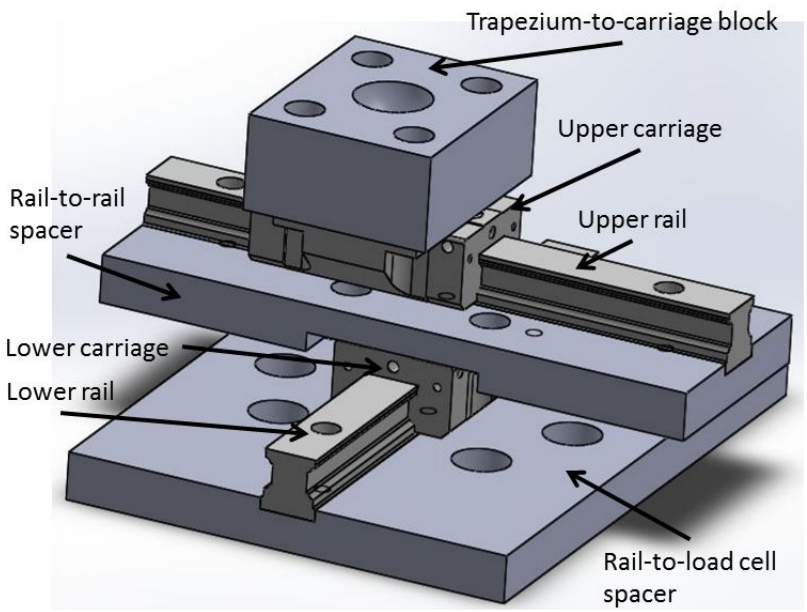

Figure 3.30: Trapezial attachment fixture (TAF) showing box for restraint of the trapezium, crossed linear rails allowing for horizontal translation of attached trapezium, and spacer plates for fixture mounting.

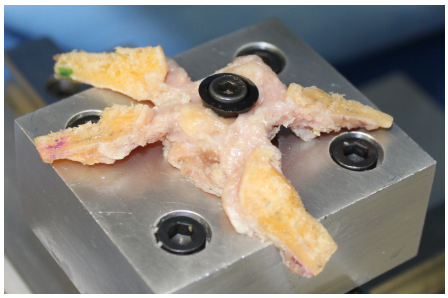

(a)

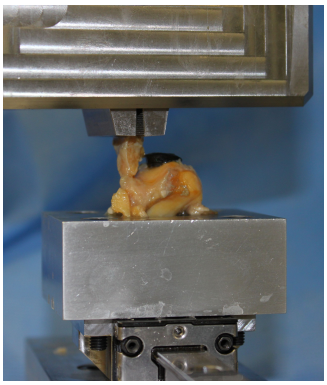

(b)

Figure 3.31: (a) TAF showing fixation of trapzium through its short axis. Figure shows ligaments/bone complexes to be tested. (b) Fixture showing the ability to position the ligament under investigation in line with test actuator using crossed linear rails.

3.4.4 Methodology

Custom made LAF and TAF fixtures were attached to a servohydraulic load frame. The LAF was used to fix the first metacarpal ligament attachment ends to the load frame actuator. The TAF was used to fix the trapezium to the base of the load frame with crossed linear rails enabling positioning of the ligament under investigation to be placed in line with the frame actuator. (Figure 3.31b) Each specimen was individually mounted to the test frame ensuring that the ligament remained in a lax position. Dry ice was placed in both wells of the base of the LAF. All specimens were kept moist before and throughout testing with physiologic saline solution at room temperature (0.9% Sodium Chloride Irrigation USP, Braun Medical Inc.).

An MTS Systems Mini Bionix servohydraulic load frame (Model 858, MTS Systems, Eden Prairie, MN) and 50lb load cell were used for testing. Specimens were pre-tensioned to a load of 0.5 lbs. A displacement controlled protocol was used to apply tensile loads at a rate of 1.5mm per second following a high strain rate methodology

by Bettinger et al. [24] It has been reported that high strain rate failure typically occurs at the midsubstance of the tissue. [57] This technique was chosen in order to obtain mechanical data on the ligament and not the bone/ligament interface. The maximim displacement of the actuator was 30mm or until failure of the ligament occurred. Tensile load and strain were measured from the MTS load cell and displacement of the actuator, respectively.

Ultimate tensile load of each ligament was defined as the peak load prior to failure. Ultimate tensile stress is defined as the ultimate tensile load divided by the cross-sectional area of the specimen. Ultimate failure strain was defined as change in length of the ligament (from actuator displacement) divided by the original length. Stiffness was defined as the load divided by the displacement at the most linear region of the load-displacement curve.

3.4.5 Results

The length, width, and thickness of the DRL, POL, AOL, and UCL ligaments are shown in Table 3.2. A one-way analysis of variance (ANOVA) was used to test for differences among each ligament type. Length, width, and thickness differed significantly among the four ligament types (p = 5.5e-8, p=0.01, p=0.002, respectively). Tukey post hoc analysis was used for pairwise comparisons. The length of the POL is significantly greater than the AOL (p=1.5e-4) and UCL (p=6.7e-6). The length of the DRL is significantly greater than the AOL (p=1.5e-4) and UCL (p=3.0e-6). The width of the POL (p=0.003) and DRL(p=3.0e-4) is significantly greater than the UCL. The POL (p=0.005), DRL (p=0.001), and UCL (p=0.01) are significantly thicker than the AOL. Boxplots of length, width, and thickness are shown in Figures 3.32, 3.33, and 3.34, respectively.

Table 3.2: Morphometric characteristics of the dorsal radial (DRL), posterior oblique (POL), anterior oblique (AOL) and ulnar collateral (UCL) ligaments.

Ligament	Length (mm)	Width (mm)	Thickness (mm)
DRL	12.8±1.5	8.4±1.3	1.5±0.3
POL	13.3±1.9	8.0±1.5	1.4±0.3
AOL	9.7±1.5	6.9±2.2	1.1±0.2
UCL	9.1±1.0	6.2±1.0	1.3±0.2
*Values are given as mean and standard deviation			

Due to the small size of the TMC joint ligaments, preliminary testing showed early failure due to embrittlement of the ligaments from the significant decrease in temperature due to the dry ice. For final testing, the dry ice was omitted from the study. No slippage of the bone was seen during testing. The ultimate tensile load, stiffness, ultimate tensile strength, and ultimate strain for the DRL, POL, AOL, and UCL ligaments are shown in Table 3.3. A one-way analysis of variance (ANOVA)

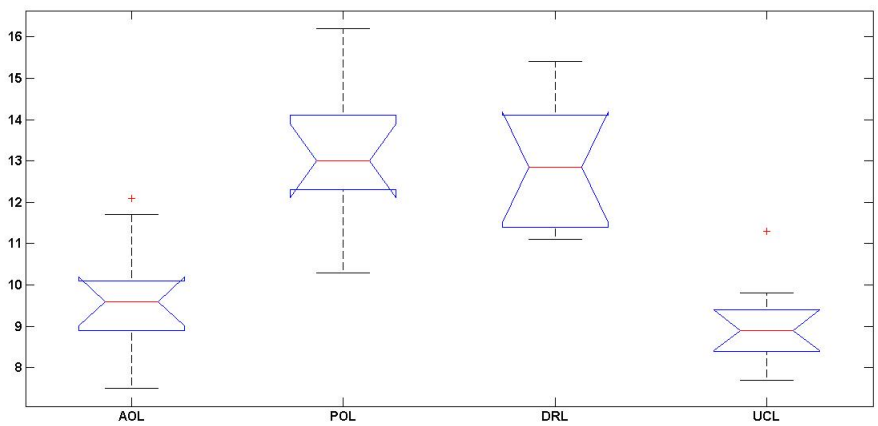

Figure 3.32: Box plot of lengths for the DRL, POL, AOL, and UCL ligaments. Red line shows the median, edges of the box are 25th and 75th percentiles, whiskers extend to most extreme points not considered outliers, outliers are denoted by red stars.

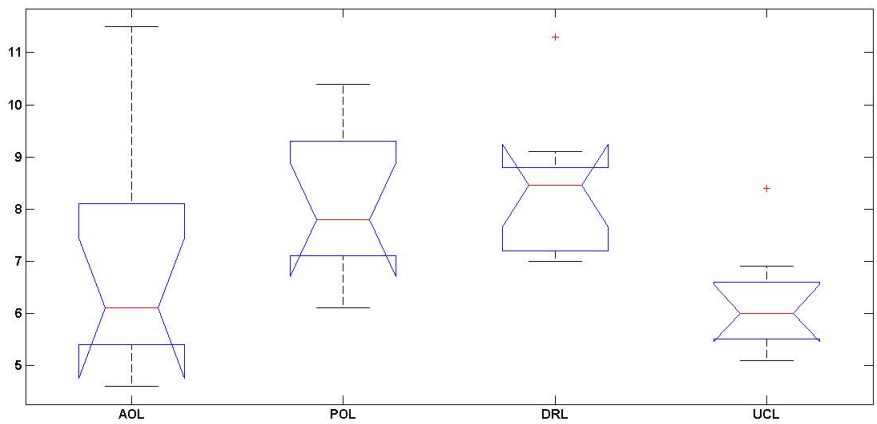

Figure 3.33: Box plot of widths for the DRL, POL, AOL, and UCL ligaments.

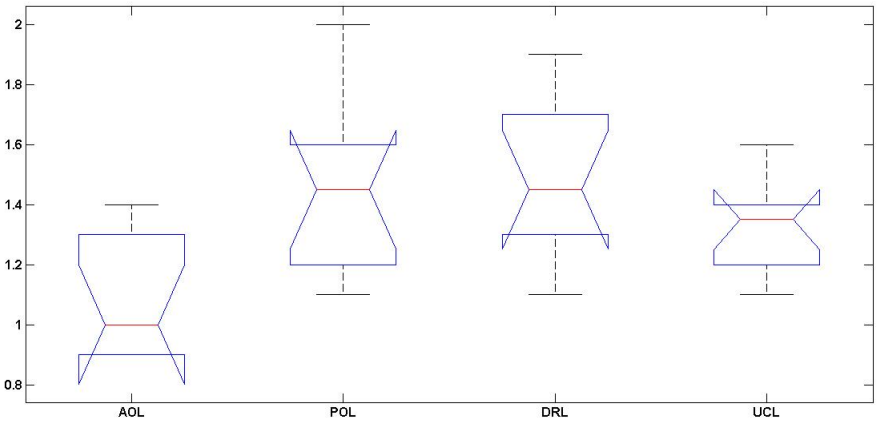

Figure 3.34: Box plot of thickness for the DRL, POL, AOL, and UCL ligaments.

was used to test for differences among each ligament type. No significant difference in ultimate tensile load, stiffness, or ultimate tensile strength was found between the groups (p=0.08, p=0.13, and p=0.39, respectively). A significant difference in strain was found between the groups (p=0.02). Pairwise comparison of ultimate load showed that POL (p=0.004) and DRL (p=0.02) are significantly greater than UCL.

Table 3.3: Mechanical test results for the DRL, POL, AOL, and UCL ligaments under uniaxial tensile loading.

Ligament	UTL (N)	Stiffness (N/mm)	UTS (N/mm^2)	Strain (mm/mm)
DRL	143.10±67.93	47.90±17.91	14.86±6.86	0.41±0.22
POL	131.13±24.74	32.70±12.87	15.49±5.28	0.44±0.13
AOL	110.94±79.05	49.16±27.06	17.41±8.08	0.36±0.15
UCL	77.24±45.58	32.72±21.03	12.05±7.16	0.71±0.44

*Values are given as mean and standard deviation
UTL - Ultimate tensile load, UTS - Ultimate tensile strength

Pairwise comparison of stiffness showed that DRL is significantly stiffer than POL (p=0.04). Pairwise comparisons of strain showed significantly higher strain in UCL than AOL ligaments (p=0.03). Load-displacement plots for DRL, POL, AOL, and UCL testing are shown in Appendix E in Figures E.1, E.2, E.3, and E.4, respectively. A representative example of a single ligament loaded to failure is shown in Figure 3.35.

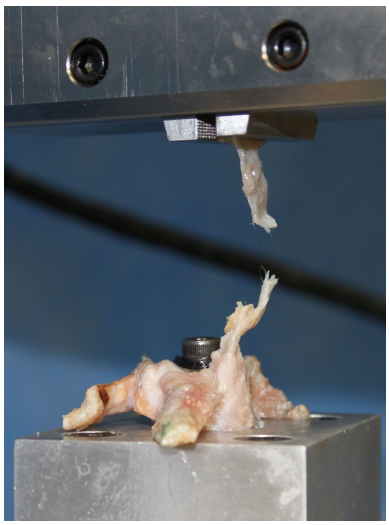

Figure 3.35: Representative example of a single ligament loaded to failure. Note that the failure point is at its midsubstance due to the high rate of loading.

3.4.6 Discussion

The present study investigated the mechanical properties of the TMC joint ligaments when subject to uniaxial tensile loading. The morphological length, width, and thickness results are compared with studies by Tan et al. and Ladd et al. [17, 18]. DRL and POL results for length compare closely with Tan et al. (12mm and13 mm, respectively). UCL, POL, and AOL results for length and all thickness results compare closely with Ladd et al. (length: 9.36mm, 13.03mm, and 9.38mm, respectively). Results for length and width of the DRL and width of the POL are greater in the present study than reported by Ladd et al. One reason for this may be due to their introduction of a previously undescribed ligament that they refer to as the dorsal central ligament (DCL). They propose that this ligament lies between the DRL and POL ligaments, but it is not possible to delineate this ligament in all subjects. In the present study, the presence of a structure that may be defined as the DCL was only present in a single subject. For this reason, the width of the DRL and POL measurements in our study may exceed that of Ladd et al. The overall width of the DRL and POL ligaments are comparable with the overall width of the DRL, DCL, and POL ligaments in their study accounting for an equivalent width of the dorsal ligament complex.

Results of mechanical testing are compared with studies by Bettinger et al. [24] and Najima et al. [21] with normal joint pathologies. Our results show inconsistencies in results for all measurable values. Najima et al. reports ultimate strengths for the AOL (8.82 N), UCL (5.46 N), IML (7.26 N), POL (10.15 N), and DRL (9.97 N) that are significantly lower than the present study and that of Bettinger et al. This may be a result of their low strain-rate testing methodology (crosshead speed 5mm/min). The DRL ultimate load we report is lower (143.1 N vs. 205.5 N) and the AOL is higher (110.9 N vs. 64.5 N) than reported by Bettinger et al. The ul-

timate stress for the DRL (14.9 N/mm^2 vs. 8.1 N/mm^2) and AOL (17.4 N/mm^2 vs. 5.8N/mm^2) is higher in the present study. The stiffness of the AOL is higher (49.2 N/mm vs. 24.1 N/mm) and the DRL is lower (47.9 N/mm vs. 78.3 N/mm) in the present study. These differences may be due to our limited sample size with high standard deviation of results. Additionally, the difference may be due to the rate of loading used in our study. We chose to standardize our test methodology by applying a constant 1.5mm/s displacement. Bettinger et al. used a constant strain rate method where the rate of loading was proportional to 25% of the gage length of the specimen. Our 1.5 mm/s loading rate would be equivalent to the rate of loading for a specimen 6mm in length in the Bettinger et al. study. Although 1.5 mm/s is considered a high strain rate loading protocol, this rate is proportional to less than 25% of the gage length of our specimens.

3.4.7 Conclusions

In the present study, the POL resulted in an ultimate tensile load comparable to the DRL ligament. Both ligaments may prove to play a significant role in stability of the TMC joint. The UCL resulted in a significantly lower ultimate tensile load than all investigated ligaments.

3.5 Histological Characterization of TMC Ligaments

3.5.1 Introduction

In the study of the human body, it is essential to understand that the structure of tissue has direct correlation to its function in the body. Ligaments connect bones to

other bones and are commonly structured with linearized collagen protein to resist high levels of tensile and bending loads. It is important to note that depending on their location and function in the body, some ligaments may maintain a more irregular structure. It has been reported that the quantity, type, and organization of collagen may be different between ligaments, even within the same joint. [58, 59, 60]

While ligaments of the knee and hip have been thoroughly characterized, limited information is available on the microscopic properties of the ligaments of the thumb. In the present study, histology of the dorsal radial ligament (DRL), posterior oblique ligament (POL), anterior oblique ligament (AOL) and the ulnar collateral ligament (UCL) is completed. This technique allows for visualization of the microstructural features of the ligamentous tissue. A qualitative analysis of collagen content and orientation, and cellular content is reported. This information will be compared with mechanical test data to determine whether a correlation exists between the quantity and structure of collagen fibers in each ligament and its ability to resist tensile loads.

3.5.2 Methodology

The trapezium and ligaments were removed en bloc from the eleven specimens analyzed in the motion analysis study. These specimens were labeled and frozen at -20°C immediately following completion of the motion study, then thawed for 24 hours prior to use in the present study. The ligament-bone complexes were fixed in neutral buffered, 10% formalin solution (100ml 37% formaldehyde, 900ml distilled water, 4.0g sodium phosphate - monobasic, 6.5g sodium phosphate - dibasic) in 50ml centrifuge tubes for a minimum of 48 hours prior to tissue processing. The DRL, POL, AOL, and UCL ligaments from each specimen were dissected from their attachment to the trapezium. Five millimeter sections were cut from the midsubstance of each ligament for histological analysis. The tissue processing, embedding, and sec-

tioning protocols have been standardized by the University of New Mexico Clinical and Translational Science Center and are briefly noted in each section.

Tissue Processing

The first step for histology of specimens is to place the tissue in histology cassettes in preparation for processing through dehydration, clearing, and infiltration with the embedding medium. For this step, a Thermo Scientific Spin Tissue Processor (Microm STP-120) takes the tissue samples through a series of graded ethanol baths to dehydrate the tissue. (Figure 3.36) This is essential because wet tissue cannot be directly infiltrated with the embedding medium. Xylene is then used to clear the tissue. Clearing is the process of removal of the dehydrant with a substance that is miscible with the embedding medium. Finally, the tissue is infiltrated with the embedding medium (paraffin wax). This protocol is defined as follows:

Dehydration:
70% ethanol for 1.5 hrs
85% ethanol for 1.5 hrs
95% ethanol for 1.5 hrs
100% ethanol for 1.5 hrs
100% ethanol for 1.5 hrs
100% ethanol for 1.5 hrs

Clearing:
50:50 (100% ethanol:xylene) for 1 hr
100% xylene for 1 hr
100% xylene for 1 hr

Figure 3.36: Thermo Scientific Spin Tissue Processor for dehydration, clearing, and infiltration of tissue for histology.

Infiltration:

Paraffin wax at 63° (Fisher Scientific, melting point 56-57°C) for 1 hr

Paraffin wax at 63° for 1 hr

Embedding

The second step for histology of specimens is to embed the specimens in the embedding medium (paraffin wax). (Figure 3.37) This process is very important because the tissue must be positioned properly depending on the orientation of the desired imaging of the sample. Additionally, the paraffin must be cleared of all air bubbles and completely encapsulate the tissue. Failure to properly embed will make sectioning (next step) difficult or impossible. The protocol used for this process is as follows:

Figure 3.37: Tissue embedding station showing hot plate (left), tissue holder cassettes (center), and paraffin wax dispenser (right).

1. Specimens are removed from the tissue processor and placed immediately on a hot plate for 1 minute (58°C) to remove excess paraffin that may be fixing the tissue to the cassette.

2. A small amount (approximately 2 drops) of paraffin is placed in the metallic tissue block. Specimens are then transferred from the cassette and placed atop the paraffin. Note: The tissue is oriented so that longitudinal sections of each ligament can be analyzed.

3. Paraffin wax is added to the block to completely encapsulate the tissue.

4. The lower end of the tissue holder cassette is placed atop the paraffin wax. Note: This will be used for mounting the specimen in the microtome for sectioning.

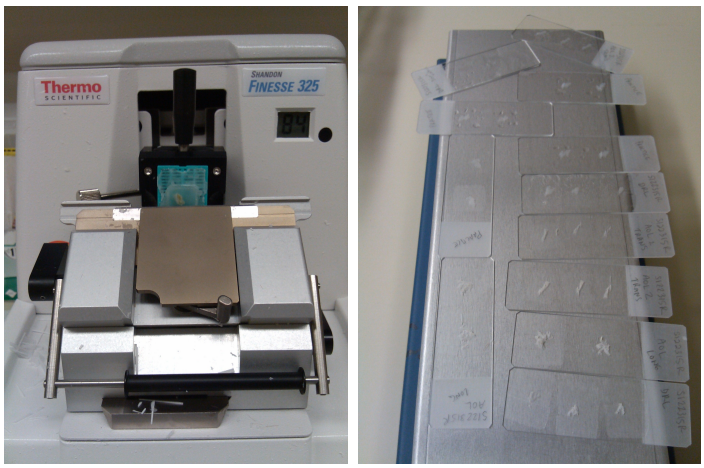

(a) (b)

Figure 3.38: (a) Microtome for tissue sectioning at 10 micron thickness. (b) Tissue sections mounted on glass slides sitting on hot plate.

5. The specimen block is placed over ice for a minimum of 24 hours to allow the wax to harden.

Sectioning

The third step for histology of tissue is to cut the samples into small sections that can be placed on slides for imaging. This process is completed with a Thermo Scientific Shandon Finesse 325 microtome - a mechanical device that allows for advancing the paraffin block while cutting with a knife mechanism. (Figure 3.38a) The protocol for this process is as follows:

1. The tissue holder cassette is removed from the specimen block and transferred to the microtome specimen holder. (Figure 3.38a)

2. The microtome knife stage is advanced toward the specimen until it touches the surface of the paraffin.

3. Adjust the section thickness. The section thickness for this study was 10 microns.

4. Advance the paraffin block toward the knife (approximately 30 rotations) until the embedded specimen is completely exposed.

5. Slowly advance the specimen while flattening the released section with a camel-hair paintbrush until the section is complete. Note: This may be repeated to form a ribbon of sequential slices.

6. Remove the sectioned tissue with tweezers and transfer it to a water bath (53°C) to remove wrinkles.

7. A glass slide is angled in the water bath and the sectioned tissue is directed toward the slide until it becomes fully attached.

8. The glass slide is removed from the water bath and placed on a hot plate for 20 minutes so the section can adhere to the slide. (Figure 3.38b)

Staining

The fourth step for histology of specimens is to stain the sectioned tissue with a variety of dyes that are chosen for their ability to stain select components of the tissue. Masson's Trichrome Stain Kit (Sigma-Aldrich, St. Louis, MO) was selected for use in the present study. This formulation is used commonly for connective tissue, staining cell nuclei black, the cytoplasm is stained red, and collagen is stained blue. The protocol as defined by Sigma-Aldrich is as follows:

1. Place glass slides into slide rack for preparation and staining.

2. Deparaffinize the sectioned tissue using a reverse embedding process (xylene to ethanol to distilled water) to allow soluble dyes to penetrate the sections.

a) 3 minutes in xylene (repeat 2 times)
b) 3 minutes in 100% ethanol (repeat 2 times)
c) 3 minutes in 95% ethanol
d) 3 minutes in 80% ethanol
c) 5 minutes in deionized water

3. Mordant in Bouin's Solution at 56°C for 20 minutes. This allows for better coloration of the final stain. (Figure 3.39a)

4. Wash slides in deionized water to remove yellow color.

5. Place in Weigert's working hematoxylin (25mL Solution A: 5g hematoxylin, 500mL 95% alcohol; 25mL Solution B: 20mL 29% ferric chloride, 475mL distilled water, 5mL hydrochloric acid) for 5 minutes. Rinse in deionized water. Hematoxylin stains the nuclei black. (Figure 3.39b)

6. Move the slide rack into Biebrich scarlet (2.7g biebrich scarlet, 0.3g acid fuchsin, 300mL distilled water, 3mL glacial acetic acid) for 5 minutes. Rinse in deionized water. Scarlet-fuchsin stains the cytoplasm red. (Figure 3.39c)

7. Move the slide rack into Phosphotungstic-phosphomolybdic acid (25g phosphotungstic acid, 25g phosphomolybdic acid, 1000mL distilled water) for 9 minutes. This allows for better uptake of the Aniline blue.

8. Move the slide rack directly into Aniline blue (2.5g aniline blue, 100mL distilled water, 1mL glacial acetic acid) for 5 minutes. Rinse in deionized water. (Figure 3.39d)

9. Move the slide rack into 1% acetic acid for 4 minutes. Rinse in deionized water. This renders the colors more delicate and transparent.

10. Dehydrate and clear.

    a) 3 minutes in 95% ethanol (repeat 1 time)
    b) 3 minutes in 100% ethanol (repeat 1 time)
    c) 5 minutes in xylene (repeat 2 times)

11. Coverslip for imaging (Cytoseal Mounting Media, Thomas Scientific)

Imaging

Imaging of the slides is completed with a Nikon Eclipse TS100 microscope mounted with a SPOT Insight 14.2 Color Mosaic camera. A 10x lens with 0.25 numerical aperture (NA), 20x lens with 0.40 NA, 40x lens with 0.65 NA, and 100x lens with 0.90 NA were used for imaging of stained tissue samples.

3.5.3 Results

Masson's trichrome stain allowed for analysis of the composition of the collagen and presence of cells in AOL, DRL, POL, and UCL tissue. All specimens were imaged

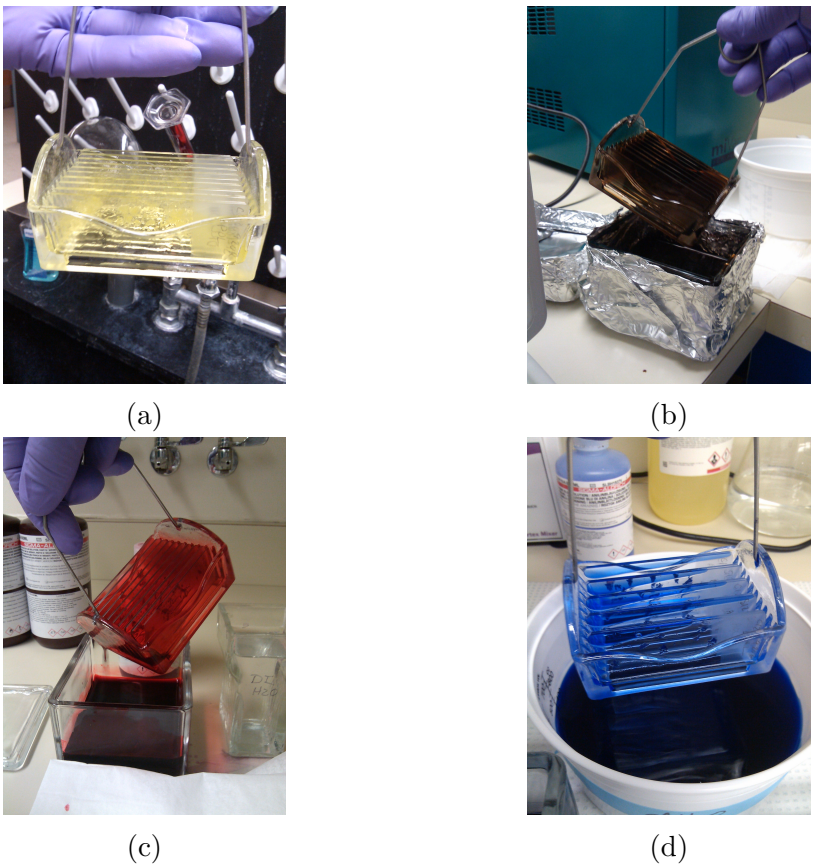

Figure 3.39: Primary steps in the staining process: (a) Mordant in Bouin's Solution for better coloration of final stain; (b) Weigert's working hematoxylin stains the nuclei black; (c) Biebrich scarlet fuchsin stains the cytoplasm red; (d) Aniline blue stains the collagen blue.

along their longitudinal axis.

The AOL consisted of a combination of disorganized (Figure 3.40a) and organized (Figure 3.40b) bundles of tightly packed collagen seen at 10x magnification. The disorganized regions displayed short, packed bundles with varied orientation. The organized regions displayed long, tightly packed crimped collagen fibers (Figure 3.40c). This non-uniformity was seen as the level of sectioned slice varied. Disorganized fibers were primarily present on the superficial layers of the tissue. The fibers be-

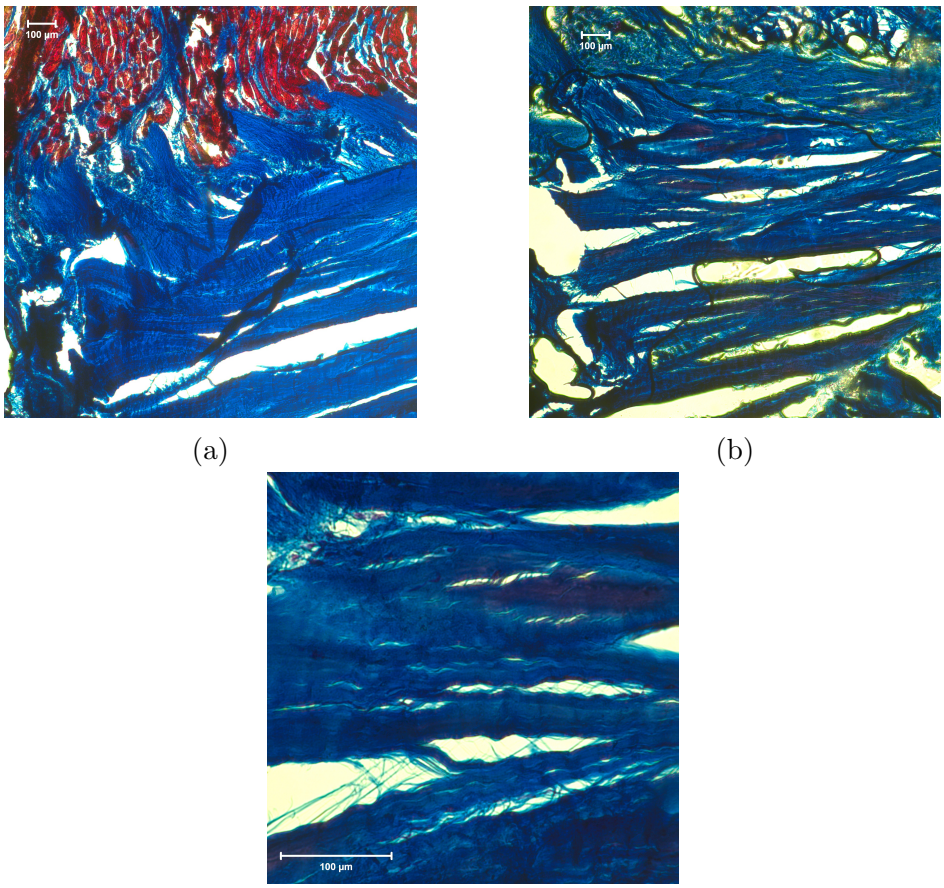

(a) (b)

(c)

Figure 3.40: Masson's trichrome stain of the AOL (a) Disorganized collagen fibers seen at 10x magnification; (b) Organized collagen fibers seen at 10x magnification; (c) Highly organized bundles of tightly packed collagen fibers seen at 40x magnification.

came more organized with increasing depth. In both, disorganized and organized regions, cellularity was limited.

The DRL consists of long, highly organized collagen fibers throughout the bulk of the tissue as seen in Figure 3.41. At 20x and 40x magnification, it is possible to visualize the long, continuous bands of fibers. At 100x, the tightly packed structure of collagen fibers is apparent. The presence of cells between bundles of collagen fibers

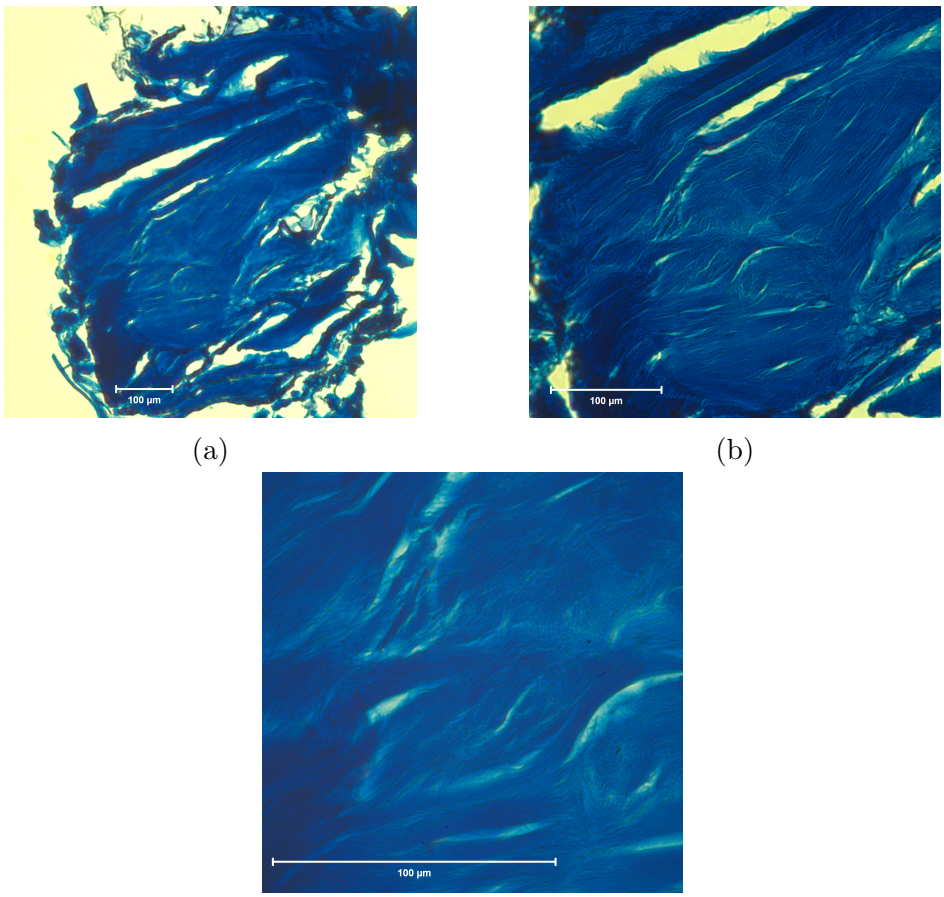

(a) (b)

(c)

Figure 3.41: Masson's trichrome stain of the DRL (a) Organized collagen fibers seen at 20x magnification; (b) Organized collagen fibers seen at 40x magnification; (c) Highly organized bundles of tightly packed collagen fibers seen at 100x magnification.

is visible under 100x magnification.

The POL consists of long, highly organized collagen fibers throughout the bulk of the tissue as seen in Figure 3.42. At 40x magnification, it is possible to visualize the long, continuous bands of crimped fibers. At 100x, the tightly packed structure of collagen fibers is apparent. The presence of cells between bundles of collagen fibers is visible under 100x magnification.

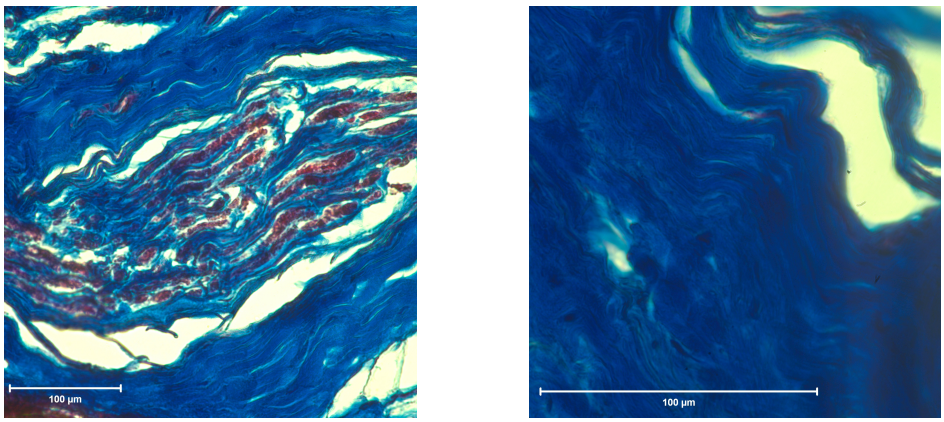

(a) (b)

Figure 3.42: Masson's trichrome stain of the POL (a) Organized collagen fibers seen at 40x magnification - note the presence of muscle in the field of view; (b) Highly organized bundles of tightly packed collagen fibers seen at 100x magnification.

The UCL consists of short, highly organized collagen fibers throughout the bulk of the tissue as seen in Figure 3.43. At 20x and 40x magnification, it is possible to visualize the short, discontinuous bands of crimped fibers. At 100x, the tightly packed structure of crimped collagen fibers is apparent. The presence of cells between bundles of collagen fibers is visible under 100x magnification.

3.5.4 Discussion

The dorsal ligaments (DRL and POL) consisted of long, continuous, and highly organized collagen fibers with the presence of cells visible under 100x magnification. Results of our study are consistent with findings by Ladd et al. [18] which found that the DRL, POL, and UCL ligaments consisted of organized, collinear bundles of collagen. We found that the UCL consisted of organized bundles of collagen fibers, but the length of these bundles were shorter than those seen in the POL and DRL.

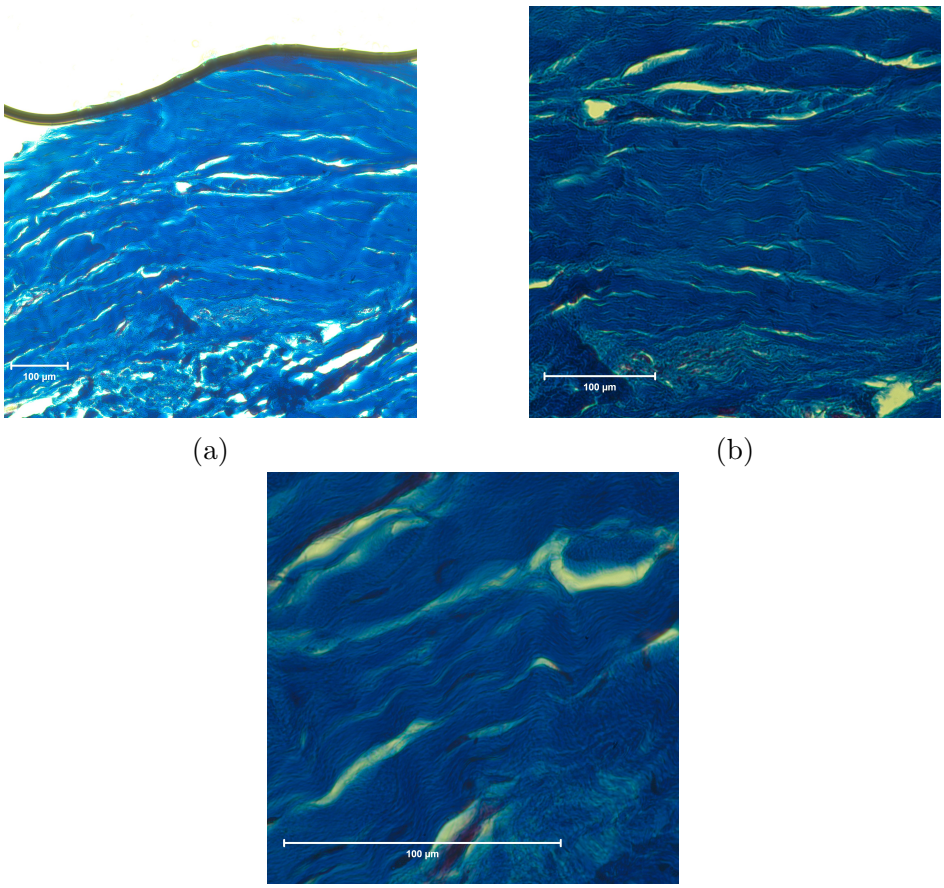

(a) (b)

(c)

Figure 3.43: Masson's trichrome stain of the UCL (a) Short, packed collagen fibers seen at 20x magnification; (b) Short collagen fibers seen at 40x magnification; (c) Short bundles of tightly packed collagen fibers seen at 100x magnification.

The most controversial finding of the present study was that the AOL consists of non-uniform groupings of disorganized and organized collagen fibers. Ladd et al. [18] reported that the AOL is a thin, disorganized structure that is not capable of static joint stability. While we agree that the ligament may not be a primary stabilizer, the organized regions may provide limited stability to the joint in the longitudinal direction of organized fibers. This may not necessarily be along the longitudinal axis of the ligament.

A limitation of the present study is that the small sample size may limit our ability to establish a proper consensus on the organizational structure of the ligaments investigated. A larger sample size may provide better representation of the consistency of protein organization. Additionally, the ligaments used for histology were used secondary to use in the high-resolution motion analysis study. The motion study required the intact specimens to be thawed for 24 hours prior to analysis and an additional 24 hours throughout the testing period. It is possible that the quality of the tissue may have been reduced due to repeat freeze/thaw cycles. This may affect our ability to identify cellular presence and collagen packing.

3.5.5 Conclusion

The long, highly organized, and tightly packed collagen of the DRL and POL provide support to the argument that the dorsal ligaments are primary stabilizers of the TMC joint. We found that the AOL consisted of non-uniform groupings of organized and disorganized collagen fibers. This ligament may provide only limited stability along the direction of organized collagen fibers. These findings contradict early reports that the AOL is of primary importance to stability of the TMC joint.

Chapter 4

Development of Surgical Treatment Options for TMC OA

4.1 Opening Wedge Trapezial Osteotomy (Early Stage Treatment)

4.1.1 Background

Experimental analysis of native joint motion of the non-arthritic hand show the trapezium and first metacarpal translate in a dorsal, proximal, and ulnar direction when subject to lateral pinch. A study of the trapezial tilt angle of normal and arthritic subjects shows that as the level of osteoarthritis increases, the tilt angle of the trapezium increases. [61] This increase in tilt angle of the trapezium may allow for the metacarpal to translate from an ulnar to radial direction, resulting in metacarpal subluxation. Increased radial loading may result in increased contact force and contact area on the dorsal radial region of the trapezium, thus increasing the severity of OA of the joint. In 2002, Kapandji and Heim [44] reported on the

technique of opening wedge osteotomy of the trapezium as a possible treatment for early TMC arthritis. They concluded that a reorientation of the trapezium may reduce the amount of subluxation of the metacarpal base in the dorsal radial direction. The following study was published in the April 2012 edition of the *American Journal of Hand Surgery.* [62]

The purpose of this cadaveric study was twofold. First, we sought to quantify the contact area and contact pressure on the trapezial surface during lateral pinch loading before and after trapezial osteotomy. Second, we sought to determine whether opening wedge osteotomy of the trapezium is successful in reducing radial subluxation of the metacarpal on the trapezium. We hypothesized that this procedure would successfully alter the contact mechanics of the TMC joint. In addition, we believed that it would reduce the amount of radial subluxation of the joint, thus addressing the two preeminent theories for initiation and progression of OA.

4.1.2 Methodology

Eight fresh-frozen human cadaveric forearms were used in this study. The wrists were X-rayed to confirm that the TMC joints were free of pathological defects including OA. Prior to preparation and testing, the specimens were stored at -25°F and thawed for 24 hours at room temperature. During preparation and testing the specimens were wrapped in gauze and irrigated with physiologic saline solution in order to avoid dehydration. The skin superficial to the flexor pollicis longus (FPL), abductor pollicis longus (APL), adductor pollicis (ADD), abductor pollicis brevis (APB) and flexor pollicis brevis/opponens pollicis (FPB-OPP) was dissected in order to expose the tendons for loading. All dissections, osteotomies, and wedge placements were performed by a trained orthopedic surgeon specializing in hand surgery.

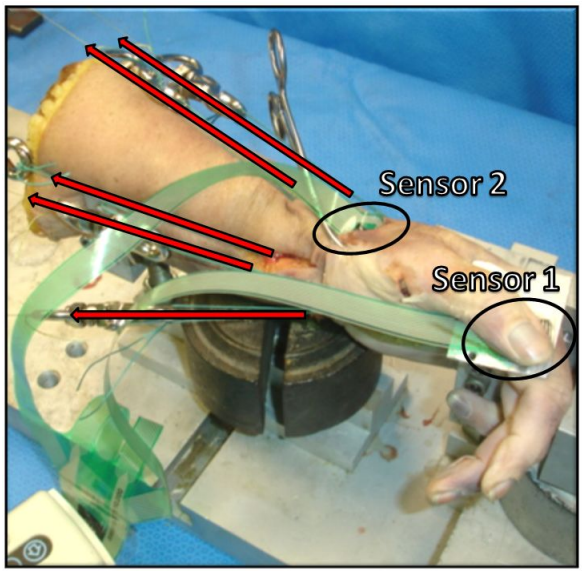

Figure 4.1: Custom built setup to restrain forearm in position to produce lateral pinch motion. Arrows indicate tendon loading trajectories. Sensor 1 is placed between the thumb and a fixed plate to monitor continuous lateral pinch. Sensor 2 is placed in the TMC joint.

The specimen was mounted in a custom-built testing device designed to keep the hand in a lateral pinch position during testing. The device restricted flexion and extension as well as radial and ulnar deviation of the wrist while allowing full motion of the TMC joint. With the arm in position, suture was attached to each exposed tendon, and load was applied in a near anatomical direction. Figure 4.1 shows a specimen in the testing fixture with arrows indicating the trajectory of the tendon loading. The tendon forces were derived from the average values reported by Cooney et al. [50]. Using a 3-dimensional analysis of static force and an assumed pinch force of 1 kilogram through the thumb pulp, Cooney et al. determined a range of values applied to each tendon along its anatomic loading position that provided information on the joint constraint forces in the TMC joint. In the present study, a 2.5kg force was applied to the FPL and APL tendons while each additional tendon had a 1.5kg force applied. Similar to the study by Cooney et al., we assumed that the FPB

and OPP act as one force vector and were thus sutured together with the applied load acting as one. Two real-time pressure sensors were used in this study (Model 6900, Tekscan, Inc., South Boston, MA). Calibration of the sensors was completed following the manufacturers specified guidelines using a Model 858 Bionix servo-hydraulic actuator to apply the calibration pressure (MTS Systems, Minneapolis, MN). This calibration test was completed to confirm that the chosen sensors were capable of detecting pressure changes in the range typically observed by the joint (60-700kPa). Each ultra-thin sensor matrix was 196 mm^2 and had 121 individual sensing elements. Sensor 1 was placed between the thumb and a plate supported by the radial side of the distal interphalangeal joint of the index finger. This sensor was monitored throughout the loading cycles to guarantee continuous lateral pinch. Sensor 2 was placed in the TMC joint space by an orthopedic surgeon. The soft tissue and joint capsule superficial to the TMC joint were incised longitudinally to allow access to the joint space. The incision size was only slightly larger than the width of the sensor to allow for insertion with minimal disruption of the joint and disturbance of the surrounding stabilizing ligaments. The sensor was folded gently and set deep in the joint using hemostatic forceps, taking care not to damage the sensor matrix. The folded sensor was then allowed to open up in the joint, and a Freer elevator instrument was used to lay the sensor flat in the joint space. Following placement of the sensor, the surrounding tissue was sutured to stabilize the sensor arm and prevent the sensor from backing out of the joint. Proper orientation of the sensor was confirmed with X-ray images from a portable c-arm. This sensor was used to measure contact area and contact pressure on the trapezial surface before and after wedge placement. Sensor placement is shown in Figure 4.1.

Each specimen was loaded and unloaded five times with contact pressure and contact area measurements taken at the TMC joint at each step for a total of 10 measurements. The sensor was divided into four equal quadrants in order to visualize any

shift in contact pressure distribution from one quadrant to another. For each unload cycle, the raw pressure (unit-less) value for each quadrant was recorded and subtracted from the corresponding raw pressure value for the load cycle. This was done to ensure that the pressure recorded during loading of the joint did not include any pressure induced in the joint due to inclusion of the sensor. Figure 4.2 illustrates the method currently described. Figure 4.2A shows a typical loaded pressure sensor while Figure 4.2B shows the corresponding reading of the same unloaded sensor for one load/unload cycle of one specimen. The unloaded reading has recorded pressure due to inclusion of the sensor in the tight joint space. The value recorded in each quadrant of the sensor in Figure 4.2B is then subtracted from the corresponding value of the same quadrant in Figure 4.2A. The final raw pressure reading for each quadrant of this load/unload cycle is: ulnar-dorsal (UD) =30-11=19, ulnar-volar (UV) =17-7=10, radial-dorsal (RD) =30-9=21, radial-volar (RV) =21-6=15. Additional

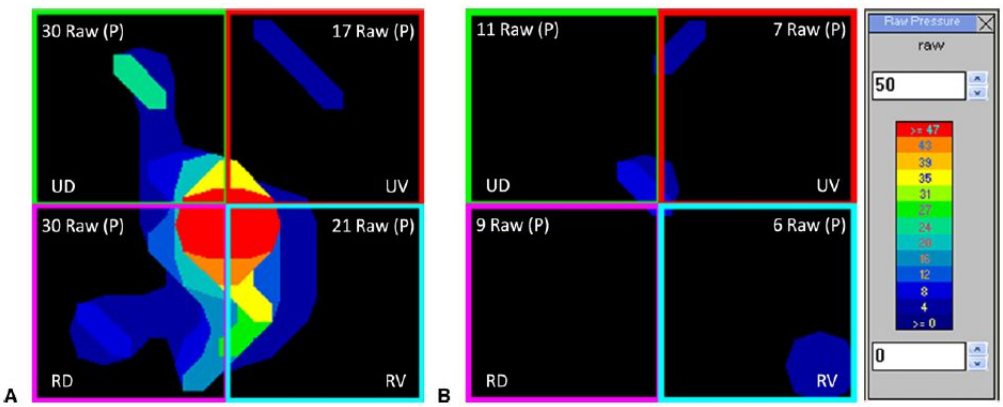

Figure 4.2: A. Typical loaded pressure sensor values. B. Corresponding unloaded pressure sensor values. Images illustrate the method used to determine the final raw pressure value for each load-unload cycle. The value recorded in each quadrant of the sensor in B is subtracted from the corresponding value of the same quadrant in A. The final raw pressure reading for each quadrant of this load-unload cycle is: ulnar-dorsal (UD) = 30-11=19, ulnar-volar (UV) = 17-7=10, radial-dorsal (RD) = 30-9=21, and radial-volar (RV) = 21-6=15. The legend shows a maximum raw pressure value of 50.

post-processing of the sensor outputs enabled collection of contact area data (cm^2) for analysis.

Anteroposterior radiographs were taken at each load/unload cycle to measure radial subluxation of the metacarpal on the trapezium (total of ten images). For each unload cycle the measured subluxation was recorded and subtracted from the measured subluxation for the load cycle to account for any induced subluxation due to frictional effects caused by the sensor in the joint space. Figure 4.3 illustrates an example of radial subluxation measurement of loaded and unloaded specimens. A line was first drawn along the lateral aspect of the first metacarpal. A second line was drawn parallel to the first line along the superior lateral aspect of the trapezium. The distance between the two parallel lines was denoted as the radial subluxation of the metacarpal on the trapezium. This procedure was performed on each radiograph and repeated 3 times by 3 of the authors independently, and the average radial subluxation for each specimen was reported in this study.

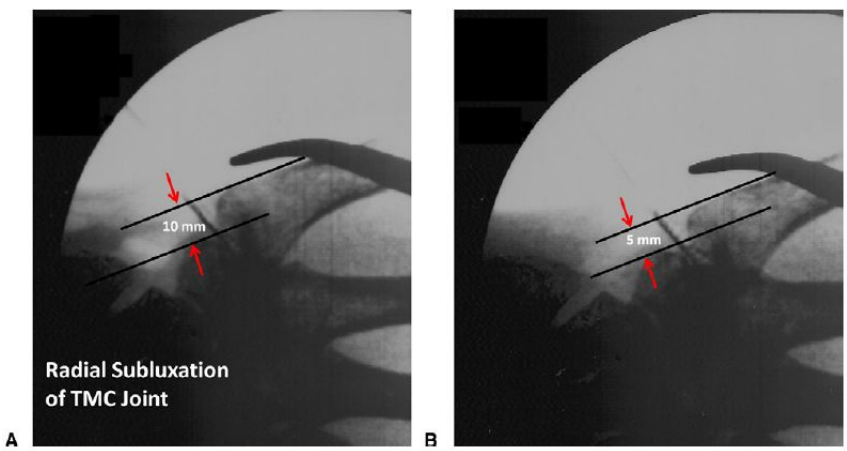

Figure 4.3: A. Typical anteroposterior radiograph showing subluxation of the metacarpal on the trapezium during loading. B. Corresponding anteroposterior radiograph of unloaded specimen.

An orthopedic surgeon then performed a dorso-lateral opening wedge trapezial osteotomy with 15° correction on each specimen. Initial bone penetration to produce the osteotomy was performed using an osteotome and mallet. The surgeon made certain not to penetrate the far cortex, leaving enough remaining bone to allow for deliberate plastic deformation in the volar region upon placement of the wedge. A 15° angle aluminum wedge was gently inserted into the osteotomy site to perform the correction. The tip of the wedge was first placed in the free space and advanced delicately to allow for gradual crack propagation, without breach of the volar cortex, until the entire wedge was positioned appropriately. The size of the wedge was chosen based on the mean value from preoperative tracing performed in a previous study. [63] Each specimen was subsequently loaded and unloaded five times with contact area and contact pressure measurements taken at each load/unload step. Moreover, anteroposterior radiographs were taken at each loading and unloading step and radial subluxations were analyzed. A paired t-test (P=0.05) was performed on the contact area, contact pressure, and radial subluxation data collected from the specimens to determine whether the opening wedge osteotomy had a significant effect on the joint characteristics.

4.1.3 Results

Our research showed that the center of force in the normal joint under lateral pinch loading was primarily located in the dorsal region of the trapezium (Figure 4.4). An average of the center of force coordinates for each bone accounting for all trials has shown the center of force to be in the radial-dorsal region in three cases, in the ulnar-dorsal region in three cases, and in the radial-volar region in two cases. Following placement of the 15° wedge, the center of force trended toward the center of the sensor but did not always deviate from its pre-wedge quadrant. In every case, addition of the wedge caused a shift in the center of force away from the dorsal

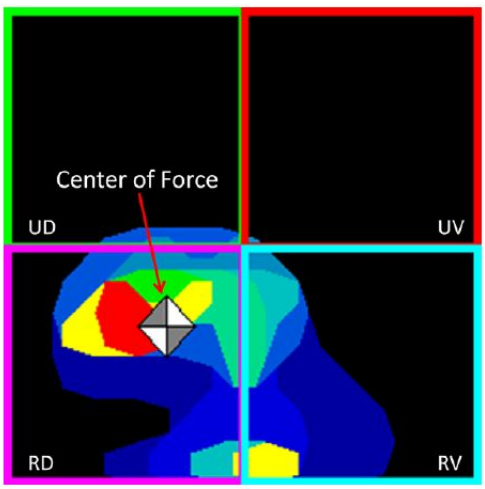

Figure 4.4: Pressure sensor showing center of force located in the radial-dorsal region of the trapezium under lateral pinch loading condition.

and/or radial edge of the sensor.

Analysis of the mean contact pressure on the trapezium showed a significant increase in the ulnar-dorsal region by 76% (p=0.030), with a slight increase in the ulnar-volar region (44%, p=0.371). Reduction in mean contact pressure in the radial-volar region (8%, p=0.632) and in the radial-dorsal region (41%, p=0.151) was not significant. Contact pressure distribution results can be found in Figure 4.5. Analysis of the mean contact area showed a significant increase in the ulnar-dorsal region from 0.05 cm^2 to 0.07 cm^2 (p=0.032) and in the ulnar-volar region from 0.003 cm^2 to 0.024 cm^2 (p=0.006). Mean contact area was not significantly decreased in the radial-dorsal region (0.12 cm^2 to 0.10 cm^2, p=0.503) or in the radial-volar region (0.085 cm^2 to 0.079 cm^2, p=0.645). Contact area results can be found in Figure 4.6. Mean radial subluxation was 4.1 mm before and 1.9 mm after the wedge osteotomy. After placement of the 15° wedge, the average radial subluxation was significantly reduced by 64% (p=0.002).

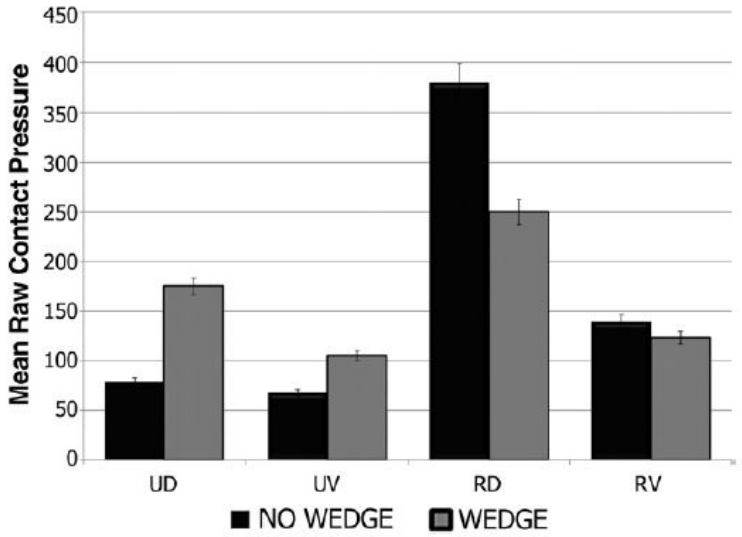

Figure 4.5: Contact pressure results showing an increase in pressure in the ulnar region and a decrease in pressure in the radial region of the trapezium after trapezial osteotomy with 15° wedge placement.

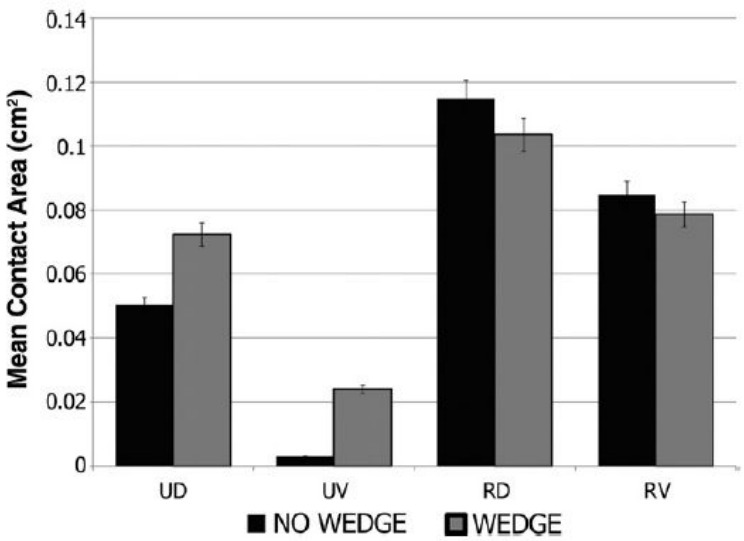

Figure 4.6: Contact area results showing a significant increase in the contact area in the ulnar region and a minor decrease in the radial region of the trapezium after trapezial osteotomy with 15° wedge placement.

4.1.4 Conclusions

In the present study, we sought to determine whether 15° opening wedge osteotomy of the trapezium would be successful in reducing radial subluxation of the metacarpal base and to quantify the shift in contact area and contact pressure on the trapezial surface under simulated lateral pinch loading. We found that the metacarpal base primarily deviated toward the dorsal and/or radial segments of the trapezium in the untreated specimens. Following an opening wedge trapezial osteotomy, the loading study was repeated, and results showed contact pressure and area distribution in the TMC joint increased ulnarly.

A study on cartilage degeneration by Momose [64] reported that the most degenerated region of the trapezium was the radial aspect. Koff et al. [30] showed that major wear occurs early in the dorsal-radial segment of the trapezium and progresses to the volar segments in late stage OA with the thickest cartilage found in the dorsal-ulnar region. Kovler et al. [65] found that the dorsal-radial aspect of the trapezium showed consistently higher levels of OA degeneration in a pooled sample of normal to highly osteoarthritic cadaveric specimens. Conversely, Pellegrini et al. [13, 14, 66, 67] reported eburnation, or hardening, of the TMC joint articular surfaces during lateral pinch loading started in the volar regions of the joint in early OA but progressed to the dorsal regions in later stages. Though the location of excessive cartilage degeneration and subsequent initiation of TMC OA has been a subject of debate for over 50 years, most authors agree that dorsal-radial degeneration and subluxation shows a high correlation to TMC joint OA.

There are some limitations to our study. In order to quantify the contact area and contact pressure across the TMC joint, it was necessary to disrupt the joint capsule for placement of the sensor. Another limitation is in our use of cadaveric

specimens with no osteoarthritic changes in the joint. Joint kinematics will likely be affected by the use of normal specimens, but they are necessary to provide a baseline for biomechanical characterization. Future studies should include a multitude of arthritic specimens with varying levels of osteoarthritis. An additional limitation was in the quantification of contact pressure on the trapezium. In order to provide meaningful results, it is necessary to calibrate the sensor in an environment identical to that used in testing. Although we followed the manufacturer guidelines for calibration, we did not use a concave structure to represent the trapezium or a convex structure to represent the metacarpal. To avoid estimations due to uncertainty in the calibration process, we quantified the percent difference in contact pressure using raw pressure measurements for each specimen before and after placement of the 15° wedge. This provides feedback on how effective the procedure was at shifting the pressure distribution across the trapezium but does not provide a numerical value for the contact pressure applied.

The present study has shown an increase in contact pressure and area in the ulnar regions of the trapezium, with a non-significant reduction in pressure in the radial regions. As described in the methods section above, we performed a static analysis of pressure and area on the trapezial surface. This analysis is capable of providing information on the initial and final states of the metacarpal on the trapezium but provides no information on how the change of geometry affects the motion of the metacarpal during loading. We know that the initial trajectory of the metacarpal during lateral pinch loading is off center and toward the dorsal and radial aspects. The change we expected with addition of the wedge was in the reduction of shear stresses due to the inability of the metacarpal to deviate toward the dorsal and/or radial edge of the trapezium. Bringing the radial surface of the trapezium closer to the metacarpal (as done by wedge placement) would theoretically reduce shear stresses, but simultaneously increase normal stresses to this region of the joint in-

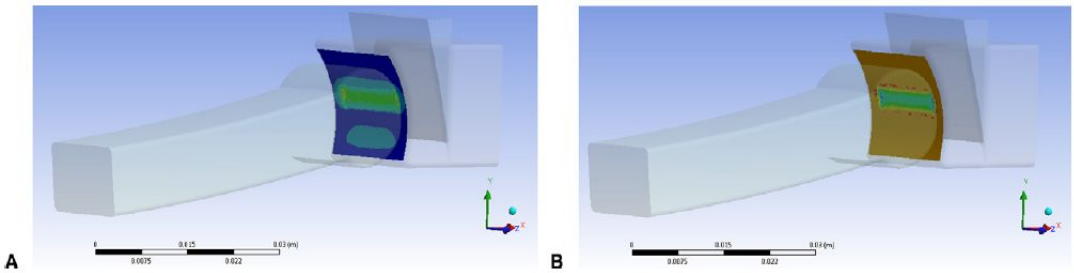

Figure 4.7: Simplified finite element model of wedge-treated specimen. A. Trapezial surface **shear** stress contour plot. B. Trapezial surface **normal** stress contour plot. Addition of the wedge moves the dorsal-radial contact surface of the trapezium closer to the metacarpal, as we observed in the experimental study.

dicated by a non-significant reduction in pressure. In order to provide quantitative data to support this hypothesis, a simplified finite element analysis was developed to compare the untreated (no wedge) joint to the treated (wedge included) joint. Results of this analysis confirmed that shear stress was decreased (0.9τ) and normal stress was increased (1.3α) on the surface of the trapezium due to inclusion of the wedge (Figure 4.7). It is uncertain which of these stresses is more detrimental to the articular surface of the joint and which of these promotes greater cartilage degeneration. Shear in the joint may promote greater initiation and propagation of OA. [61, 68] To further investigate this issue, we analyzed the position of the center of force of the loaded joint to provide information on the post-wedge trajectory of the metacarpal on the trapezium. We found that the center of force trended toward the center of the trapezium but did not always deviate from its pre-wedge quadrant. Theoretically, if the center of force remains in the dorsal-radial quadrant but moves closer to the center of the joint following wedge placement, the shear in the joint has been reduced and the potential for initiation and propagation of OA is limited. We suggest that a future patient-specific computational finite element analysis will provide greater insight into the shear and normal stresses on the trapezium before and after wedge placement.

4.2 Partial Trapeziectomy with Capsular Interposition (Advanced Stage Treatment)

4.2.1 Background

Based on results of the experimental study in Chapter 3, we found that the primary and secondary stabilizing ligaments of the TMC joint are the posterior oblique (POL) and dorsal radial (DRL) ligament. These ligaments had the greatest effect on motion of the trapezium and first metacarpal base when subject to thumb extension, lateral pinch, and grip. This research provides preliminary information for further investigation of the theory that laxity and/or damage to the primary stabilizing ligaments may predispose to TMC OA. Furthermore, damage or removal of these ligaments may result in increasing the effects of OA or joint instability if they are removed as part of a surgical technique for treatment of OA. Removal of ligamentous tissue is necessary during the commonly used technique known as total trapeziectomy. The following study proposes a surgical technique that allows the surgeon to retain ligamentous attachment of the primary and secondary stabilizers. This study is currently in review by the *British Journal of Hand Surgery*.

In the present study, we propose a surgical technique for treatment of TMC OA characterized by partial removal of the metacarpal base and partial removal of the trapezium, utilizing the joint capsule for local tissue interposition. This technique will be referred to as the partial trapeziectomy with capsular interposition (PTCI). While other authors have described partial resection of the trapezium, partial resection of the metacarpal, or the use of redundant capsular tissue for capsular interposition [69, 70, 71, 72, 73, 74], we know of none that have combined partial resection of the trapezium with resection of the base of the metacarpal or combined partial trapezium resection with local tissue interposition. We hypothesize that re-

moval of the irregular arthritic surface of the metacarpal base in conjunction with distal trapezium resection may lead to less hard and soft tissue disruption and therefore less metacarpal subsidence under load when compared to complete trapezium resection. The first aim of this study is to report on clinical results of PTCI in a short-term (6 month) retrospective chart review of clinical cases from 2003-2009 and medium-term patient follow-up (40-80 months). The second aim of this study is to compare this technique with the commonly used total trapeziectomy technique, both utilizing capsular interposition in a matched-paired cadaveric biomechanical study. A custom-made software tool measures thumb metacarpal to scaphoid distance in antero-posterior radiographs of key-pinch loaded specimens. We hypothesize that the PTCI group will result in less thumb subsidence when compared to the total trapeziectomy group.

4.2.2 Methodology

Surgical Technique

Exposure of the TMC joint begins with elevation of the periosteum and abductor pollicus longus tendon from the base of the metacarpal. After joint exposure, approximately 2mm of bone is resected from the base of the metacarpal and 2 mm of bone is resected from the distal aspect of the trapezium. (Figure 4.8a) Local, redundant capsular tissue is utilized for interposition. (Figure 4.8b) The joint is closed by reefing, or securing with suture, the periosteal flap and abductor pollicus longus tendon on the dorsal surface of the first metacarpal. No internal fixation is utilized. The thumb is splinted post-operatively for four weeks follow by home or supervised occupational therapy.

(a) The proximal two millimeters of the base of the first metacarpal are excised using a micro sagittal saw.

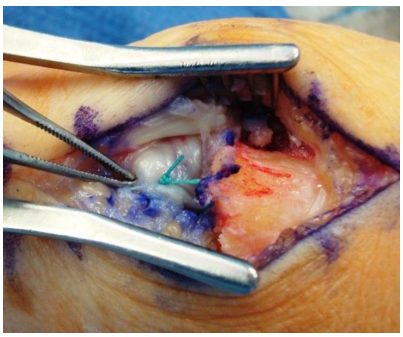

(b) Two non-absorbable sutures between the trapezium capsule and the deep capsular tissue.

Figure 4.8: Surgical technique for partial trapeziectomy with capsular interposition.

Clinical Subjects

Institutional approval from the IRB, informed consent, and HIPPA consent were obtained (HRRC, 10-563). Inclusion criteria were all patients over the age of 18 who presented with osteoarthritis of the TMC joint treated surgically with PTCI by the senior surgeon at a single institution over a 6 year period (January 2003-December 2009). The main surgical indication was pain localized to the TMC joint not alleviated by non-operative treatment including rest, anti-inflammatory medication, splinting, or injections. A total of 62 patients met these criteria. Exclusion criteria were bilateral thumb basal joint arthroplasty, the presence of injury or other upper extremity disorder including rheumatoid arthritis, and lack of pre-operative and post-operative pinch and grip measurements. 25 patients were excluded based on these criteria. 37 patients were included in the study.

Clinical Evaluation

Data were collected via a retrospective chart review on all eligible patients (n=37). These included demographics, handedness, side of surgery, post-surgical complications, as well as pre- and post-operative grip and key pinch strength values collected

Table 4.1: Group characteristics from short-term retrospective chart review.

Number of patients	37
Male/female	11/26
Operative side, right/left	16/21
Handedness, right/left	2/35
Average age at surgery, years	58
Average follow-up, months	6.3

at a mean duration follow-up of 6 months. (Table 4.1) Assessment of short-term pinch and grip strength outcomes were completed utilizing a Students t-test. Potential complications are reported and the complication rate is calculated.

All patients were invited, via phone call, to return for a follow-up visit to assess medium-term outcomes. The patients were asked to complete a Disabilities of the Arm, Shoulder and Hand (DASH) questionnaire and submit to a physical examination including grip and pinch strength (treated and contralateral limb), first web measurement (measured in centimeters, from the most ulnar aspect of the thumb IP crease to the most radial aspect of the mid palmar crease), and MCP joint range of motion. DASH questionnaires are scored based on disability/symptoms (pain) and performance. All physical examinations were completed by one hand fellow and one chief resident assigned to the study. Mean values for first web-space measurements and MCP range of motion are compared to the contralateral limb using a Students t-test. The difference in preoperative key pinch and grip strength and that measured at the medium-term clinical follow-up appointment was also calculated and compared using a Students t-test. Mean DASH score is reported.

Biomechanical Cadaveric Testing

Nine matched pairs of fresh frozen cadaveric hands were utilized for this study. Each pair was randomized to the total trapeziectomy (TTCI) or partial trapeziectomy

(PTCI) group. Capsular tissue was used as interposition for both techniques. Randomization controlled for inherent differences in strength and stability between hands in any given pair. Group assignment was performed utilizing a computer generated random number program. All TMC joints were imaged prior to commencing the study to ensure the joints were free of degenerative changes.

A custom aluminum jig was fabricated to stabilize the hand with the thumb in the lateral (key) pinch position. Utilizing a braided suture locking stitch, the flexor pollicus longus (FPL), adductor pollicus (ADD), opponens pollicus (OPP)/flexor pollicus brevis (FPB), abductor pollicus longus (APL), and abductor pollicus brevis (APB) tendons were dissected, tagged, and fixed with acrylic thread for physiologic loading. We loaded these six muscles in line with the direction of pull of the muscle fibers as described by Cooney and Chao. [50] The FPL and APL were each loaded with 2.5kg. The ADD/OPP/FPB group was loaded with 3kg. The APB was loaded with 1.5kg. (Figure 4.9) As a reference for relative metacarpal motion and

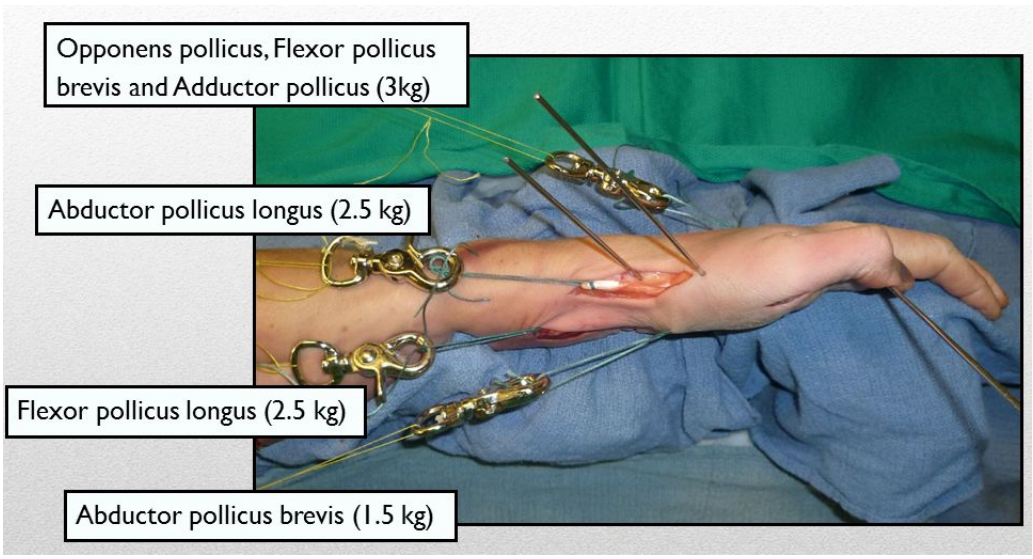

Figure 4.9: Specimen placed in custom-built fixture to restrain the hand for anatomical loading of tendons to simulate lateral pinch.

metacarpal to scaphoid distance, we utilized two K-wires which we securely embedded into the bone of the first metacarpal base and distal scaphoid. The K-wires were placed free of soft tissue tethers. We loaded all thumb joints prior to performing the surgical procedure to evaluate group similarity in metacarpal to scaphoid distances prior to bone resection. All surgical procedures were then performed by a fellowship-trained hand surgeon following the outlined procedure for partial trapeziectomy with capsular interposition. The procedure for total trapeziectomy has been frequently described based on a technique by Gervis published in 1949. [75] Modification to the total trapeziectomy technique was made in order to include the capsular interposition technique outlined in this manuscript. Antero-posterior radiographs were taken of the untreated and treated wrists in three loaded and three unloaded positions giving a total of twelve fluoroscan images per specimen. To account for differences in magnification between images, a 19.1mm diameter metal sphere was used as a calibration marker. A custom-designed software tool utilizing the Hough Transform model was developed to calibrate the linear distance between K-wire ends to the diameter of the spherical marker. [76]

Statistical Analysis

We performed a power analysis prior to conducting the biomechanical study utilizing 2 mm as the clinically significant difference in metacarpal to scaphoid distance based on previously described functional analysis. [30, 77] A sample size of eighteen or nine matched pairs was adequate to detect a 2mm difference between surgical groups with α=0.05 and β=0.20. In order to evaluate inter-rater reliability in the cadaveric study, three readers independently measured all radiographic images. Measurements were obtained independently by each reader and blinded to the measurements taken by the other readers. We first evaluated the data for systematic bias across readers and across trials using a three-way analysis of variance (ANOVA); significance was set at $p \leq 0.05$. If no bias was encountered, we planned to average measurements across

trials and reviewers utilizing a Students t-test for comparison of relative metacarpal to scaphoid means in the native specimens and between the TTCI and PTCI groups. If bias was encountered we planned to analyze the data for each individual reviewer and then compare this mean across the three reviewers utilizing a three-way ANOVA.

4.2.3 Results

Clinical Results

Thirty-seven patients met the inclusion criteria and were included in the short-term retrospective review. There were no significant differences found between pre- and post-operative grip strength (p=0.45; 24.6±10.5kg and 24.4±8.6kg, respectively) and pinch strength (p=0.16; 5.7±3.3kg and 5.1±1.6kg, respectively). The overall complication rate was 5.41% (2 patients). The first patient developed a septic wrist with osteomyelitis of the distal ulna three months postoperatively. This was successfully treated with irrigation and debridement followed by six weeks of intravenous antibiotics. The second patient developed proximal migration of the first metacarpal with resultant impingement on the trapezial remnant. This was successfully treated with revision metacarpal excision. The results of the retrospective review are summarized in Table 4.2.

Fifteen patients returned for medium-term follow up (42% of the qualifying patients). Patient characteristics are shown in Table 4.3. The mean follow up period was 51 months. A statistically significant difference was found when comparing pre-operative to medium term post-operative grip strength. (p=0.01; 25.3±10.1kg and 32.0±12.8kg, respectively) No significant difference was found between pre-operative and medium term post-operative pinch strength. (p=0.14; 5.7±3.4kg and 7.2±2.7kg, respectively) Contralateral limb grip and pinch strength were measured (36.3±14.5kg and 9.3±4.6kg, respectively). Grip strength averaged 69.9% of contralateral strength

Table 4.2: Results of short-term retrospective chart review.

	Pre-operative	Post-operative	P-value
Grip strength, kg	24.6±10.5	24.4±8.6	0.45
Pinch strength, kg	5.7±3.3	5.1±1.6	0.16
Complication rate = 5.41% (2 patients)			
Patient 1: Septic wrist w/osteomyelitis of the distal ulna 3 months post-operatively successfully treated with irrigation and debridement followed by six weeks of intravenous antibiotics.			
Patient 2: Proximal migration of the first metacarpal with impingement on the trapezial remnant; successfully treated with revision metacarpal excision and capsular interposition.			

pre-operatively and increased to 88.2% at medium-term follow-up (p=0.02; 18.3% increase). Pinch strength averaged 61.3% of contralateral strength pre-operatively and increased to 77.1% at medium-term follow-up (p=0.27; 15.8% increase). No significant difference was found in first web space distance between treated and contralateral limb (4.6±0.7mm and 4.8±0.6mm, respectively). No significant difference was found in MCP flexion range of motion between treated and contralateral limb (43.3±12.5° and 46.0±13.9°, respectively). Excellent DASH scores were reported (median = 4.17 w/range 0.83-15.52)). No additional complications were reported. A typical radiograph of a patient pre-operatively and at two years following the PTCI procedure is shown in Figure 4.10. The results of the medium-term clinical follow-up

Table 4.3: Group characteristics from medium-term clinical follow-up.

Number of patients	15
Male/female	6/9
Operative side, right/left	4/11
Handedness, right/left	14/1
Average age at surgery, years	59
Average follow-up, months	51

Figure 4.10: A. Preoperative and B. 2 years postoperative follow-up x-ray on a patient treated with partial trapeziectomy with capsular interposition. Note the removal of the articular surfaces of the trapezium and first metacarpal.

group are summarized in Table 4.4.

Table 4.4: Results of medium-term clincal follow-up. (51 months)

	Pre-operative	Post-operative	P-value
Grip strength, kg	25.3±10.1 (69.9%)*	32.0±12.8 (88.2%)*	0.01
Pinch strength, kg	5.7±3.4 (61.3%)*	7.2±2.7 (77.1%)*	0.14
	Short-term	Post-operative	P-value
Pinch strength, kg	5.5±1.7	7.2±2.7	0.02
	Post-operative	Contralateral	P-value
First web space, cm	4.6±0.7	4.8±0.6	0.18
MCP range of motion, deg	43.3±12.5	46.0±13.9	0.58
*percentage of contralateral limb			
Dash score (median) = 4.17			
Complication rate = 0% (No complications reported)			

Biomechanical Test Results

We found no main effect or interaction between reviewers (p=0.98) or between trials (p=0.90). Bland-Altman plots showing favorable correlations between each reviewer are shown in Figure 4.11. We averaged across trials to illustrate the lack of measured

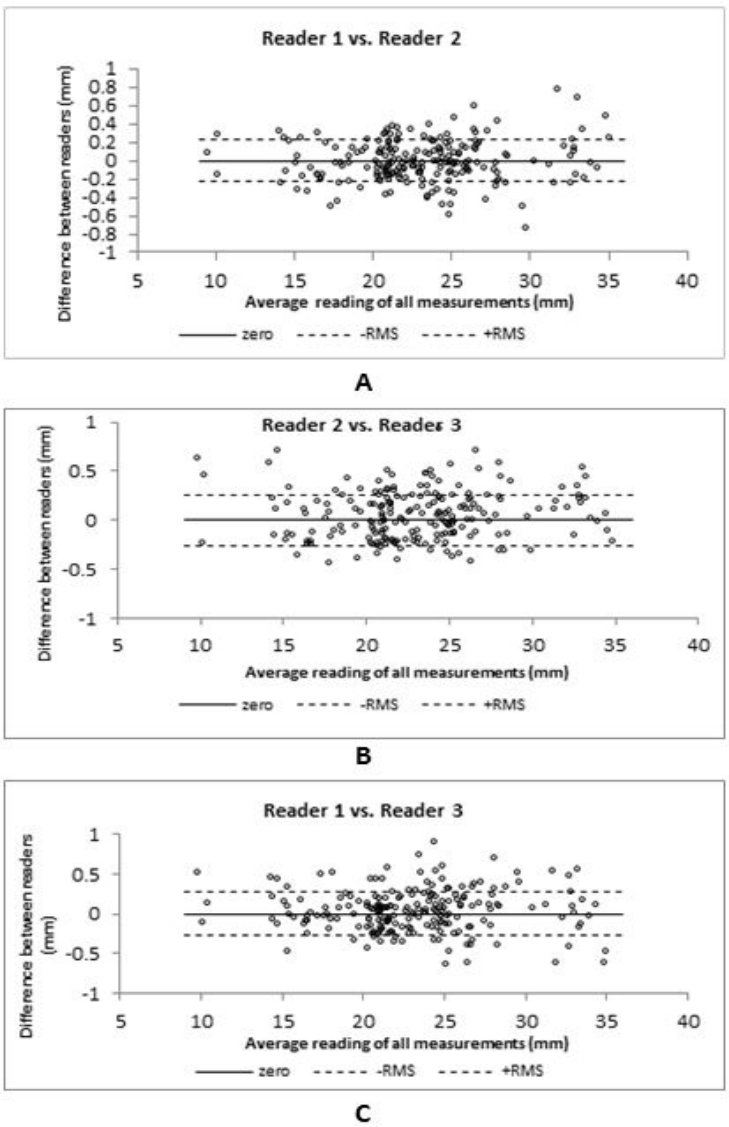

Figure 4.11: Bland-Altman plots showing correlations in measured difference in metacarpal to scaphoid distance among the three reviewers. A. Reader 1 vs. Reader 2. B. Reader 2 vs. Reader 3. C. Reader 1 vs. Reader 3.

difference in metacarpal to scaphoid distance among the three reviewers. We found no difference between metacarpal to scaphoid distance measurements obtained by each reviewer (t-tests all with $p \gg 0.88$). As there was no difference in measurements between reviewers or across trails, we were able to average metacarpal to scaphoid distance values across reviewers and trials to compare a single mean pre and post TMC joint loading for each specimen.

Mean metacarpal to scaphoid distance in the native specimens under applied load was 23.13±3.40mm for TTCI and 25.61±3.31mm for PTCI groups. Mean metacarpal to scaphoid distance in the treated TTCI and PTCI groups under applied load were 15.38±2.48mm and 21.30±2.72mm, respectively. The difference in metacarpal to scaphoid distance was statistically significant between the TTCI (34% reduction) and PTCI (17% reduction) groups (p=0.05; 7.75±3.09mm and 4.28±3.25mm, respectively) indicating greater metacarpal subsidence with the TTCI group.

4.2.4 Conclusions

We describe a technique of partial trapezium resection and first metacarpal base resection with utilization of local capsular tissue interposition for treatment of TMC joint arthritis. In the clinical portion of the study, we did not identify any differences in pre-operative to short-term post-operative pinch or grip strength. However, at medium-term follow-up, differences were noted. The treated patients had better grip strength and maintained first web space distance and MCP flexion range of motion at final follow up. Excellent functional outcomes on the DASH score were reported and no additional complications were reported. We have demonstrated in a cadaveric model that this technique, when compared to complete trapezium excision, results in less proximal translation of the first metacarpal under a simulated physiological load. The maintenance of overall thumb length may be important as it

may lead to a more stable and biomechanically sound thumb. Clinically, it has been shown that metacarpal subsidence correlates with decreased thumb strength due to a reduction in the length of the lever arm.

Our clinical results compare well with other described surgical procedures when utilizing grip and pinch strength as an outcome measure. Vermuelen et al. demonstrated final grip and pinch strengths of 21.0 kg and 5.6 kg, respectively, 12 months following treatment with ligament reconstruction arthroplasty (Weilby technique) for TMC OA. [78] In their study, pre-operative to post-operative grip strength increased significantly (p=.015; 17.9 kg to 21.0 kg), but the increase in pinch strength was not significant (p=.642;5.3 kg to 5.6 kg). At medium-term follow-up, our final grip and pinch strengths are 32.0±12.8 kg and 7.2±2.7 kg, respectively. Like the Vermuelen et al. study, we saw a significant increase in grip strength (25.3±10.1 kg to 32.0±12.8 kg; p=0.01), but the increase in pinch strength did not reach significance (5.7±3.4 kg to 7.2±2.7 kg; p=0.14). In the series by Sandvall et al., grip and lateral pinch strength 24 months following treatment with LRTI were 22.1±9.6 kg and 6.3±2.1 kg, respectively, and for hematoma distraction arthroplasty (HDA) were 29.3±14.7 kg and 6.9±2.4 kg, respectively. [79] In a study by Soejima et al., 22 thumbs receiving ligament reconstruction with the abductor pollicis longus, showed final grip and pinch strength were 16 kg and 4 kg, respectively. [80]

Our biomechanical results compare well with the study by Yao et al 2010 which measured the distance from the metacarpal base to the distal surface of the trapezium, before and after complete trapezial excision. [81] They found the difference between native and excised specimen space height was 12.8mm in one group (n=10) and 13.2 mm in the second group (n=10) studied. We found a difference between the native and treated TTCI group of 7.75±3.09mm. It should be noted that our study included capsular interposition with the total trapezial excision while no interposition

treatment was used in Yao et al. Additionally, our results compare well with a radiographic study by Downing et al. [82] They found an average difference in trapezial space height of 6.3 mm when comparing pre-operative measures to 1-year follow-up measurements of total trapeziectomy with 1. no interposition (n=73), 2. palmaris longus interposition (n=23), and 3. flexor carpi radialis ligament reconstruction and tendon interposition (n=24) . A clinical study by Sandvall et al. reported that treatment with LRTI or HDA resulted in 49% and 50% thumb metacarpal subsidence, respectively, at mean follow-up of 24 months. [79] We report a 17% subsidence following PTCI in cadaveric specimens (4.28±3.25mm).

Some limitations exist in both arms of the present study. In the clinical study, retrospective analysis is a limitation, as it has the risk of introducing bias compared with a prospective study. As with all retrospective cohorts, there is no randomization. Additionally, we had a relatively low percentage of subjects return for the medium-term follow-up portion of the study (42%). We live in a large rural state, with a transient population, where a majority of our patients live remotely. In many cases, the patients declined to return for follow-up due to a lack of time, money, or effort required to return to our city for evaluation. In the biomechanical study, cadaveric tissue can be variable in quality and we cannot control for the quality of the tissue between specimens. A matched-paired study minimizes this risk in variability. Cadaveric specimens do not have the biological healing which could change the behavior of the TMC joint dynamics. Additionally, we did not use specimens with TMC OA. Our study was focused on gathering baseline measurements of metacarpal to scaphoid distance between matched paired specimens and we wanted to avoid the potential for adjacent joint arthritis or compromised ligaments associated with TMC OA that may affect joint kinematics. Moreover, our model did not assess displacement in the three dimensional plane. In vivo, the TMC joint is subject to load in multiple planes by various muscle groups which is not easily reproduced in the lab-

oratory setting. The biomechanics of thumb movement, and joint variable loading and interplay between bone stability and muscle stability is not well understood and is an area of further research.

Our study has several strengths. First, utilization of local capsular tissue for interposition does not require graft harvest. This is required in many other described techniques for thumb basal joint surgery, a common procedure being ligament reconstruction with tendon interposition. The capsular tissue after removal of 4mm of bone from the TMC joint becomes redundant and is adequate for utilization as an interposition graft into the created joint space. Others have shown that removal of the trapezium can lead to proximal thumb migration and thumb instability. [74, 80, 83, 84] We have shown in the biomechanical study that avoiding removal of the entire trapezium may avoid this complication. The addition of metacarpal base resection may be beneficial in that the irregular, arthritic, eburnated bone, a potential pain generator in patients with TMC arthritis, is removed. In the clinical study, all surgeries were performed by a single surgeon, resulting in less variability in surgical technique, thus increasing the validity of our results.

In conclusion, we present an alternative technique for treatment of TMC OA. In a medium-term follow-up, PTCI resulted in significantly improved outcomes in clinically relevant measurements such as grip strength and DASH scores making it competitive with other common treatment options. We found in a cadaveric model that this technique has less proximal displacement of the metacarpal, or better maintenance of thumb length while under lateral pinch load, when compared to total resection of the trapezium.

Chapter 5

Patient-Specific Finite Element Model of the Thumb

5.1 Introduction

Mechanical motion analyses in Section 3.3 have provided fundamental information necessary for understanding the native motion of the trapezium and first metacarpal base when subject to daily physiologic activities. Testing and histology in Sections 3.4 and 3.5 have provided information on mechanical properties and microstructural features of TMC joint ligaments. Additionally, testing has provided a means of investigating new techniques for the treatment of TMC OA. While experimental testing has served as an essential first step to normal joint TMC analyses, the small size and intricate architecture of the joint limits the information that can be obtained through traditional experimental techniques. For this reason, Chapter 5 introduces the development of a patient-specific, high-resolution finite element model of the thumb. This model may be used investigate the effects of new surgical techniques for treatment of OA, to increase understanding of joint motion when subject to a variety

of physiologic activities, and can be used to understand contact mechanics of the normal and OA joint. This model may be expanded in future studies to investigate new surgical interventions or implants, for pre-surgical planning, or investigation of the effects of OA on neighboring joints.

5.2 High-Resolution Quantitative Computed Tomography

Prior to mechanical testing, the fifteen matched pairs of fresh-frozen cadaveric hands used in the experimental study were thawed for 24 hours and placed in a lateral pinch position using Scotchcast plus Casting Tape (3M, St. Paul, MN). (Figure 5.1) This position was selected because it was a neutral pinch position allowing for optimal imaging and matched one of the positions investigated in the motion analysis study. This would enable the computational model to be validated with the lateral pinch motion analysis data. The specimens were then transferred to the New Mexico Office of the Medical Investigator (OMI) for high-resolution quantitative computed tomography (QCT) imaging. The OMI is the only medical investigation facility in the United States with state-of-the-art imaging services using CT and magnetic resonance scanners.

With assistance from Gary Hatch, MD (Forensic Radiologist at OMI and Visiting Assistant Professor in Radiology and Pathology) and Chandra Gerard, BS/RT (Supervisor, Center for Forensic Imaging at OMI), a scanning protocol was created for the Brilliance CT scanner (Philips Healthcare, Andover, MA) to capture high-resolution images of the bones of the hand and wrist. The following protocol was used for CT scanning [85]:

Figure 5.1: Cadaveric specimen (right hand) was placed in a lateral pinch position using fiberglass tape with plaster casting resin (Scotchcast plus Casting Tape by 3M) in preparation for high-resolution computed tomography.

1. A QCT calibration phantom is placed on the scanner table (Mindways Inc., Austin, TX). This phantom is positioned within the field of view of the specimen and will allow for conversion of scanner Hounsfield grey-scale units (HU) to equivalent potassium phosphate (K_2HPO_4) density which is assumed to be equal to bone ash density.

2. The cast specimen is placed within a modified forearm splint similar to that used for motion analysis testing and fixed to the top surface of the QCT phantom. (Figure 5.2)

3. The CT table is advanced into the x-ray gantry. Laser alignment markers are positioned at the level of the TMC joint.

4. Each specimen was scanned using the following parameters: The scanner was operated at 120kVp and 216mAs. A sharp reconstruction kernel was used (higher spatial frequency) for ease with image segmentation.

Figure 5.2: Cadaveric specimen (right hand) placed in a modified forearm splint attached to the top surface of a QCT calibration phantom for CT scanning.

Slice increment and thickness were 0.56mm and 0.8mm, respectively. The field of view was 512 x 512 pixels and captured the full hand, wrist and distal 1/4 of the radius and ulna.

5.3 Patient-specific Finite Element Models

A patient-specific three-dimensional model was generated from the high-resolution QCT images using the Materialise Interactive Medical Image Control System (MIMICS 15.0, Materialise, Plymouth, MI). The following procedure was used to develop the three-dimensional model:

1. QCT dicom files for the scanned specimen were imported into the MIMICS software program. Figure 5.3 shows two-dimensional slices of the hand in coronal and sagittal planes displayed in MIMICS.

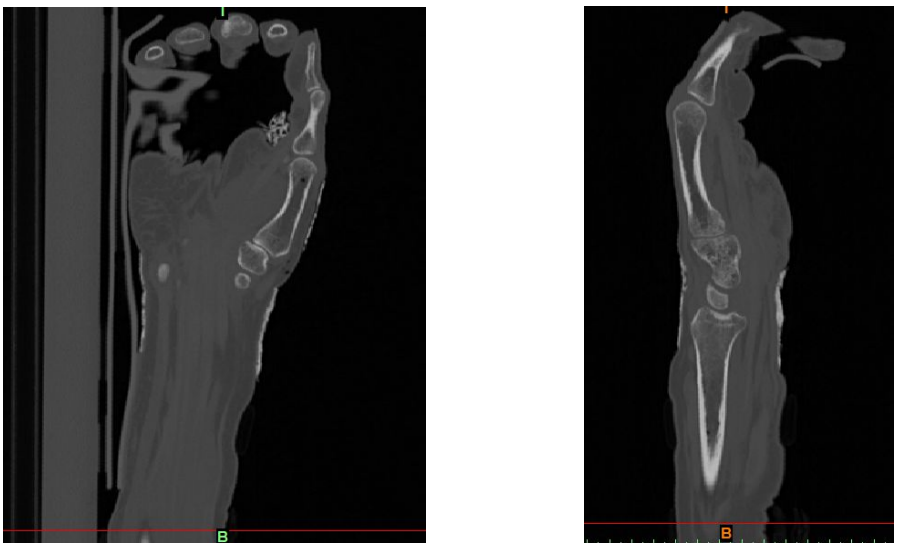

(a) (b)

Figure 5.3: Two-dimension CT slices of the hand displayed in MIMICS (a) Coronal view; (b) Sagittal view

2. A manual segmentation procedure was used to isolate the bones of the hand from the surrounding soft tissue. Figure 5.4 shows a transverse view of the bones of the wrist. The cyan mask is created to identify the bony structures. Black polylines are generated from the mask for filling the cavity of the bones.

3. A three-dimension model of the segmented CT images is generated from the masked coronal, sagittal, and transverse CT slices.

4. A series of smoothing and wrapping procedures is used to close small gaps in the model due to poor segmentation or effects of CT slice thickness. Smoothing filters outliers while preserving boundaries. Wrapping filters small inclusions. Figure 5.5 shows the three-dimensional model of the hand and wrist to be used for finite element mesh generation.

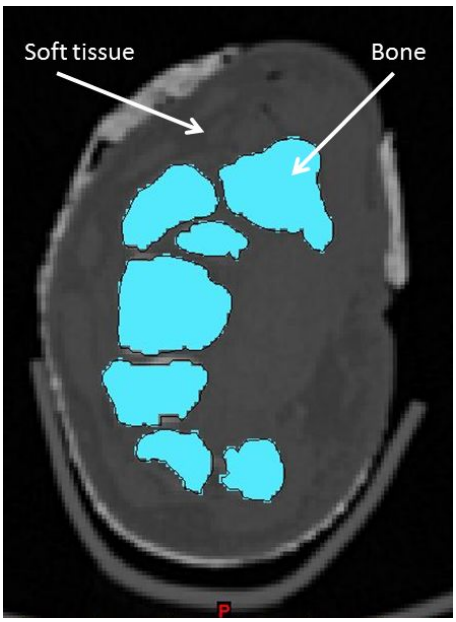

Figure 5.4: Two-dimensional, transverse cross-sectional image of the hand showing the manual segmentation process to isolate the bones of the hand and wrist.

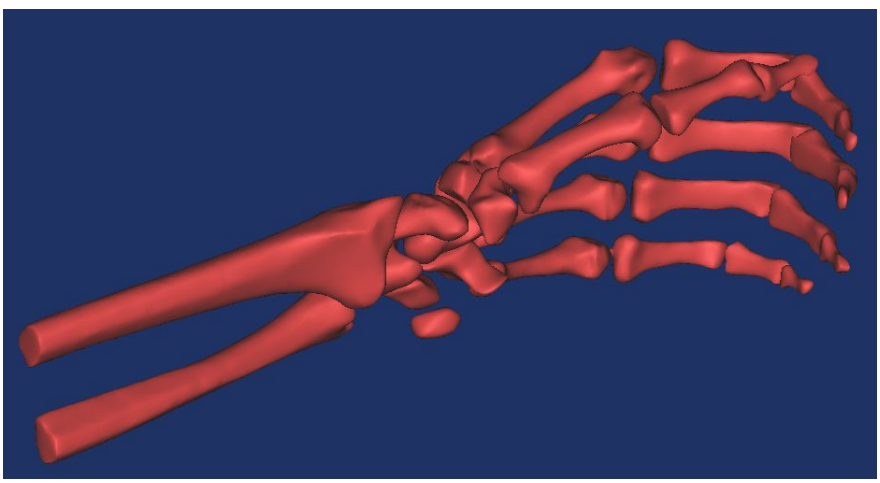

Figure 5.5: Three-dimension model of the hand and wrist to be used for finite element analysis.

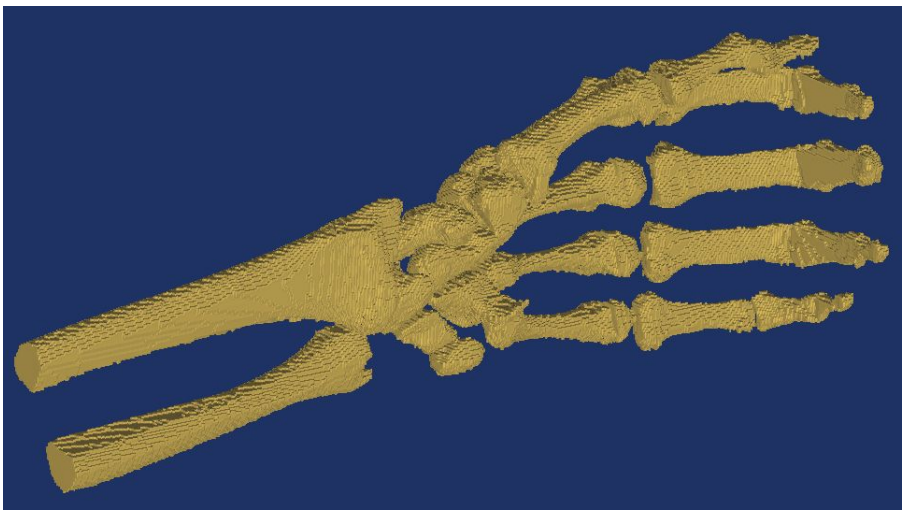

Figure 5.6: Three-dimension model with voxel based finite element mesh.

In the present study, a voxel based finite element meshing technique is used. A voxel mesh is generated using the MIMICS finite element analysis package. A mesh size is selected to be equivalent to the in-plane pixel size and thickness of CT settings (0.56 mm x 0.8 mm). This mesh resulted in 590,577 elements and 703,560 nodes. Discrete material properties were then assigned to each voxel element based on the density (Hounsfield unit) of the QCT voxel. The following equation was used to calculate the isotropic elastic modulus from the apparent density of the voxel: $E = 14664\rho^{1.49}$. [86] Poisson's ratio was selected to be 0.3. [85] The finite element mesh is shown in Figure 5.6 and the material distributions are shown in Figure 5.7.

In the event that a focused analysis of the trapeziometacarpal (TMC) joint is preferred, or that computational limits prevent analysis of a large finite element model, it is possible to isolate the first and second metacarpals, trapezium, trapezoid, and scaphoid from the current mesh. (Figure 5.8) This new mesh resulted in 112,123 elements and 134,195 nodes. The material distributions for the thumb only mesh is shown in Figure 5.9.

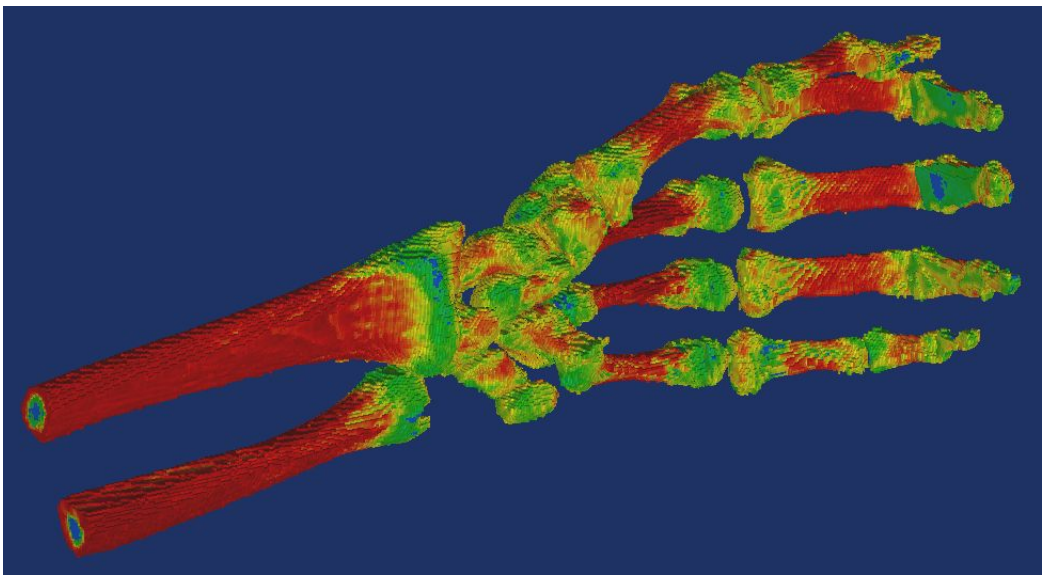

Figure 5.7: Material properties applied to the finite element mesh. The red regions show the dense cortical sections of the shaft of the long bones and fingers. The blue regions show the less dense cancellous bone near articular surfaces.

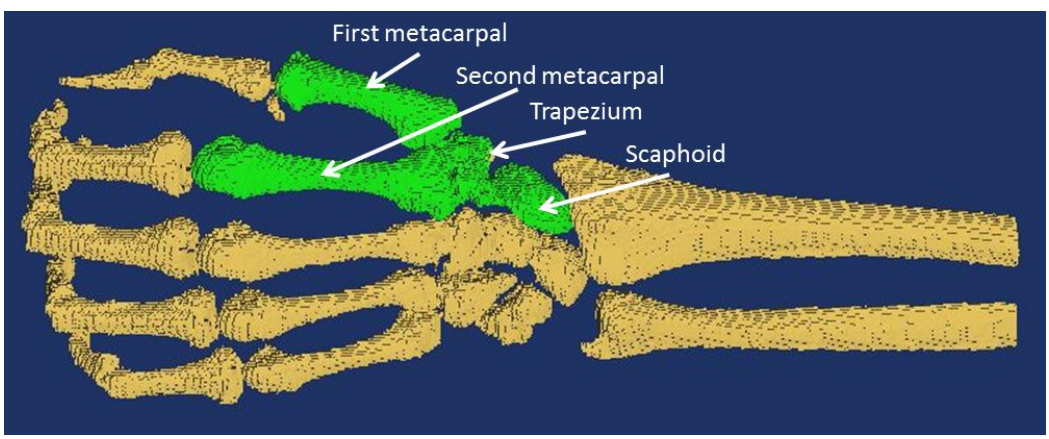

Figure 5.8: Three-dimensional model with voxel based finite element mesh of the first and second metacarpals, trapezium, trapezoid, and scaphoid (green).

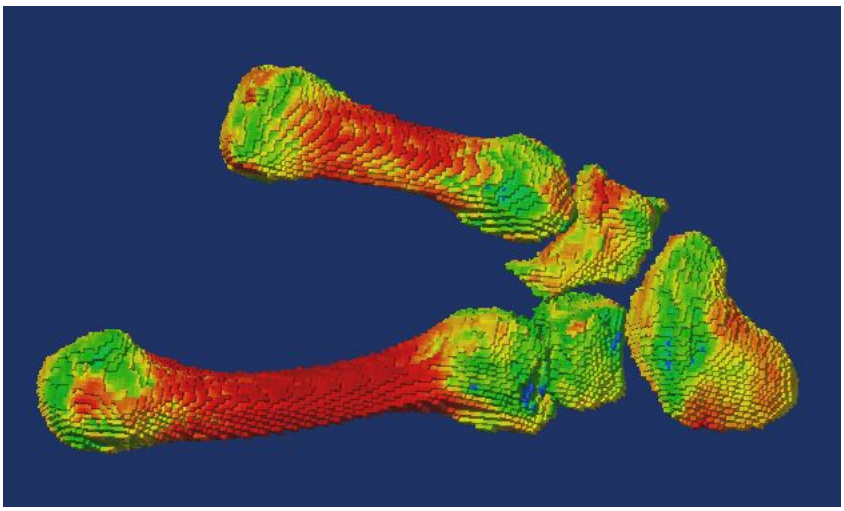

Figure 5.9: Material properties applied to the finite element mesh of the isolated thumb.

5.4 Boundary Conditions

Once the material distributions have been applied to the finite element mesh, it can be exported as an ansys preprocessor file (.cdb) to the Ansys®Workbench finite element software package (or any finite element package desired). If using the Workbench package, it is necessary to import the .cdb file using the Finite Element Modeler (FEM) component system. The skin detection tool is then used to create the three-dimensional geometry of the thumb using curvatures from the legacy mesh. The FEM can then be linked to the Model section of a Structural Analysis component system for applying boundary conditions and solving the finite element model. In the present example, the thumb only mesh is imported to the Workbench system for application of boundary conditions.

Ligaments

The first step is to introduce the trapeziometacarpal (TMC) joint ligaments investigated in the motion analysis study in Chapter 3. Body-body spring elements are

used to simulate the dorsal radial (DRL), posterior oblique (POL), anterior oblique (AOL), ulnar collateral (UCL), and intermetacarpal (IML) ligaments. Connection of each spring element matches the origin and insertion of each ligament on the trapezium, first metacarpal, or second metacarpal based on a study of the ligamentous attachments of the TMC joint by Nanno et al. [15] The spring element stiffness for each ligament is based on results of the uniaxial tensile stiffness results from the experimental study presented in Chapter 3.

Dorsal Ligaments

Figure 5.10 shows the spring elements representing the dorsal and intermetacarpal ligaments of the TMC joint.

1. The spring element for the DRL is attached to the dorsal radial tubercle of the trapezium and to the dorsal radial edge of the base of the first metacarpal (1st MC base). The stiffness for the DRL is 47.9 N/mm.

2. The element for the POL is attached proximal to the dorsal and ulnar edge of the trapezium and attached distally to the dorsal and ulnar edge of the 1st MC base. The stiffness for the POL is 32.70 N/mm.

3. The element for the IML is attached ulnar to the dorsal radial tubercle of the second metacarpal and attached radial to the dorsal ulnar side of the first metacarpal. The stiffness for the IML was not determined in our study and is not reported in literature. A stiffness of 49.16 N/mm was used. This value is equivalent to the stiffness of the AOL.

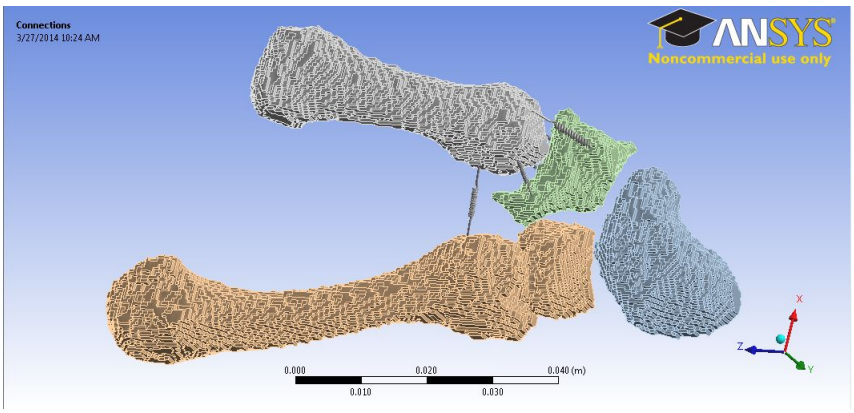

Figure 5.10: Finite element model of the thumb. Dorsal view showing inter-metacarpal, dorsal radial, and posterior oblique ligaments applied to model as springs with stiffness defined from experimental test data.

Volar Ligaments

Figure 5.11 shows the spring elements representing the volar and inter-metacarpal ligaments of the TMC joint.

1. The spring element for the AOL is attached proximal to the volar edge of the trapezium and distal to the volar edge of the 1st MC base. The stiffness for the AOL is 49.16 N/mm.

2. The element for the UCL is attached proximally from the distal edge of the trapezial ridge and distally on the ulnar volar side of the 1st MC base. The stiffness for the UCL is 32.72 N/mm.

Contacts

To simplify the analysis time for this model, bonded contact can be used between the following bone-bone junctions: scaphoid and trapezium, scaphoid and trapezoid, trapezoid and second metacarpal, trapezoid and trapezium. A frictional contact is placed between the trapezium and first metacarpal with a coefficient of friction of

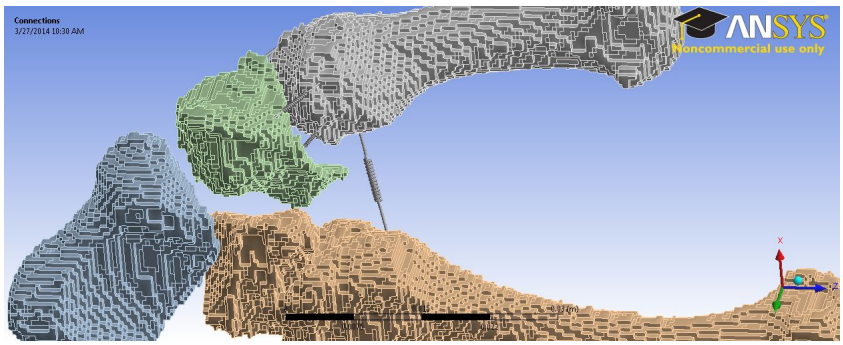

Figure 5.11: Finite element model of the thumb. Volar view showing intermetacarpal, ulnar collateral, and anterior oblique ligaments applied to model as springs with stiffness defined from experimental test data.

0.01. [87] Note: This coefficient of friction can be used between any two adjacent bones to simulate healthy joint contact.

Load and Supports

A fixed support is applied to the proximal ulnar surface of the scaphoid to prevent rigid body motion during analysis. A resultant force of 5N is applied along the central axis of the first metacarpal in a proximal, dorsal, and ulnar direction. This is the direction of motion of the 1st MC base of the native joint found from experimental motion analyses in Chapter 3.

5.5 Conclusion

The methodology for the development of patient-specific finite element models of the hand and thumb is presented. Three-dimensional solid models are developed from two-dimensional computed tomography scans of the specimens taken prior to experimental testing. Material properties are applied to the models using density information from calibrated scans to allow for patient-specific representations of bone

density. Stiffness results from mechanical testing are supplied as inputs to the spring elements representing the ligaments of the TMC joint. Trajectory for the load applied to the first metacarpal is defined from results of the displacement of the 1st MC base from native motion analysis.

Chapter 6

Conclusions

6.1 Conclusions

In Chapter 3, experimental testing and characterization of the anterior oblique (AOL), posterior oblique (POL), ulnar collateral (UCL), dorsal radial (DRL), and intermetacarpl (IML) ligaments is completed using high-resolution motion tracking with sequential sectioning, uniaxial tensile testing, and ligament histology. These analyses provide a clear understanding of the importance of each ligament to stability of the trapeziometacarpal (TMC) joint. To our knowledge, this study is the first to investigate native joint motion and the effects of ligament sectioning when subject to thumb extension, lateral pinch, and varied grip loading. Additionally, this study is the first to investigate the uniaxial, tensile mechanical properties of POL and UCL ligaments. Experimental conclusions about the contribution of each ligament to stability is drawn based on a compilation of mechanical testing and tissue characterization results.

Native joint motion analyses of extension and lateral pinch showed that the trapezium

and first metacarpal (1st MC base) translate along the same x-, y-, and z-directions but at different magnitudes. 1st MC base dorsal and proximal displacement is higher in extension but lower in lateral pinch than the trapezium. This finding is intuitive since the 1st MC base is actively moving dorsally in extension, but the trapezium is limiting dorsal motion during lateral pinch. A significant finding of native joint motion when subject to grip is that the trapezium and 1st MC base displace ulnarly at low grip sizes (1/2 and 1 inch) but displace radially at high grip sizes (1-1/2 and 2 inch). This information may be beneficial for future joint contact studies to analyze the effects of contact on the incidence of TMC joint osteoarthritis (OA). Activities which require repeated grasp of large objects may show a significant increase in dorsal, radial contact force on the trapezium. Repeated contact loads have been implicated in the initiation and progression of thumb OA.

Based on findings from motion analysis following ligament sectioning, tensile testing, and histology, we report that the primary stabilizer of the TMC joint is the posterior oblique ligament. In the motion analysis study, sectioning the POL resulted in greater dorsal and radial displacement during thumb extension and it caused a shift from dorsal to volar displacement of the 1st MC base during lateral pinch. During grip, it acted as a restraint to dorsal displacement with dorsally directed loads and prevented significant volar displacement with volarly directed loads. Uniaxial tensile test results showed the POL to have an ultimate tensile load of 131.13 N, secondary only to the DRL (143.10 N). Histological analysis showed the POL consists of long, highly organized bands of crimped collagen fibers.

We find that the secondary stabilizing structure of the TMC joint is the dorsal radial ligament. In the motion anlaysis study, sectioning the DRL resulted in greater dorsal and radial displacement of the 1st MC base during extension. During grip, it acted as a restraint to dorsal displacement of the trapezium. In uniaxial testing,

this ligament had the highest ultimate tensile load (143.10 N). Histological analysis showed the DRL consists of long, highly organized bands of crimped collagen fibers.

In Chapter 4, two surgical techniques for treatment of TMC OA are presented. The opening wedge trapezial osteotomy (OWTO) technique for early TMC OA has been hypothesized to alter the contact mechanics of the TMC joint by reducing dorsal radial subluxation, and shifting contact away from the dorsal radial aspect of the trapezium (which is susceptible to increased wear). This treatment has the added benefit of being an extracapsular procedure and does not damage the ligaments stabilizing the joint. This study provides baseline contact area and pressure measurements on the trapezium during lateral pinch loads. This information, when coupled with motion analysis testing, provides a more thorough view of TMC joint motion. Interestingly, while the motion analysis study found that the base of the first metacarpal is directed in an ulnar, dorsal, and proximal direction in the normal joint under lateral pinch, the contact analysis study found that the center of force was split between the ulnar-dorsal and radial-dorsal quadrants of the trapezium. Ultimately, we found that OWTO is successful at reducing dorsal radial subluxation and increases ulnar contact of the first metacarpal on the trapezium. We conclude the section by introducing a highly simplified finite element model to describe the process by which this occurs. This technique is shown to be successful at addressing two theories hypothesized for the initiation and progression of TMC OA - increased contact loads and excessive metacarpal subluxation.

The partial trapeziectomy with capsular interposition (PTCI) technique for advanced TMC OA is introduced, and mechanical testing is used to compare results of thumb subsidence to the commonly used total trapeziectomy technique. This outcome measure is selected because thumb subsidence has been associated with reduced pinch and grip strength. Total trapeziectomy is characterized by complete removal of the

trapezium and all ligamentous attachments to the first metacarpal. PTCI, though an intracapsular treatment option, is hypothesized to reduce the amount of thumb subsidence by preserving ligamentous attachments thought to maintain stability of the joint. This technique has the added benefit of removing the diseased articular surfaces of the joint which can be associated with pain. Results of this study show that PTCI is successful at limiting metacarpal subsidence. Early results of clinical studies show that PTCI is successful at increasing grip strength from pre-operative measures. Comparisons to the contralateral limb show an increase of 18.3% in grip and 15.8% in pinch compared to pre-operative measures.

In Chapter 5, the methodology for the development of advanced patient-specific finite element models of the thumb and/or full hand and wrist is presented. This model is built by providing inputs to the model based on results of experimental test data of motion analysis and uniaxial tensile testing.

6.2 Future Work

In the motion analysis study, each specimen was placed in an experimental test group where the ligaments to be investigated were assigned (Table 3.1). Each specimen was subject to native joint motion characterization followed by sequential sectioning of the ligaments assigned to that specimen. In the present work, only the native motion of the trapezium and base of the first metacarpal (1st MC base) and the motion of these bones following sectioning of the first ligament was analyzed. Future work will include the analysis of the additional ligaments sectioned for each specimen. Appendix A shows plots of the trapezium and 1st MC base displacement in x-, y-, and z-directions for all ligaments sectioned. A qualitative analysis of these plots show that sectioning of subsequent ligaments provides further information on the relative

contribution of each ligament to joint stability. A quantiative analysis is necessary.

A limitation of the motion analysis study was a lack of cadaveric specimens available for determining the effects of individual ligament sectioning on the motion of the trapezium and 1st MC base. Results obtained were useful in examining a clinical significance in the relative displacement of the bones when compared to their native joint motion. Unfortunately, statistical significance could not be obtained without an increase in available test specimens. Future work will include the acquisition of a larger group of cadaveric specimens and the motion analysis study will be repeated. Corrections to the methodology, including the automation of specimen loading, will be implemented to improve outcome measures.

Similar to the motion analysis study, the uniaxial tensile tests lacked a sufficient sample size of cadaveric specimens to reduce the effects of specimen variability (high standard deviations). This study will be repeated with a larger sample size to increase the contribution of mechanical test data on the ligaments of the thumb. Motion analysis results show the intermetacarpal ligament (IML) to play a substantial role in the stability of the 1st MC base. While it is not clearly a primary stabilizer of the joint, data on the ultimate strength and stiffness of this ligament is limited. Future studies will include the IML so that results can be compared with motion analysis data in an effort to determine its relative contribution to stability. Like the motion study, methodology may be modified (strain rate, fixture attachment, grip method etc.) to improve outcome measures and limit variability.

In Chapter 4, a study of contact pressure and area of the TMC joint before and after opening wedge trapezial osteotomy is presented. Tekscan pressure sensing pads were placed within the joint space to determine the change in contact area and pressure as a result of correction. Unfortunately, these sensing pads require disruption

of the dorsal ligaments in order to place these sensors within the joint space. Motion analysis testing has shown that the dorsal ligaments are the primary stabilizing ligaments of the joint and removal of these ligaments may affect results of the contact study. A simplified finite element model was developed to analyze the change in contact pressure on the trapezial surface, but a patient-specific computational model is preferred. In Chapter 5, the development of a patient-specific model of the thumb is presented. In future studies, this model will be validated through experimental testing and a computational study simulating the experimental joint contact study will be completed. These models may be used for a wide number of thumb and hand exploratory studies.

While this body of work is succesful at introducing new information on native and damaged joint motion when subject to daily physiologic activities, the ultimate goal is to identify potential causes for the intiation and progression of osteoarthritis. Future work may include an investigation of the motion of the TMC joint and mechanical characterization of joint ligaments with varying degrees of osteoarthritis. This will provide information on how diseased tissue may affect joint motion. Additionally, a histologic analysis of diseased ligaments may provide information on whether a change in the macromolecule's structure or organization affects mechanical properties.

References

[1] Neumann DA and Bielefeld T. The carpometacarpal joint of the thumb: stability, deformity, and therapeutic intervention. *J Orthop Sports Phys Thera*, 33(7):386–399, 2003.

[2] Iqbal A. Carpometacarpal joint of thumb, Accessed 10 Apr. 2014. http://www.mananatomy.com/body-systems/skeletal-system/carpometacarpal-joint-thumb.

[3] Morphopedics. Scaphoid fractures, Accessed 10 Apr. 2014. http://morphopedics.wikidot.com/scaphoid-fractures.

[4] Muir H. Proteoglycans as organizers of the intercellular matrix. *Biochem Soc Trans*, 11:613–622, 1983.

[5] Muir H. The chondrocyte, architect of cartilage: biomechanics, structure, function and molecular biology of cartilage matrix macromolecules. *Bioessays*, 17:1039–1048, 1995.

[6] Mankin HJ and Thrasher AZ. Water content and binding in normal and osteoarthritic human cartilage. *J Bone Joint Surg Am*, 57(A), 1975.

[7] Bednar MS. Osteoarthritis of the hand and digits: thumb, Accessed 10 Apr. 2014. http://mmspf.msdonline.com.br/ebooks/HandSurgery/sid901079.html.

[8] Bettinger PC, Linscheid RL, Berger RA, Cooney WP 3rd, and An KN. An anatomic study of the stabilizing ligaments of the trapezium and trapeziometacarpal joint. *J Hand Surg Am*, 24(A):786–798, 1999.

[9] Kauer JM. Functional anatomy of the carpometacarpal joint of the thumb. *Clin Orthop Relat Res*, 220:7–13, 1987.

[10] Boulderinthesnow. Arm muscles unedited flashcards, Accessed 10 Apr. 2014. http://quizlet.com/4669012/arm-muscles-copy-unedited-flash-cards/.

[11] Eaton RG and Littler JW. Ligament reconstruction for the painful thumb carpometacarpal joint. *J Bone Joint Surg Am*, 55(A):1655–1666, 1973.

[12] Pagalidis T, Kuczynski K, and Lamb DW. Ligamentous stability of the base of the thumb. *Hand*, 13(1):29–36, 1981.

[13] Pellegrini Jr. VD. Osteoarthritis of the trapeziometacarpal joint: the pathophysiology of articular cartilage degeneration. i. anatomy and pathology of the aging joint. *J Hand Surg Am*, 16(A):967–974, 1991.

[14] Pellegrini Jr. VD, Olcott CW, and Hollenberg G. Contact patterns in the trapeziometacarpal joint: the role of the palmar beak ligament. *J Hand Surg Am*, 18(A):238–244, 1993.

[15] Nanno M, Buford Jr WL, Patterson RM, Andersen CR, and Viegas SF. Three-dimensional analysis of the ligamentous attachments of the first carpometacarpal joint. *J Hand Surg Am*, 31(A):1160–1170, 2006.

[16] Edmunds O. Current concepts of the anatomy of the thumb trapeziometacarpal joint. *J Hand Surg Am*, 36(A):170–182, 2011.

[17] Tan J, Xu J, Xie RG, Deng AD, and Tang JB. In vivo length and changes of ligaments stabilizing the thumb carpometacarpal joint. *J Hand Surg Am*, 36(A):420–427, 2011.

[18] Hagert E Ladd AI, Lee J. Macroscopic and microscopic analysis of the thumb carpometacarpal ligaments. a cadaveric study of ligament anatomy and histology. *J Bone Joint Surg Am*, 94:1468–1477, 2012.

[19] Hagert E, Lee J, and Ladd AL. Innervation patterns of thumb trapeziometacarpal joint ligaments. *J Hand Surg Am*, 37(A):706–714, 2012.

[20] Strauch RJ, Behrman MJ, and Rosenwasser MP. Acute dislocation of the carpometacarpal joint of the thumb: An anatomic and cadaver study. *J Hand Surg Am*, 19(A):93–98, 1994.

[21] Najima H, Oberlin C, Alnot JY, and Cadot B. Anatomical and biomechanical studies of the pathogenesis of trapeziometacarpal degenerative arthritis. *J Hand Surg Br*, 22(2):183–188, 1997.

[22] Van Brenk B, Richards RR, Mackay MB, and Boynton EL. A biomechanical assessment of ligaments preventing dorsoradial subluxation of the trapeziometacarpal joint. *J Hand Surg Am*, 23(A):607–611, 1998.

[23] Colman M, Mass DP, and Draganich LF. Effects of the deep anterior oblique and dorsoradial ligaments on trapeziometacarpal joint stability. *J Hand Surg Am*, 32(A):310–317, 2007.

[24] Bettinger PC, Smutz WP, Linscheid RL, Cooney WP 3rd, and An KN. Material properties of the trapezial and trapeziometacarpal ligaments. *J Hand Surg Am*, 25(A):1085–1095, 2000.

[25] Abhishek A and Doherty M. Diagnosis and clinical presentation of osteoarthritis. *Rheum Dis Clin North Am*, 39(1):45–66, 2013.

[26] Dias R, Chandrasenan J, Rajaratnam V, and Burke FD. Basal thumb arthritis review. *Postgrad Med J*, 83:40–43, 2007.

[27] Fontana L, Neel S, Claise JM, Ughetto S, and Catilina P. Osteoarthritis of the thumb carpometacarpal joint in women and occupational risk factors: a case-control study. *J Hand Surg Am*, 32(A):459–465, 2007.

[28] Funzoo. Base of thumb arthritis poster.

[29] Hunter DJ, Zhang Y, Sokolove J, Niu J, Aliabadi P, and Felson DT. Trapeziometacarpal subluxation predisposes to incident trapeziometacarpal osteoarthritis: the framingham study. 13:953–957, 2005.

[30] Koff MF, Ugwonali OF, Strauch RJ, Rosenwasser MP, Ateshian GA, and Mow VC. Sequential wear patterns of the articular cartilage of the thumb carpometacarpal joint in osteoarthritis. *J Hand Surg Am*, 28(A):597–604, 2003.

[31] Meenagh GK, Patton J, Kynes C, and Wright GD. A randomized controlled trial of intra-articular corticosteroid injection of the carpometacarpal joint of the thumb in osteoarthritis. *Ann Rheum Dis*, 63:1260–1263, 2004.

[32] Basford JR, Sheffield CG, Mair SD, and Ilstrup DM. Low-energy helium neon laser treatment of thumb osteoarthritis. *Arch Phys Med Rehabil*, 68:794–797, 1987.

[33] Carreira ACG, Jones A, and Natour J. Assessment of the effectiveness of a functional splint for osteoarthritis of the trapeziometacarpal joint of the dominant hand: a randomized controlled study. *J Rehabil Med*, 42:469–474, 2010.

[34] Stahl S, Karsh-Zafrir I, Ratzon N, and Rosenberg N. Comparison of intraarticular injection of depot corticosteroid and hyaluronic acid for treatment of degenerative trapeziometacarpal joints. *J Clin Rheumatol*, 11(6):299–302, 2005.

[35] Habib GS, Saliba W, and Nashashibi M. Local effects of intra-articular corticosteroids. *Clin Rheumatol*, 29(4):347–356, 2010.

[36] Leung GJ, Rainsford KD, and Kean WF. Osteoarthritis of the hand ii: chemistry, pharmacokinetics and pharmacodynamics of naproxen, and clinical outcome studies. *J Pharm Pharmacol*, 2013.

[37] Selecting splints or exercises for thumb arthritis, Accessed 10 Apr. 2014. http://www.3pointproducts.com/blog-health-arthritis-finger-and-toe-conditions/bid/61367/Selecting-Splints-or-Exercises-for-Thumb-Arthritisl.

[38] Tallia AF and Cardone DA. Diagnostic and therapeutic injection of the wrist and hand region. *Am Fam Physician*, 67(4):745–750, 2003.

[39] Knutsen RM. On advance for occupational therapy practitioners, Accessed 10 Apr. 2014. http://occupational-therapy.advanceweb.com/Features/Articles/Thumb-Therapy.aspx.

[40] Kenniston JA and Bozentka DJ. Treatment of advanced carpometacarpal joint disease: arthrodesis. *Hand Clin*, 24:285–294, 2008.

[41] Turker T and Thirkannad S. Trapezio-metacarpal arthritis: The price of an opposable thumb. *Ind J Plastic Surg*, 44(2):308–316, 2011.

[42] Taylor EJ, Desari K, D'arcy JC, and Bonnici AV. A comparison of fusion, trapeziectomy, and silastic replacement for the treatment of osteoarthritis of the trapeziometacarpal joint. *J Hand Surg Br*, 30(B):45–49, 2005.

[43] DeSmet L, Vaes F, and Van Den Broeck J. Arthrodesis of the trapeziometacarpal joint for basal joint osteoarthritis of the thumb: the importance of obtaining osseous union. *Chir Main*, 24(5):222–224, 2005.

[44] Kapandji AI and Heim UF. L'osteotomie de reorientation de la selle trapezienne. *Chir Main*, 21:124–133, 2002.

[45] Hobby JL, Lyall HA, and Meggitt BF. First metacarpal osteotomy for trapeziometacarpal osteoarthritis. *J Bone Joint Surg Br*, 80(B):508–512, 1998.

[46] Shrivastava N, Koff MF, Abbott AE, Mow VC, Rosenwasser MP, and Strauch RJ. Simulated extension osteotomy of the thumb metacarpal reduces carpometacarpal joint laxity in lateral pinch. *J Hand Surg Am*, 28(A):733–738, 2003.

[47] Freedman DM, Eaton RG, and Glickel SZ. Long-term results of volar ligament reconstruction for symptomatic basal joint laxity. *J Hand Surg Am*, 25(A):297–304, 2000.

[48] Berger RA. The ligaments of the wrist. a current overview of anatomy with considerations of their potential functions. *Hand Clin*, 13(1):63–82, 1997.

[49] Berger RA. The anatomy of the ligaments of the wrist and distal radioulnar joints. *Clin Orthop Relat Res*, 383:32–40, 2001.

[50] Cooney WP and Chao EYS. Biomechanical analysis of static forces in the thumb during hand function. *J Bone Joint Surg Am*, 59(A):27–36, 1977.

[51] Kuo LC, Cooney 3rd WP, Oyama M, Kaufman KR, Su FC, and An KN. Feasibility of using surface markers for assessing motion of the thumb trapeziometacarpal joint. *Clin Biomech*, 18:558–563, 2003.

[52] Matthews GL, Keegan KG, and Graham HL. Effects of tendon grip technique (frozen versus unfrozen) on in vitro surface strain measurements of the equine deep digital flexor tendon. *Am J Vet Res*, 57(1):111–115, 1996.

[53] Cheung JTM and Zhang M. A serrated jaw clamp for tendon gripping. *Med Eng Phys*, 28:379–382, 2006.

[54] Ng BH, Chou SM, and Krishna V. The influence of gripping techniques on the tensile properties of tendons. *Proc IMechE J Eng Med*, 219(H):349–354, 2005.

[55] Rincon L, Schatzmann L, Brunner P, Staubli HU, Ferguson SJ, Oxland TR, and Nolte LP. Design and evaluation of a cryogenic soft tissue fixation device - load tolerances and thermal aspects. *J Biomech*, 34:393–397, 2001.

[56] Kiss MO, Hagemeister N, Levasseur A, Fernandes J, Lussier B, and Petit Y. A low-cost thermoelectrically cooled tissue clamp for in vitro cyclic loading and load-to-failure testing of muscles and tendon. *Med Eng Phys*, 31:1182–1186, 2009.

[57] Noyes FR, DeLucas JL, and Torvik PJ. Biomechanics of anterior cruciate ligament failure: an analysis of strain-rate sensitivity and mechanisms of failure in primates. *J Bone Joint Surg Am*, 56(A):236–253, 1974.

[58] Petersen W and Tillmann B. Structure and vascularization of the cruciate ligaments of the human knee joint. *Anat Embryol*, 200:325–334, 1999.

[59] Amiel D, Frank C, Harwood F, Fronek J, and Akeson W. Tendons and ligaments: a morphological and biochemical comparison. *J Orthop Res*, 1(3):257–265, 1984.

[60] Rumian AP, Wallace AL, and Brich HL. Tendons and ligaments are anatomically distinct but overlap in molecular and morphological features - a comparative study in an ovine model. *J Orthop Res*, 25:458–464, 2007.

[61] Bettinger PC, Linscheid RL, Cooney WR, and An KN. Trapezial tilt: a radiographic correlation with advanced trapeziometacarpal joint arthritis. *J Hand Surg Am*, 26(A):692–697, 2001.

[62] Cheema T, Salas C, Morrell N, Lansing L, Reda Taha MM, and Mercer D. Opening wedge trapezial osteotomy as possible treatment for early trapeziometacarpal osteoarthritis: a biomechanical investigation of radial subluxation, contact area, and contact pressure. *J Hand Surg Am*, 37(A):699–705, 2012.

[63] Ropars M, Siret P, Kaila R, Marin F, Belot N, and Dreano T. Anatomical and radiological assessment of trapezial osteotomy for trapezial dysplasia in early treatment of trapeziometacarpal joint arthritis. *J Hand Surg Br*, 34(B):264–267, 2009.

[64] Momose T. Cartilage degeneration and measurement of the contact area of the trapeziometacarpal joint: morphological observation. *J Jpn Orthop Assoc*, 68(A):426–434, 1994.

[65] Kovler M, Lundon K, McKee N, and Agur A. The human first carpometacarpal joint: osteoarthritic degeneration and 3-dimensional modeling. *J Hand Ther*, 17:394–400, 2004.

[66] Pellegrini Jr. VD, Smith RL, and Ku CW. Pathobiology of articular cartilage in trapeziometacarpal osteoarthritis. i. regional biochemical analysis. *J Hand Surg Am*, 19(A):70–78, 1994.

[67] Pellegrini Jr. VD, Smith RL, and Ku CW. Pathobiology of articular cartilage in trapeziometacarpal osteoarthritis. ii. surface ultrastructure by scanning electron microscopy. *J Hand Surg Am*, 19(A):79–85, 1994.

[68] Ateshian GA, Ark JW, Rosenwasser MP, Pawluk RJ, Soslowsky LJ, and Mow VC. Contact areas in the thumb carpometacarpal joint. *J Orthop Res*, 13:450–458, 1995.

[69] Edwards SG and Ramsey PN. Prosepective outcomes of stage iii thumb carpometacarpal arthritis treated with arthroscopic hemitrapeziectomy and thermal capsular modification without interposition. *J Hand Surg Am*, 35(A):566–571, 2010.

[70] Gwynne-Jones DP, Penny ID, Sewell SA, and Hughes TH. Basal thumb metacarpal osteotomy for trapeziometacarpal osteoarthritis. *J Orthop Surg*, 14(1):58–63, 2006.

[71] Cox CA, Zlotolow DA, and Yao J. Suture button suspensionplasty after arthroscopic hemitrapeziectomy for treatment of thumb carpometacarpal arthritis. *Arthroscopy*, 26(10):1395–1403, 2010.

[72] Rai JK, Singh P, Mendonca D, and Porter M. Trapeziectomy with a capsular interposition flap. *Ann R Coll Surg Eng*, 91(4):345–346, 2009.

[73] Earp BE, Leung AC, Blazar PE, and Simmons BP. Arthroscopic hemitrapeziectomy with tendon interposition for arthritis at the first carpometacarpal joint. *Tech Hand Up Extrem Surg*, 12(1):38–42, 2008.

[74] Barron OA and Eaton RG. Save the trapezium: double interposition arthroplasty for the treatment of stage iv disease of the basal joint. *J Hand Surg Am*, 23(A):196–204, 1998.

[75] Gervis WH. Excision of the trapezium for osteoarthritis of the trapeziometcarpal joint. *J Bone Joint Surg Br*, 31(B):537–539, 1949.

[76] Smereka M and Duleba I. Circular object detection using a modified hough transform. *Int J Appl Math Comput Sci*, 18(1):85–91, 2008.

[77] Koff MF, Zhao KD, Mierisch CM, Chen MY, An KN, and Cooney WP 3rd. Joint kinematics after thumb carpometacarpal joint reconstruction: an in vitro comparison of various constructs. *J Hand Surg Am*, 32(A):688–696, 2007.

[78] Vermeulen GM, Brink SM, and Sluiter J. Ligament reconstruction arthroplasty for primary thumb carpometacarpal osteoarthritis (weilby technique): prospective cohort study. *J Hand Surg Am*, 34(A):1393–1401, 2009.

[79] Sandvall BK, Cameron TE, and Netscher DT. Basal joint osteoarthritis of the thumb: ligament reconstruction and tendon interposition versus hematoma distraction arthroplasty. *J Hand Surg Am*, 35(A):1968–1975, 2010.

[80] Soejima O, Hanamura T, Kikuta T, Iida H, and Naito M. Suspensionplasty with the abductor pollicis longus tendon for osteoarthritis in the carpometacarpal joint of the thumb. *J Hand Surg Am*, 31(A):425–428, 2006.

[81] Yao J, Zlotolow DA, Murdock R, and Christian M. Suture button compared with k-wire fixation for maintenance of posttrapeziectomy space height in a cadaver model of lateral pinch. *J Hand Surg Am*, 35(A):2061–2065, 2010.

[82] Downing ND and Davis TR. Trapezial space height after trapeziectomy: mechanism of formation and benefits. *J Hand Surg Am*, 26(A):862–868, 2001.

[83] Conolly WB and Rath S. Revision procedures for complications of surgery for osteoarthritis of the carpometacarpal joint of the thumb. *J Hand Surg Am*, 18(A):533–539, 1993.

[84] Zouzias IC, Doft MA, Uzumcugil A, and Rosenwasser MP. Treatment of hyperextension deformity of the thumb metacarpophalangeal joint in basal joint arthritis: a novel technique based on an anatomic study. *Tech Hand Up Extrem Surg*, 15(2):119–124, 2011.

[85] Dragomir-Daescu D, Op Den Buijs J, McEligot S, Dai Y, Entwistle RC, Salas C, Melton LJ 3rd, Bennet KE, Khosla S, and Amin S. Robust qct/fea models of proximal femur stiffness and fracture load during a sideways fall on the hip. *Ann Biomed Eng*, 39(2):742–755, 2011.

[86] Morgan EF, Bayraktar HH, and Keaveny TM. Trabecular bone modulus-density relationships depend on anatomic site. *J Biomech*, 36(7):897–904, 2003.

[87] Hills BA and Butler BD. Surfactants identified in synovial fluid and their ability to act as boundary lubricants. *Ann Rheum Dis*, 43(4):641–648, 1984.

Appendices

Appendix A

Raw data for motion analysis study

Table A.1: Maximum displacement (mm) of the native trapezium when subject to extension and lateral pinch loads; positive x - volar, negative x - dorsal; positive y - proximal, negative y - distal; positive z - radial, negative z - ulnar

	Extension			Pinch		
Subject	x	y	z	x	y	z
1	-1.0023	2.6043	-1.1300	-1.7448	5.0197	-0.6692
2	-1.4363	6.1664	-2.8488	-2.3323	19.0188	-2.3274
3	-2.1448	2.8822	-1.7863	-1.9861	1.8836	-2.3274
4	-2.7364	3.1125	-2.2930	-3.3974	3.8132	-0.9301
5	-2.8788	3.6121	-1.5824	-2.7503	4.3489	-1.1847
6	-0.8004	1.1912	-0.7200	-2.8975	4.2851	-1.2117
7	-0.9209	1.3500	-0.5100	-1.9091	3.5777	-1.2166
8	0.4318	0.9767	-0.5354	-1.0731	3.6825	-1.7330
9	-0.5184	0.6789	-0.4634	-2.643	3.6920	-0.9542
10	-1.1282	1.9518	-0.8132	-1.9342	2.4490	0.0649
11	-0.8919	3.5603	-2.8887	-2.1198	3.1106	-0.2397

Table A.2: Maximum displacement (mm) of the native 1st MC base when subject to extension and lateral pinch loads; positive x - volar, negative x - dorsal; positive y - proximal, negative y - distal; positive z - radial, negative z - ulnar

	Extension			Pinch		
Subject	x	y	z	x	y	z
1	-8.7754	6.5662	-0.8406	1.3035	3.5928	-1.0967
2	-1.9060	12.8610	-3.5707	3.2758	17.0199	-3.5707
3	-5.9871	4.7410	0.7175	-3.6319	0.4634	-1.7851
4	-12.8727	10.5123	-0.7510	-3.4626	3.2565	-0.6616
5	-6.2711	3.8964	-0.0558	-2.8709	2.1592	-0.3135
6	-2.9135	3.1075	-0.5995	-0.9777	1.8989	0.3349
7	-1.3644	3.3783	-0.5654	-0.2696	2.0243	-0.4029
8	-2.0017	3.7031	-1.6020	0.5504	2.7190	-1.7151
9	-2.9837	4.6522	-0.9139	1.3883	1.2798	0.0489
10	-8.0405	5.9266	-0.2549	-0.8014	0.0970	0.0324
11	-11.3608	13.8187	-2.1808	4.7001	-2.0100	-2.6051

Table A.3: Native trapzium displacement in x (palmar/dorsal), y (proximal/distal), and z (radial/ulnar) directions when subject to 1/2, 1, 1-1/2, and 2 inch grip loads.

	1/2 inch			1 inch		
Subject	x	y	z	x	y	z
1	-1.0581	4.4300	-0.5636	-2.4313	5.0687	-0.9424
2	-5.3678	8.2444	-1.5642	-4.6008	7.1303	-1.11159
3	-1.6482	2.9238	-2.1318	-2.2591	3.5728	-2.1871
4	-6.1912	4.3817	-0.5912	-6.5401	4.4490	-0.3017
5	-4.3866	4.6133	-1.2006	-4.3866	4.3074	-0.8283
6	-4.2478	4.5792	-1.3784	-5.0805	4.4901	-0.5860
7	-3.2698	4.0518	-0.7660	-3.7702	4.6460	-0.5453
8	-3.6930	5.4454	-1.2450	-3.7853	3.5708	-0.5076
9	-3.6220	3.5459	-0.3880	-4.6469	4.0580	-0.5673
10	-3.8919	2.7946	1.7602	-5.5535	3.0040	2.4330
11	-4.3147	3.2679	-0.2448	-6.0814	3.4356	-0.0130
	1-1/2 inch			2 inch		
Subject	x	y	z	x	y	z
1	-2.1587	3.9932	-0.8170	-2.2324	3.7699	-0.7011
2	-6.3500	6.6964	-1.1839	-4.3545	4.8274	-0.649
3	-8.4221	3.6568	-1.0281	-4.3238	2.2421	1.0124
4	-6.0562	3.8138	-0.2107	-6.2250	4.3152	-0.4150
5	-5.1798	4.0574	-0.5363	-4.5814	3.4259	-0.3592
6	-4.9934	3.6752	0.5003	-6.0130	3.5549	1.1520
7	-4.1730	3.0187	0.5786	-5.9593	3.3479	0.7999
8	-4.1836	3.6464	0.4091	-4.5750	2.6631	0.7541
9	-5.0836	4.0596	-0.0316	-5.8428	4.5843	-0.3102
10	-4.7080	3.0942	2.5014	-3.8722	2.6189	2.3563
11	-4.1734	2.6357	0.9119	-5.0857	2.8802	1.1660

Table A.4: Native first metacarpal base displacement in x (palmar/dorsal), y (proximal/distal), and z (radial/ulnar) directions when subject to 1/2, 1, 1-1/2, and 2 inch grip loads.

	1/2 inch			1 inch		
Subject	x	y	z	x	y	z
1	3.4514	3.3168	-1.0039	3.0173	3.7450	-1.3568
2	-1.9739	7.0544	-0.6728	-0.8025	5.9077	-0.1541
3	-2.8046	3.1046	-0.6434	-2.1273	2.8561	-1.3555
4	-1.3648	4.1010	-0.5025	-2.7847	3.4404	-0.3337
5	-2.7237	3.1424	-0.9768	-3.6739	2.4469	-0.1769
6	-1.7424	4.2668	0.2691	-2.7663	4.1736	0.4859
7	-2.1008	3.3386	-0.4143	-2.8958	3.8848	-0.2918
8	1.7533	4.7713	-1.7367	-1.9549	3.3062	-0.2335
9	-2.6835	2.1259	0.2060	-7.5123	4.1383	0.1697
10	1.4749	1.0359	-0.6803	-5.1850	2.0721	-3.7564
11	0.6751	1.8252	-0.3945	-4.8177	3.5554	0.7445
	1-1/2 inch			2 inch		
Subject	x	y	z	x	y	z
1	0.5062	3.3280	-0.8125	-1.3488	3.3164	-0.7093
2	-5.4475	6.2211	-0.0061	-1.8243	4.1145	-0.0111
3	-9.2527	2.7156	1.9461	-3.7818	1.9017	1.7962
4	-4.0387	2.7771	0.4725	-4.6602	4.0400	0.6235
5	-5.5650	2.6937	1.6534	-5.1953	1.9443	1.5314
6	-2.4894	3.1414	0.8913	-5.2032	3.1544	2.1015
7	-5.1861	2.1961	0.4828	-8.8467	2.9640	0.9088
8	-5.0500	3.8777	1.8518	-5.4958	3.0983	2.3339
9	-6.1928	3.6523	0.6915	-5.2986	3.6526	0.5744
10	-3.7564	1.9253	1.8705	-2.7384	1.5445	1.7146
11	1.5594	1.6658	-1.3969	-2.8466	0.0788	1.2002

Table A.5: Difference of means of maximum displacement (mm) of the trapezium in x (palmar/dorsal), y (proximal/distal), and z (radial/ulnar) directions when subject to ligament sectioning at extension and lateral pinch loads. (Key: neg x - dorsal displacement due to sectioning; pos y - proximal displacement due to sectioning; neg z - ulnar displacement due to sectioning)

	Extension			Pinch		
Ligament	x	y	z	x	y	z
AOL	0.1318	0.0831	-0.1487	0.0021	-0.7076	0.0288
UCL	0.0056	-0.5586	0.0784	-0.3069	-5.8363	-0.0540
IML	-0.4909	0.7306	-0.0037	1.5679	-2.1233	1.3170
POL	-0.3157	0.3256	-0.2268	-0.2190	0.1302	0.3030
DRL	0.3922	-0.2680	0.2112	0.7688	-2.6347	0.0709

Table A.6: Difference of means of maximum displacement (mm) of the 1st MC base in x (palmar/dorsal), y (proximal/distal), and z (radial/ulnar) directions when subject to ligament sectioning at extension and lateral pinch loads. (Key: neg x - dorsal displacement due to sectioning; pos y - proximal displacement due to sectioning; neg z - ulnar displacement due to sectioning)

	Extension			Pinch		
Ligament	x	y	z	x	y	z
AOL	-1.2830	0.9216	1.4858	-1.8039	1.5871	-0.8902
UCL	-0.4589	-0.3720	-0.5756	1.8239	10.2698	1.0200
IML	-4.1510	3.4480	-0.1005	1.9661	-1.2336	0.6889
POL	-4.1714	2.2535	1.0739	7.7635	-2.1535	-2.5538
DRL	-1.1560	0.8358	1.4543	-5.1198	-1.2728	0.1430

Table A.7: Difference of means of maximum displacement (mm) of the trapezium in x (palmar/dorsal), y (proximal/distal), and z (radial/ulnar) directions when subject to ligament sectioning and 1/2, 1, 1-1/2, and 2 inch grip loads. (Key: neg x - dorsal displacement due to sectioning; pos y - proximal displacement due to sectioning; neg z - ulnar displacement due to sectioning)

	1/2 inch			1 inch		
Ligament	x	y	z	x	y	z
AOL	-0.4576	0.6218	0.1133	0.2388	-0.2424	0.0545
UCL	-0.4457	-0.3226	-0.2825	-1.3511	-0.0240	0.1881
IML	-0.0589	1.3733	-0.3211	-0.9064	-0.3126	0.9827
POL	-0.1626	0.0100	0.2437	-0.1286	0.4556	0.5412
DRL	-2.1414	0.7914	-0.2104	-0.8625	0.1098	0.1351
	1-1/2 inch			2 inch		
Ligament	x	y	z	x	y	z
AOL	0.0769	-0.1420	-0.0830	0.2171	-0.4602	0.0001
UCL	-0.0525	-0.2810	0.1607	-0.1723	-0.1376	-0.0095
IML	2.6728	-0.6078	0.7525	-0.0611	-0.0929	-0.1809
POL	-1.1860	0.7861	0.0111	-1.0949	-0.1198	0.1146
DRL	-1.0172	0.7383	-0.0913	-0.5154	-0.0807	0.0423

Table A.8: Difference of means of maximum displacement (mm) of the 1st MC base in x (palmar/dorsal), y (proximal/distal), and z (radial/ulnar) directions when subject to ligament sectioning and 1/2, 1, 1-1/2, and 2 inch grip loads. (Key: neg x - dorsal displacement due to sectioning; pos y - proximal displacement due to sectioning; neg z - ulnar displacement due to sectioning)

	1/2 inch			1 inch		
Ligament	x	y	z	x	y	z
AOL	0.3171	0.6551	-0.2390	1.3510	-0.7230	-0.6640
UCL	0.2436	-0.3490	-0.6450	-0.6930	0.8050	0.0304
IML	4.1325	1.0724	-0.7730	1.9325	-0.8550	-0.1820
POL	-0.6600	0.0773	-.1059	2.6011	0.2791	0.1787
DRL	-5.6310	1.2580	0.1348	-5.5000	0.8980	0.6936
	1-1/2 inch			2 inch		
Ligament	x	y	z	x	y	z
AOL	0.4441	-0.1390	-0.3150	0.8066	-0.5480	-0.1450
UCL	1.2614	-0.5580	0.1683	0.0829	-0.1030	-0.0740
IML	3.3940	-0.6390	-0.8990	-0.4340	-0.0280	-0.1180
POL	-1.3100	0.8160	0.3622	-1.0860	-0.5250	0.0092
DRL	-0.5290	0.8485	0.0572	-0.1150	-0.1100	0.2271

Appendix B

Representative examples of the effects of ligament sectioning when subject to 1/2 inch grip

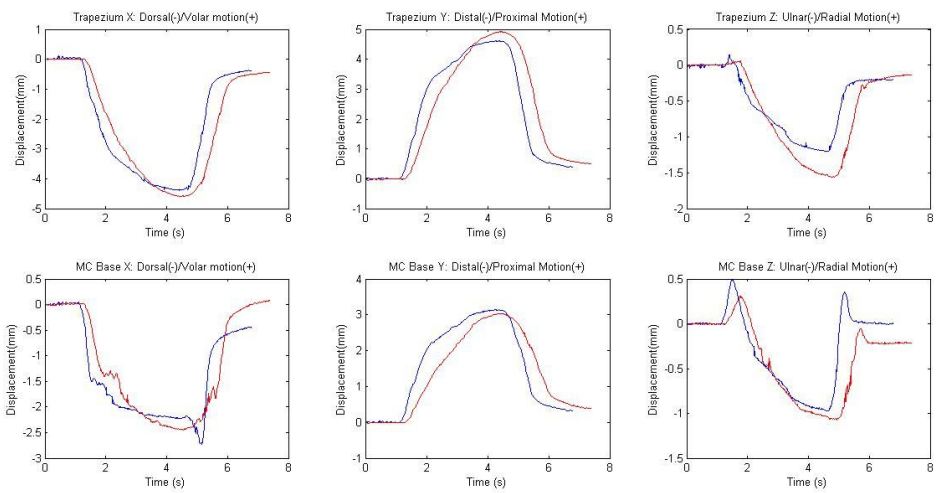

Figure B.1: Representative example of the effect of AOL ligament sectioning when subject to 1/2 inch grip

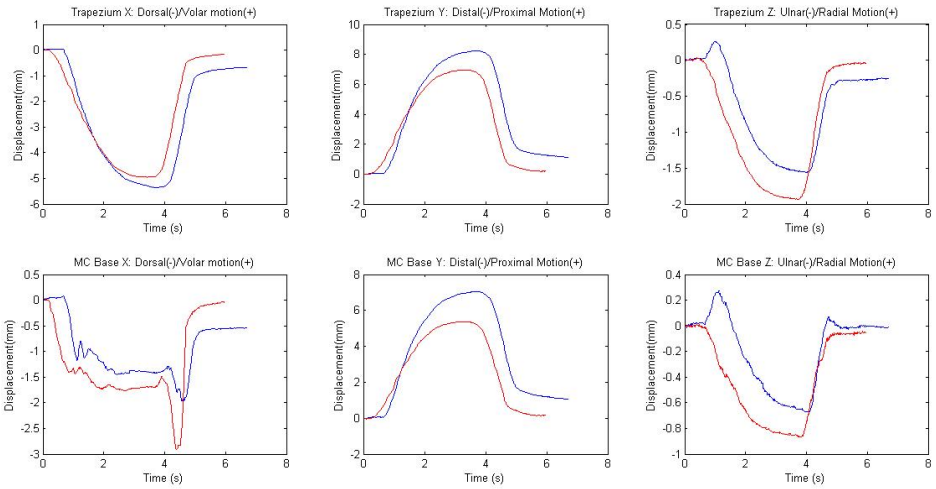

Figure B.2: Representative example of the effect of UCL ligament sectioning when subject to 1/2 inch grip

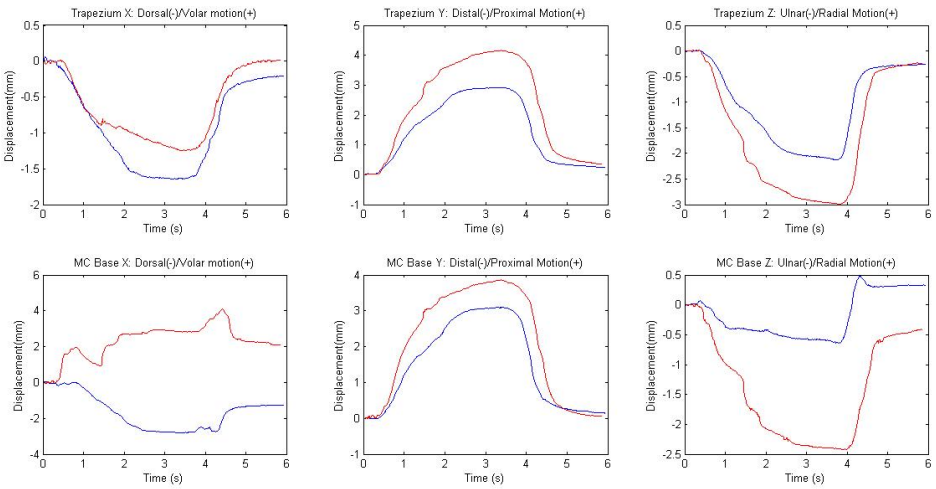

Figure B.3: Representative example of the effect of IML ligament sectioning when subject to 1/2 inch grip

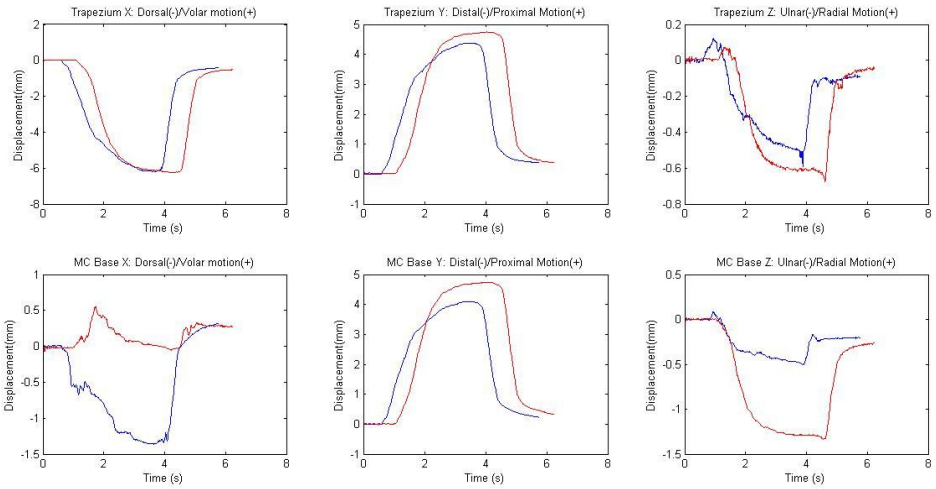

Figure B.4: Representative example of the effect of POL ligament sectioning when subject to 1/2 inch grip

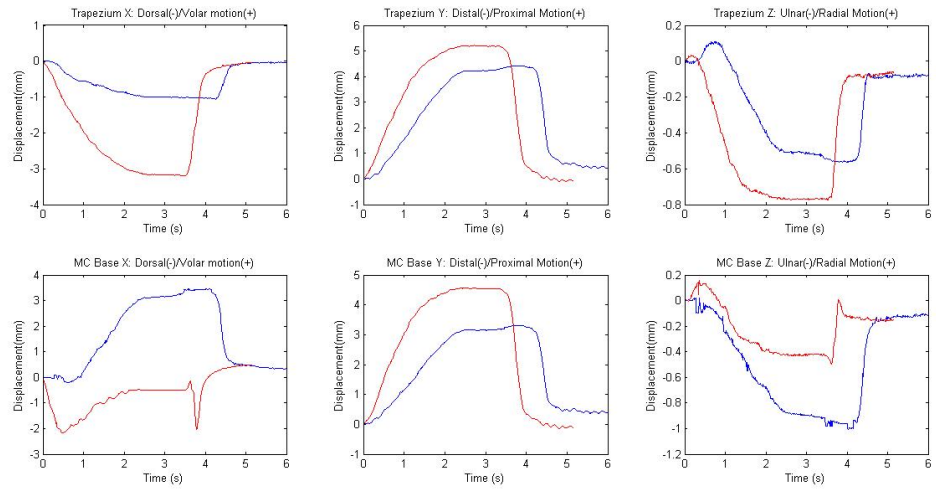

Figure B.5: Representative example of the effect of DRL ligament sectioning when subject to 1/2 inch grip

Appendix C

Plots of thumb extension and lateral pinch for all specimens and all ligaments sectioned

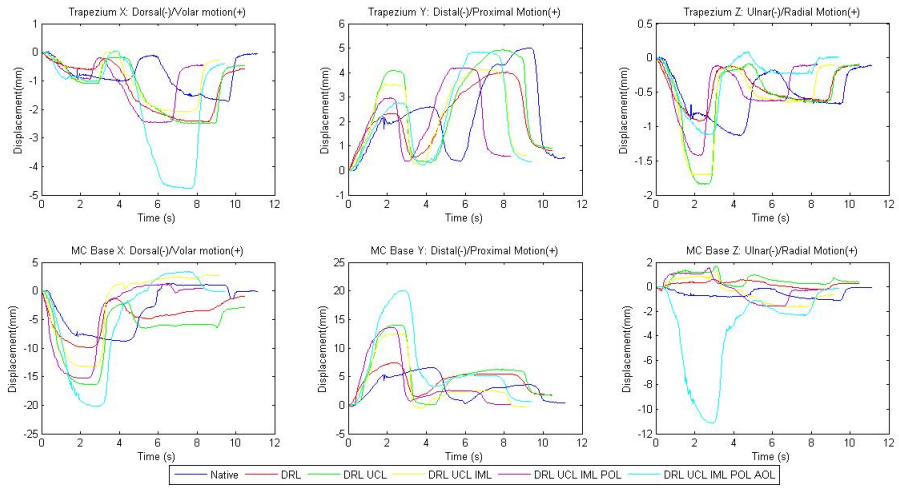

Figure C.1: Specimen 1. Plots of trapezium and 1st MC base displacement when subject to thumb extension and lateral pinch.

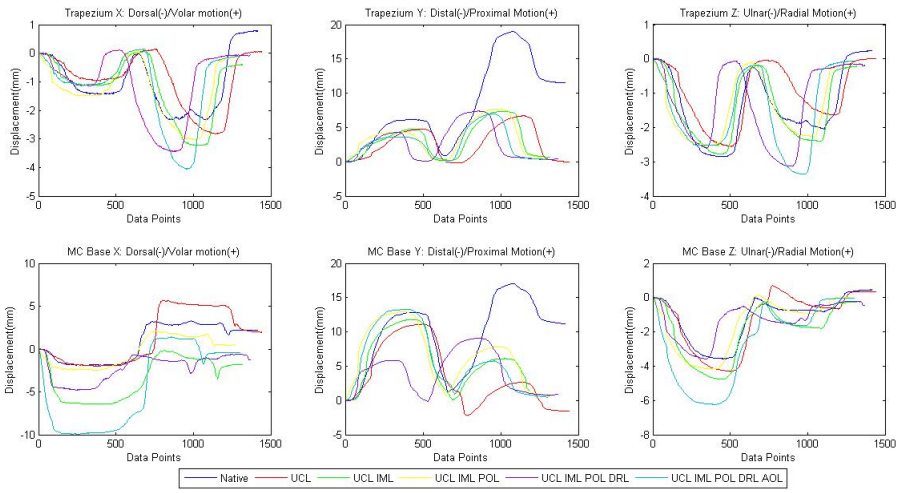

Figure C.2: Specimen 2. Plots of trapezium and 1st MC base displacement when subject to thumb extension and lateral pinch.

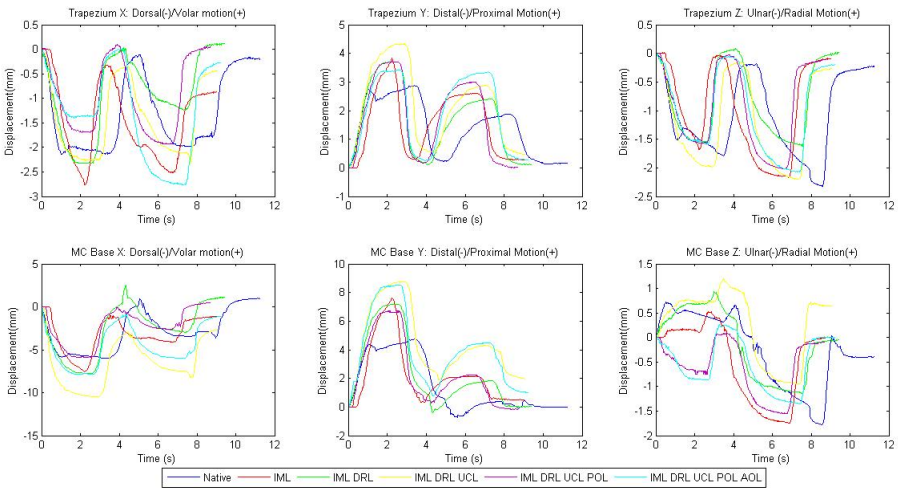

Figure C.3: Specimen 3. Plots of trapezium and 1st MC base displacement when subject to thumb extension and lateral pinch.

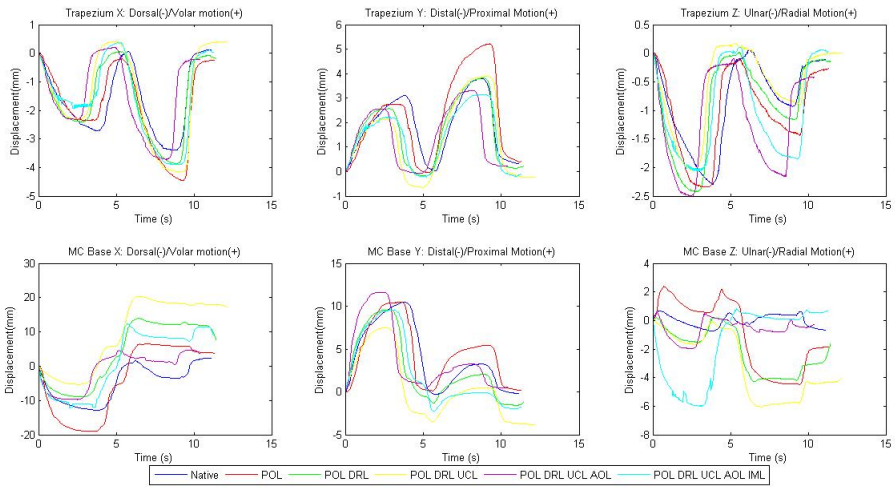

Figure C.4: Specimen 4. Plots of trapezium and 1st MC base displacement when subject to thumb extension and lateral pinch.

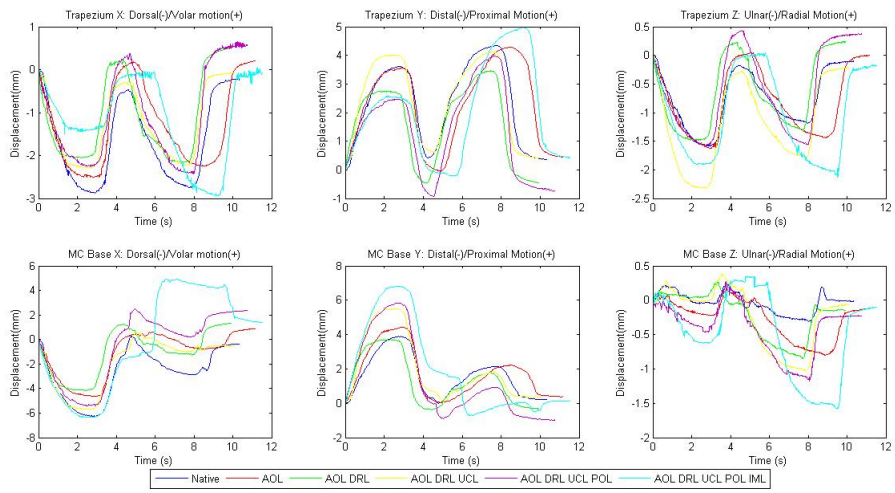

Figure C.5: Specimen 5. Plots of trapezium and 1st MC base displacement when subject to thumb extension and lateral pinch.

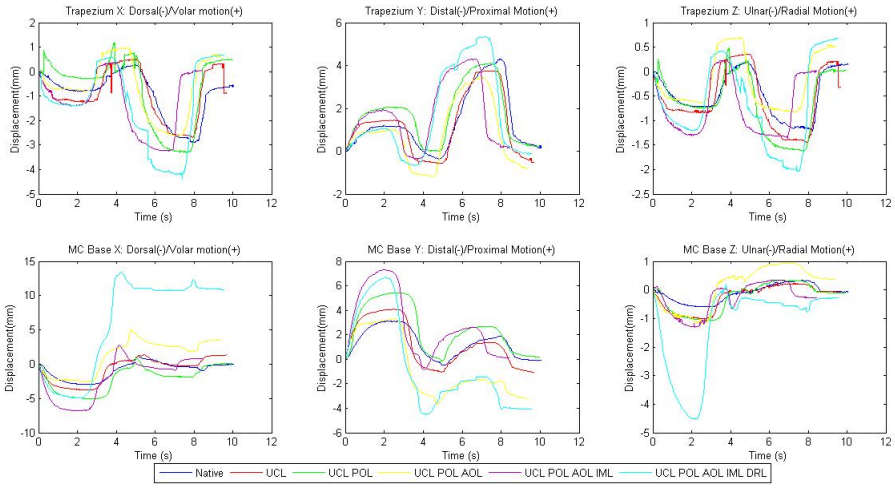

Figure C.6: Specimen 6. Plots of trapezium and 1st MC base displacement when subject to thumb extension and lateral pinch.

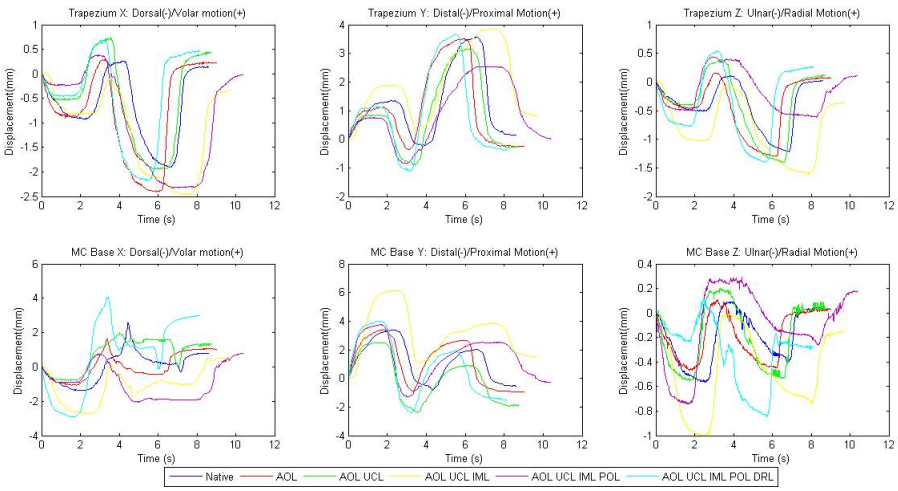

Figure C.7: Specimen 7. Plots of trapezium and 1st MC base displacement when subject to thumb extension and lateral pinch.

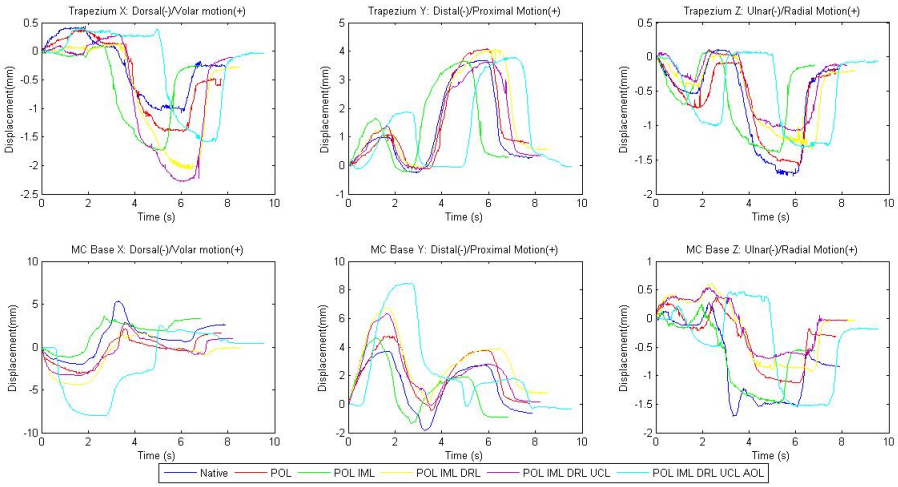

Figure C.8: Specimen 8. Plots of trapezium and 1st MC base displacement when subject to thumb extension and lateral pinch.

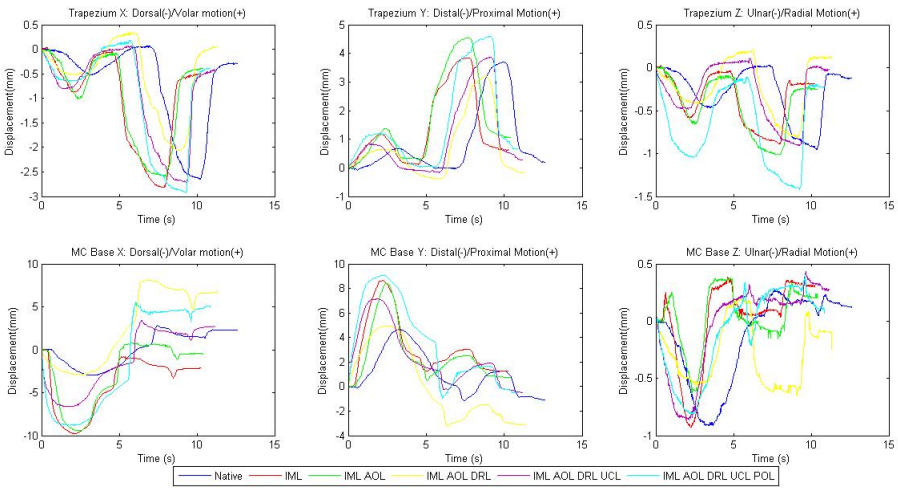

Figure C.9: Specimen 9. Plots of trapezium and 1st MC base displacement when subject to thumb extension and lateral pinch.

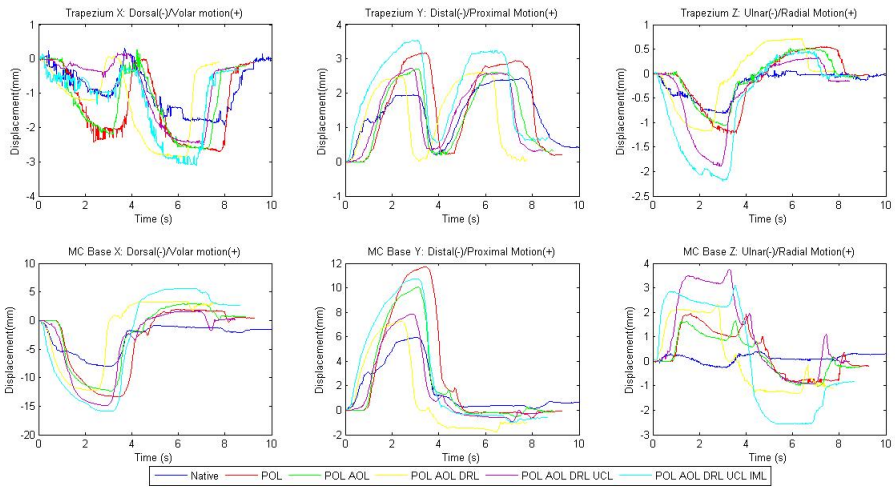

Figure C.10: Specimen 10. Plots of trapezium and 1st MC base displacement when subject to thumb extension and lateral pinch.

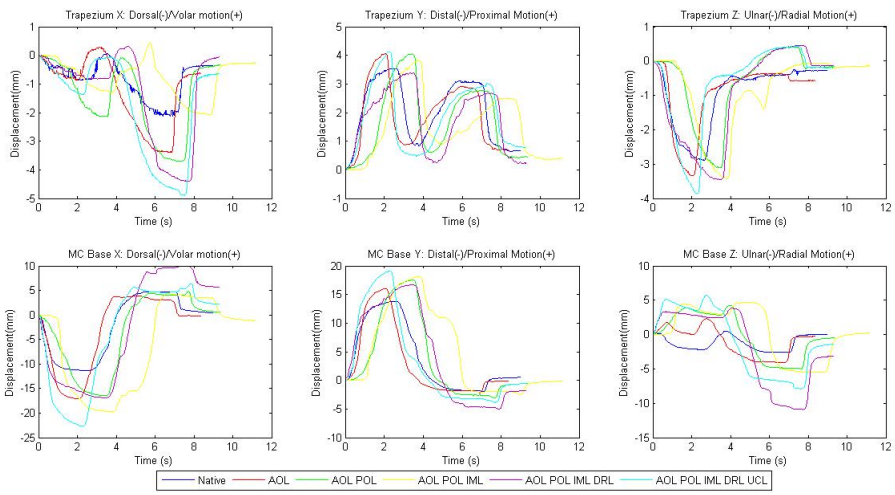

Figure C.11: Specimen 11. Plots of trapezium and 1st MC base displacement when subject to thumb extension and lateral pinch.

Appendix D

Native joint motion plots when subject to grip

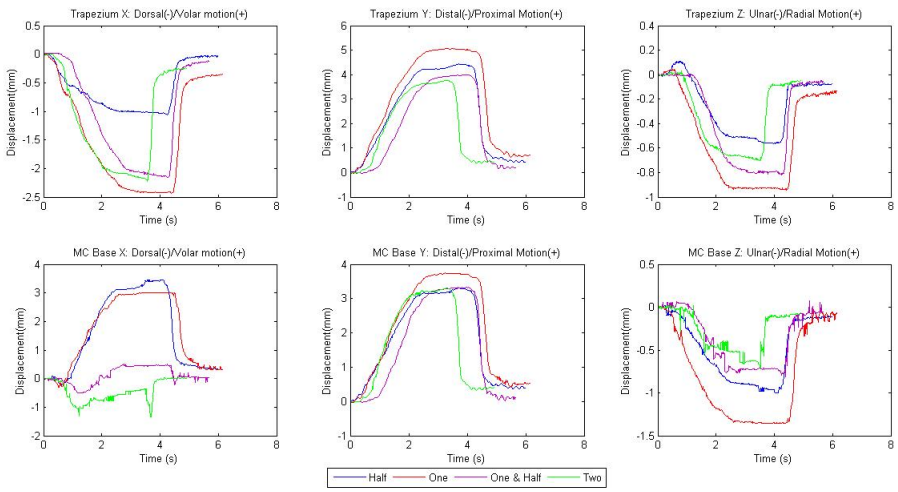

Figure D.1: Specimen 1. Plots of trapezium and 1st MC base native bone displacement in x-, y-, and z-directions when subject to 1/2, 1, 1-1/2, and 2 inch grip.

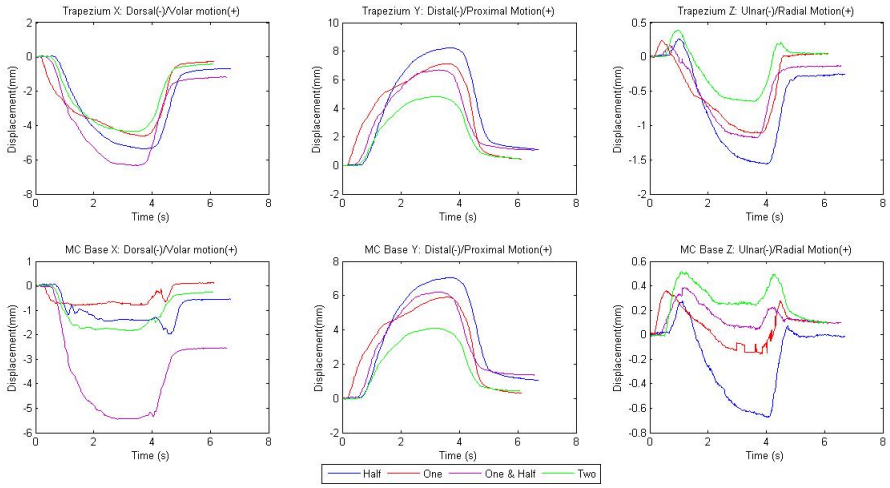

Figure D.2: Specimen 2. Plots of trapezium and 1st MC base native bone displacement in x-, y-, and z-directions when subject to 1/2, 1, 1-1/2, and 2 inch grip.

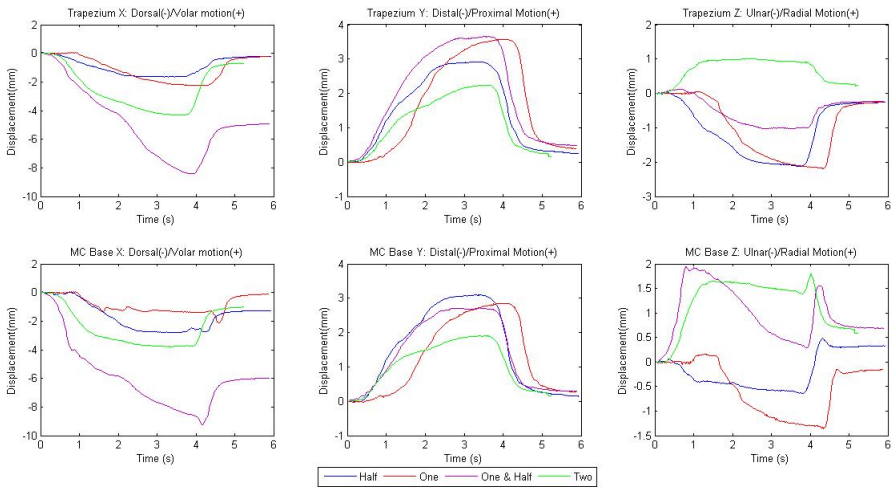

Figure D.3: Specimen 3. Plots of trapezium and 1st MC base native bone displacement in x-, y-, and z-directions when subject to 1/2, 1, 1-1/2, and 2 inch grip.

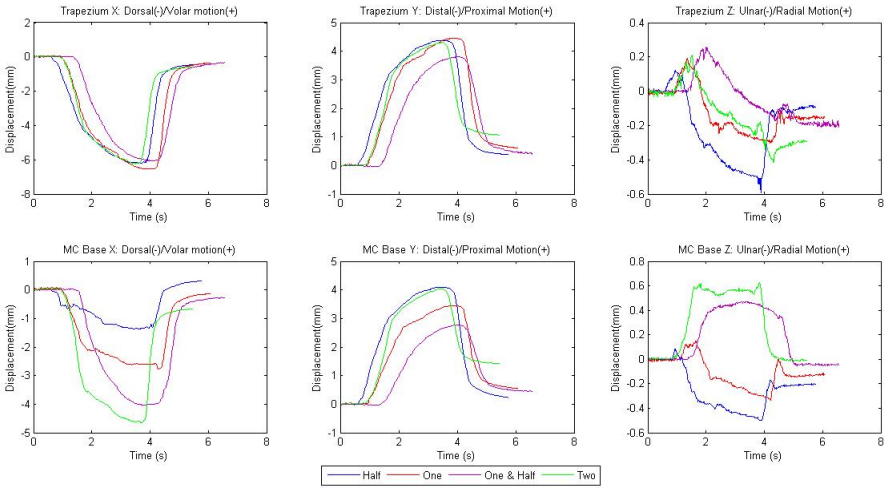

Figure D.4: Specimen 4. Plots of trapezium and 1st MC base native bone displacement in x-, y-, and z-directions when subject to 1/2, 1, 1-1/2, and 2 inch grip.

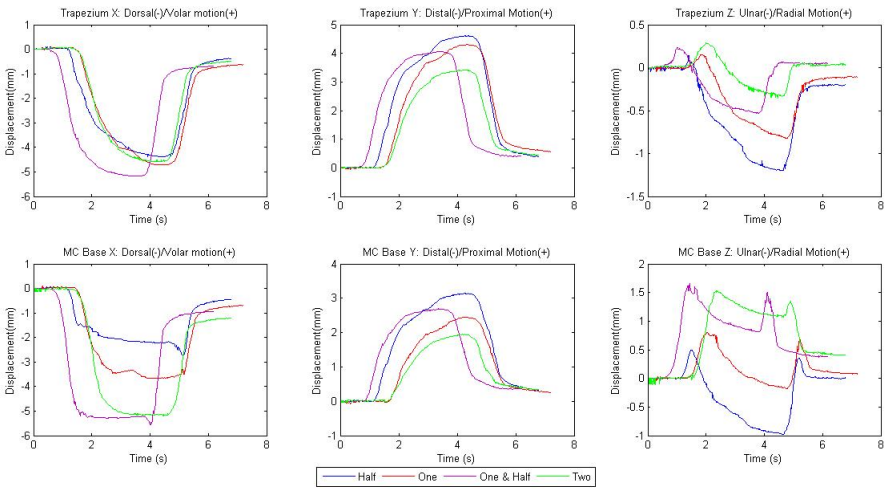

Figure D.5: Specimen 5. Plots of trapezium and 1st MC base native bone displacement in x-, y-, and z-directions when subject to 1/2, 1, 1-1/2, and 2 inch grip.

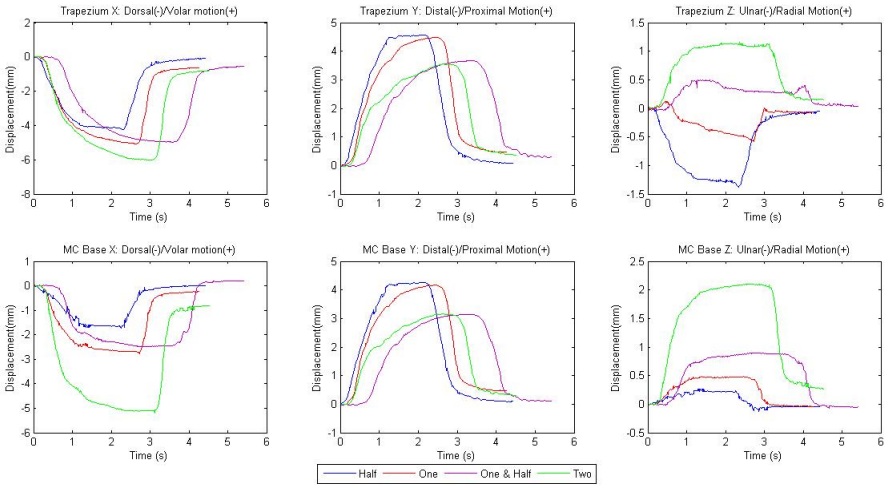

Figure D.6: Specimen 6. Plots of trapezium and 1st MC base native bone displacement in x-, y-, and z-directions when subject to 1/2, 1, 1-1/2, and 2 inch grip.

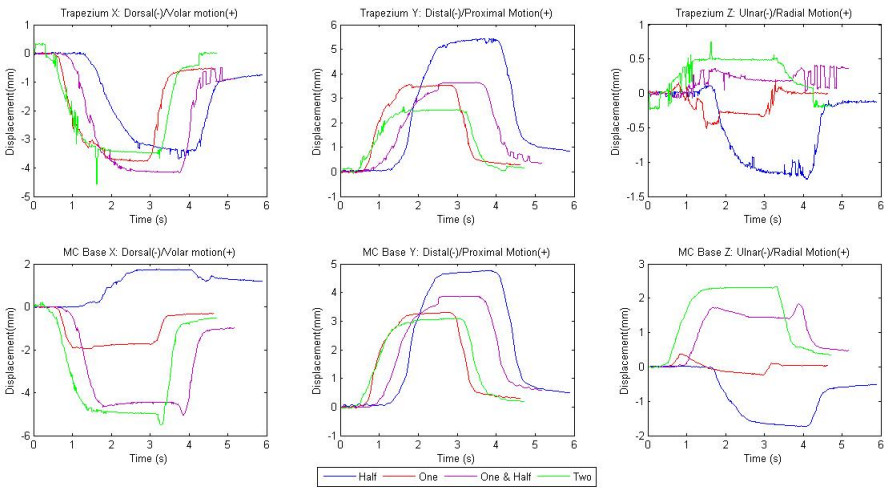

Figure D.7: Specimen 8. Plots of trapezium and 1st MC base native bone displacement in x-, y-, and z-directions when subject to 1/2, 1, 1-1/2, and 2 inch grip.

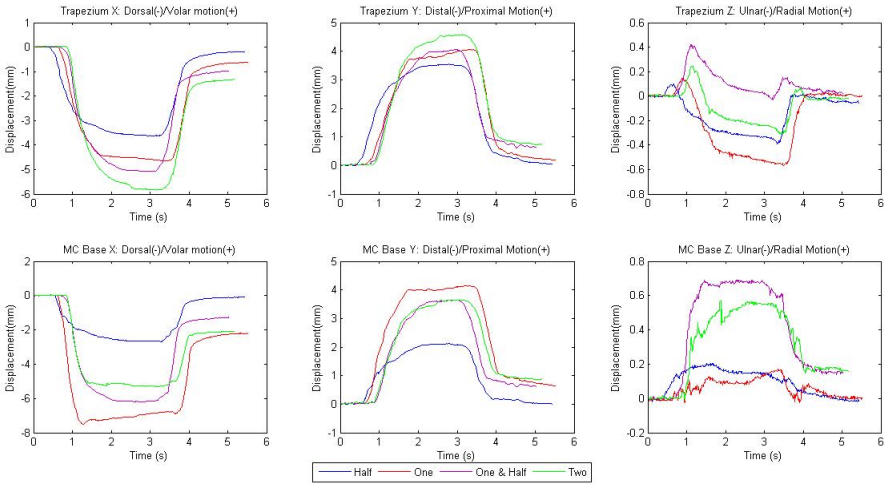

Figure D.8: Specimen 9. Plots of trapezium and 1st MC base native bone displacement in x-, y-, and z-directions when subject to 1/2, 1, 1-1/2, and 2 inch grip.

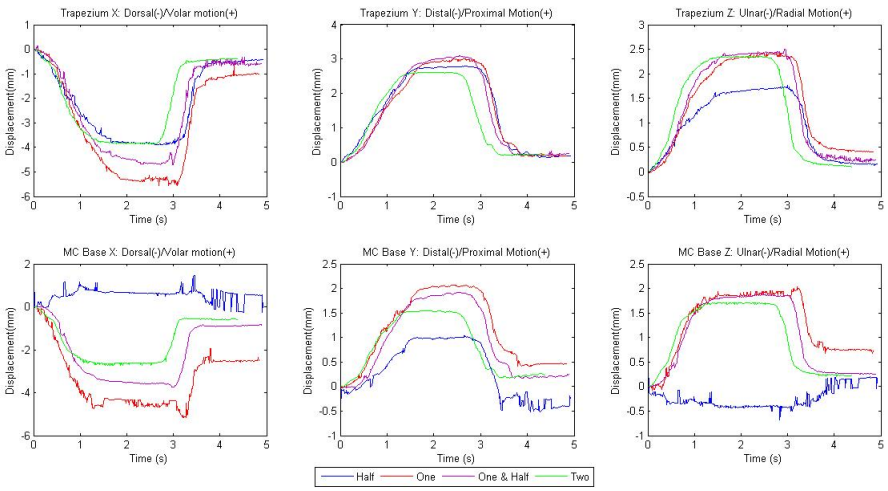

Figure D.9: Specimen 10. Plots of trapezium and 1st MC base native bone displacement in x-, y-, and z-directions when subject to 1/2, 1, 1-1/2, and 2 inch grip.

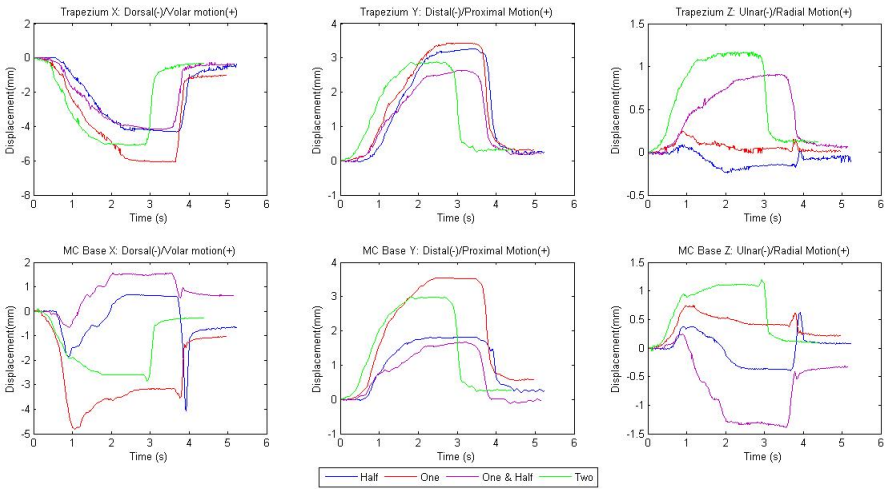

Figure D.10: Specimen 11. Plots of trapezium and 1st MC base native bone displacement in x-, y-, and z-directions when subject to 1/2, 1, 1-1/2, and 2 inch grip.

Appendix E

Load-displacement plots for the DRL, POL, AOL, and UCL ligaments

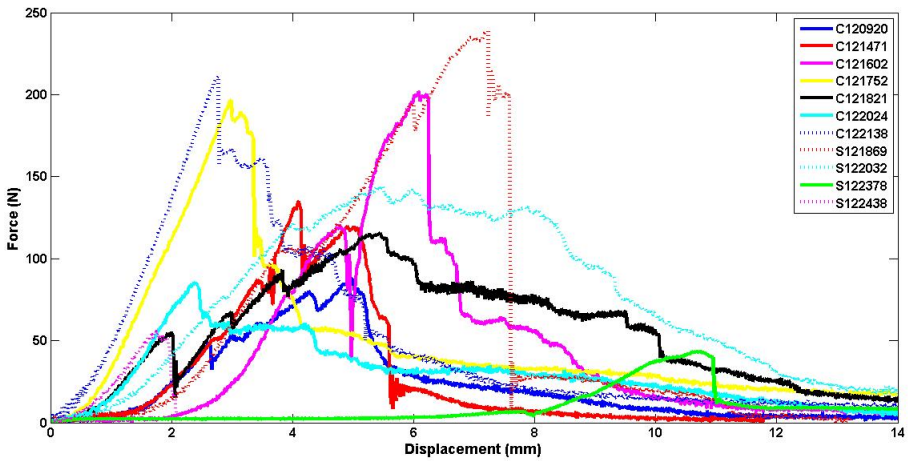

Figure E.1: Load-displacement plots for DRL ligament testing.

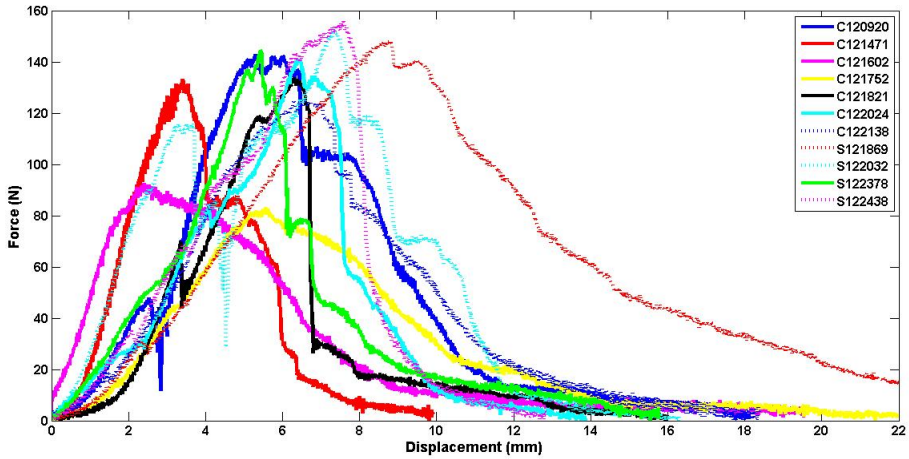

Figure E.2: Load-displacement plots for POL ligament testing.

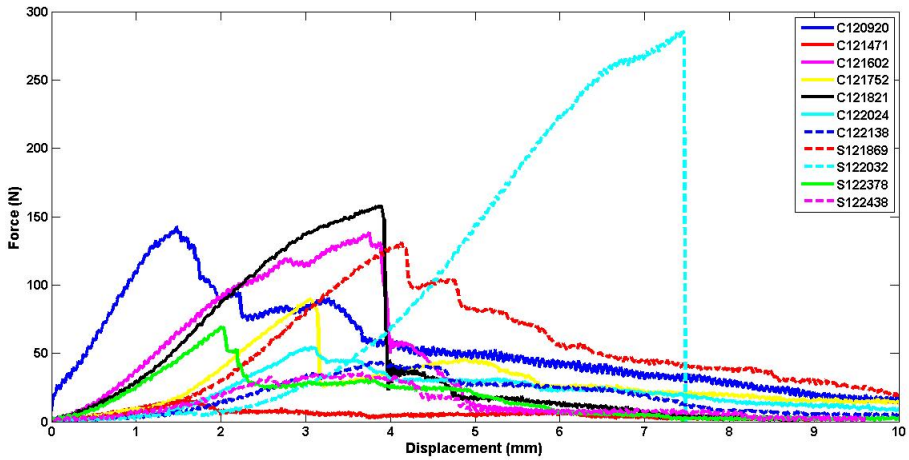

Figure E.3: Load-displacement plots for AOL ligament testing.

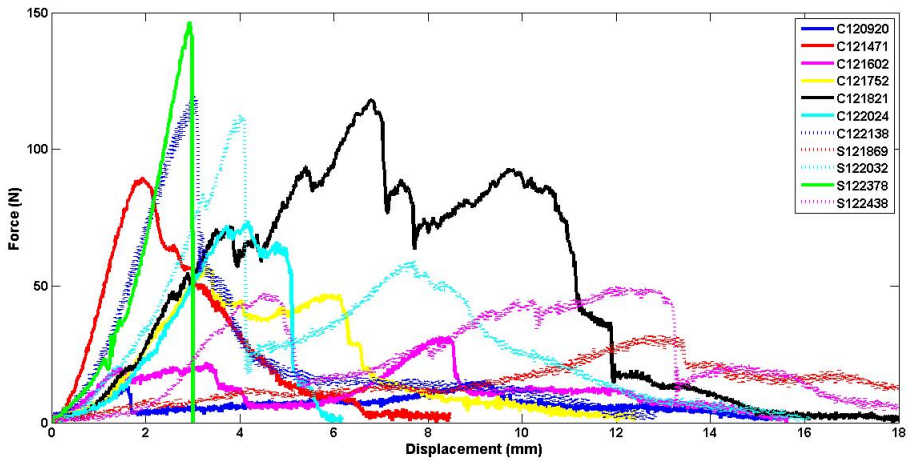

Figure E.4: Load-displacement plots for UCL ligament testing.

Appendix F

Dimensioned drawings of fixtures made for tensile testing

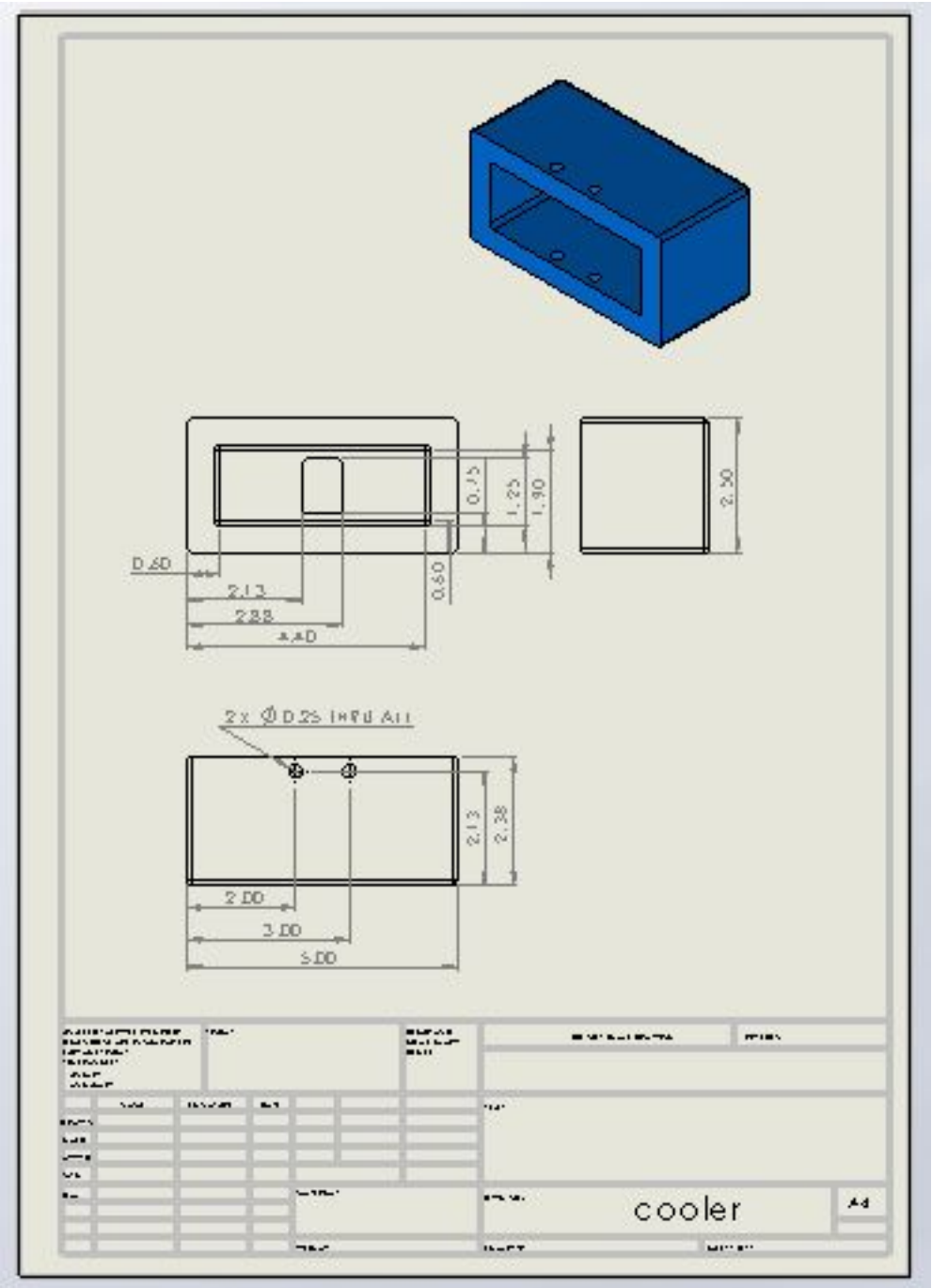

Figure F.1: Dimensioned drawing of cooler for ligament attachment fixture.

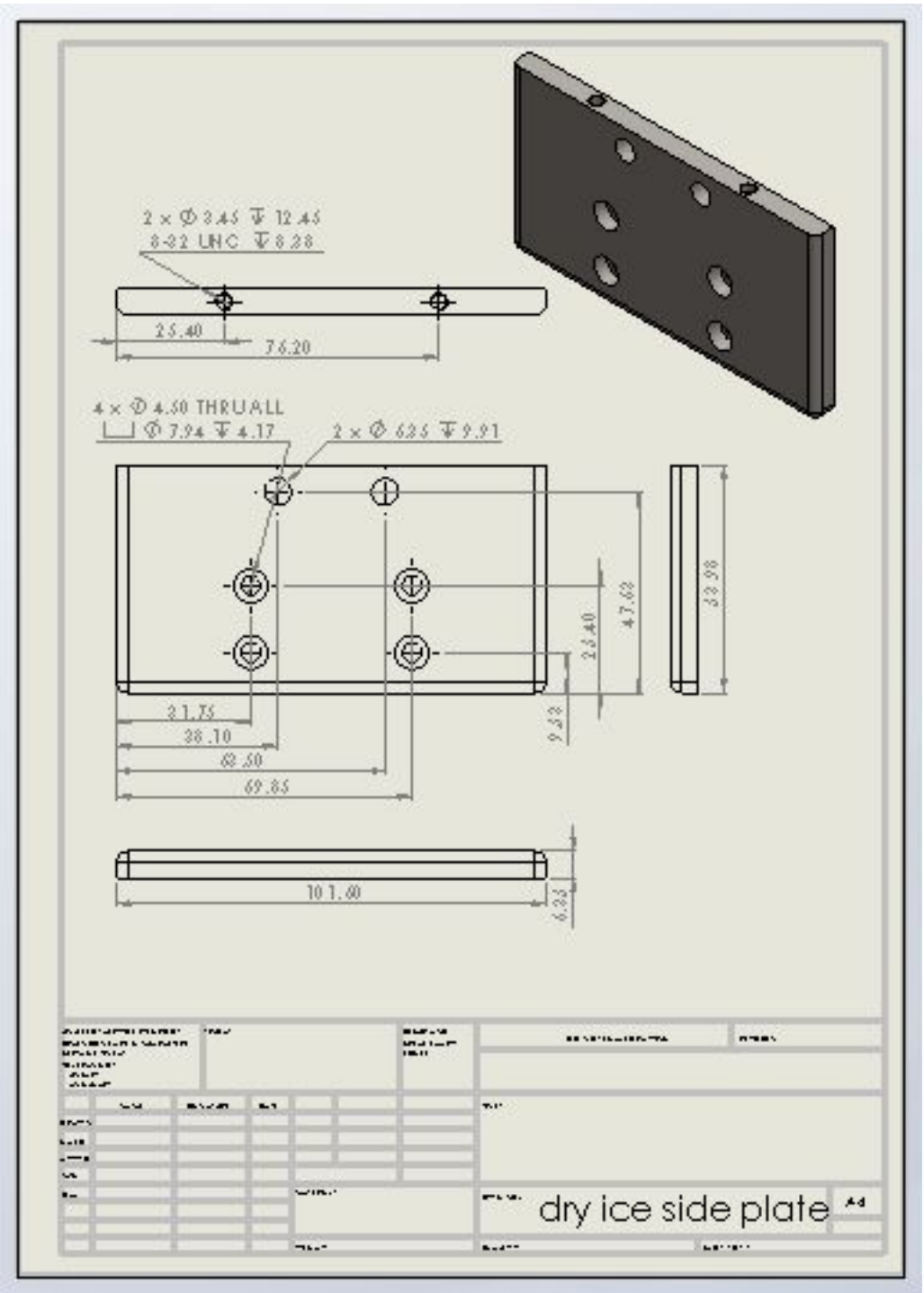

Figure F.2: Dimensioned drawing of dry ice sideplate for ligament attachment fixture.

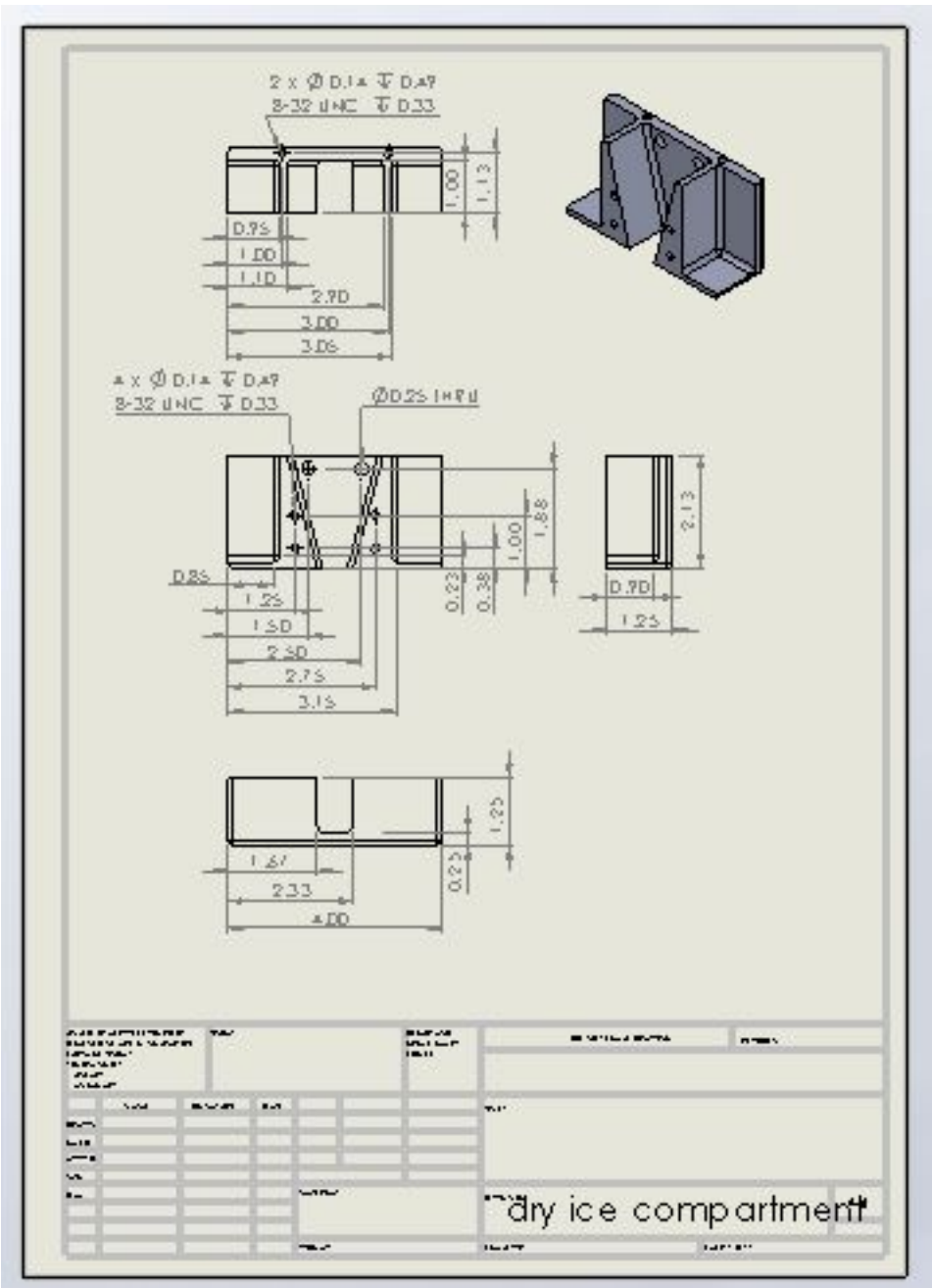

Figure F.3: Dimensioned drawing of dry ice compartment for ligament attachment fixture.

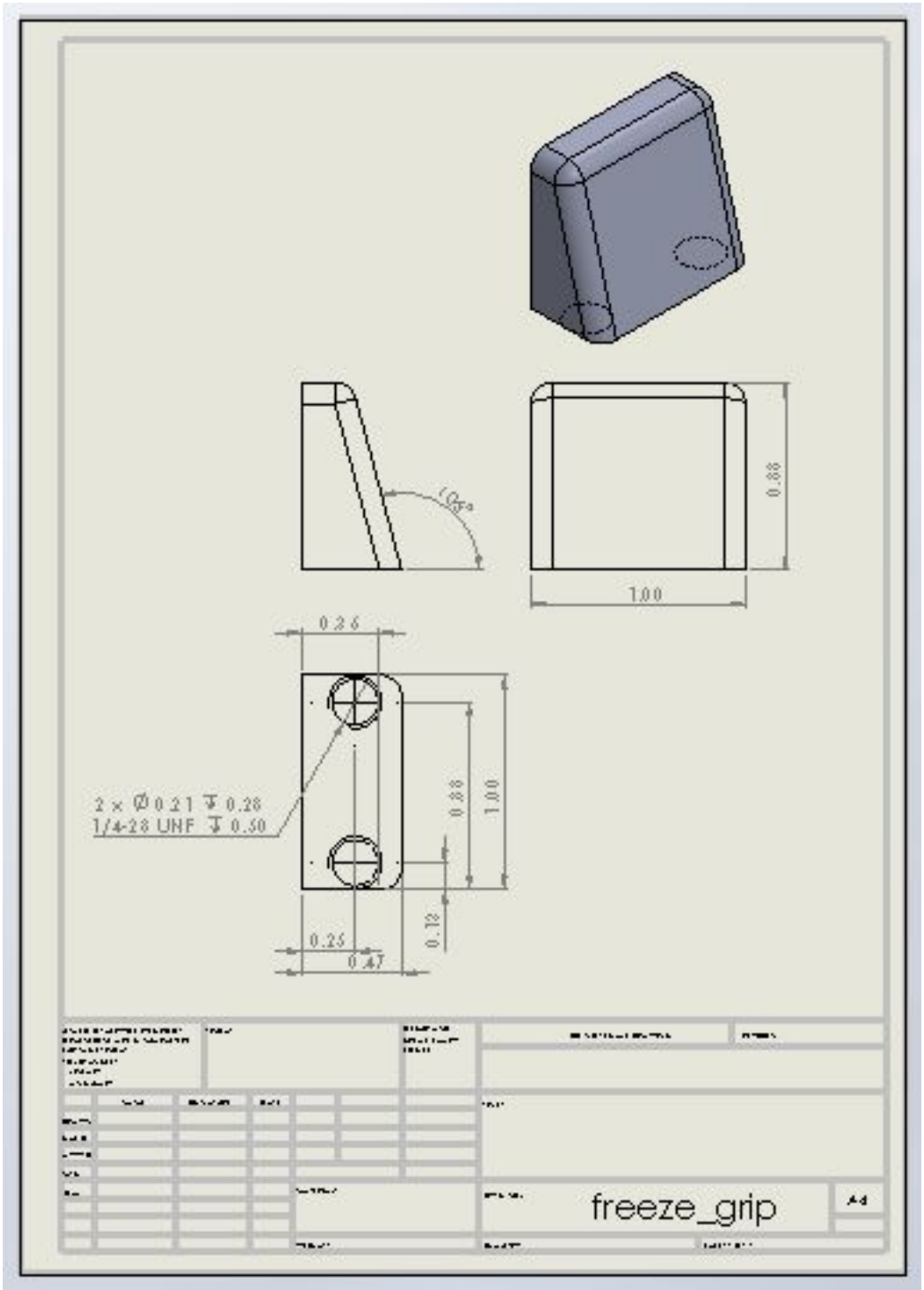

Figure F.4: Dimensioned drawing of freeze grip for ligament attachment fixture.

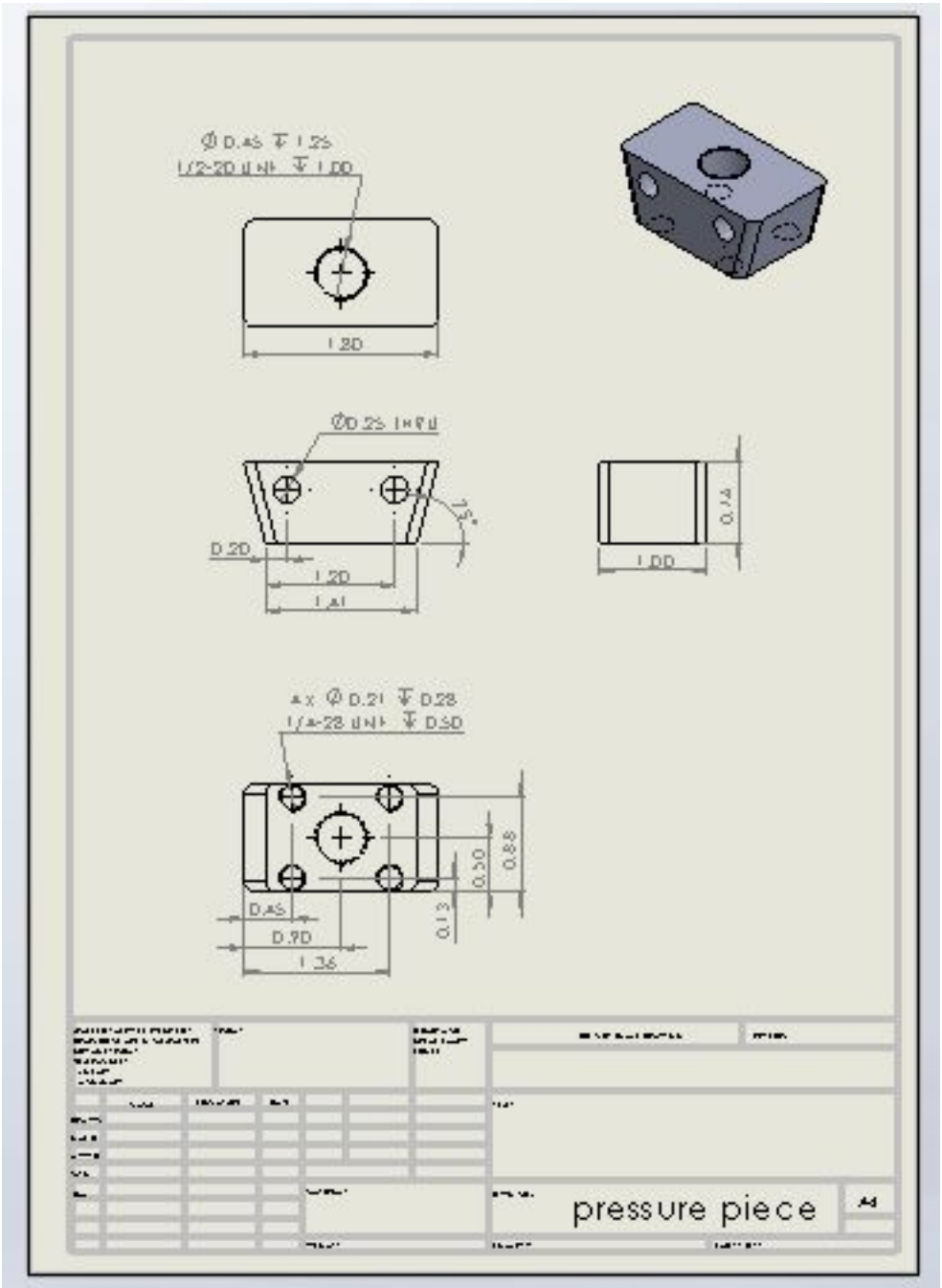

Figure F.5: Dimensioned drawing of pressure piece for ligament attachment fixture.

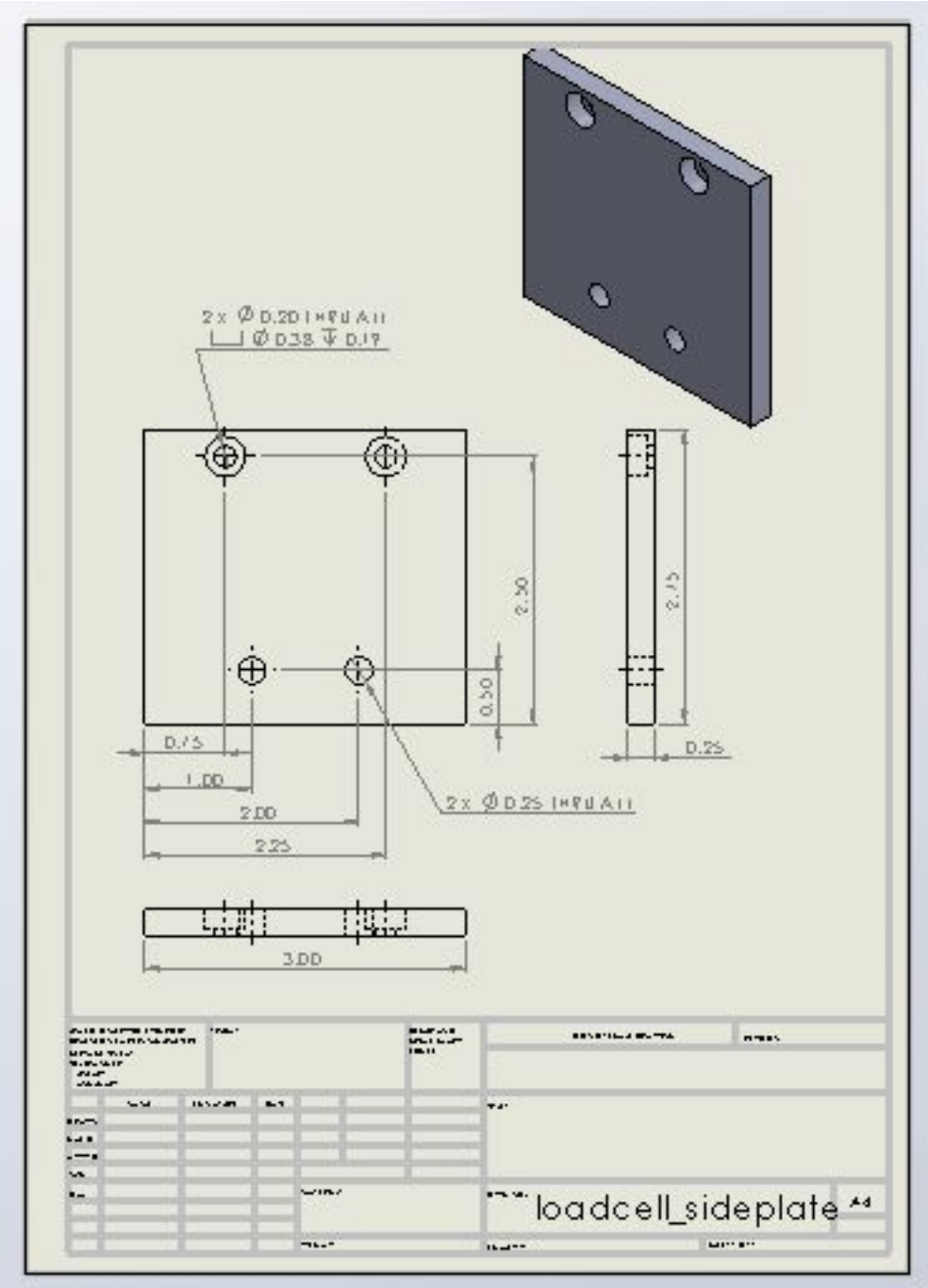

Figure F.6: Dimensioned drawing of loadcell side plate for ligament attachment fixture.

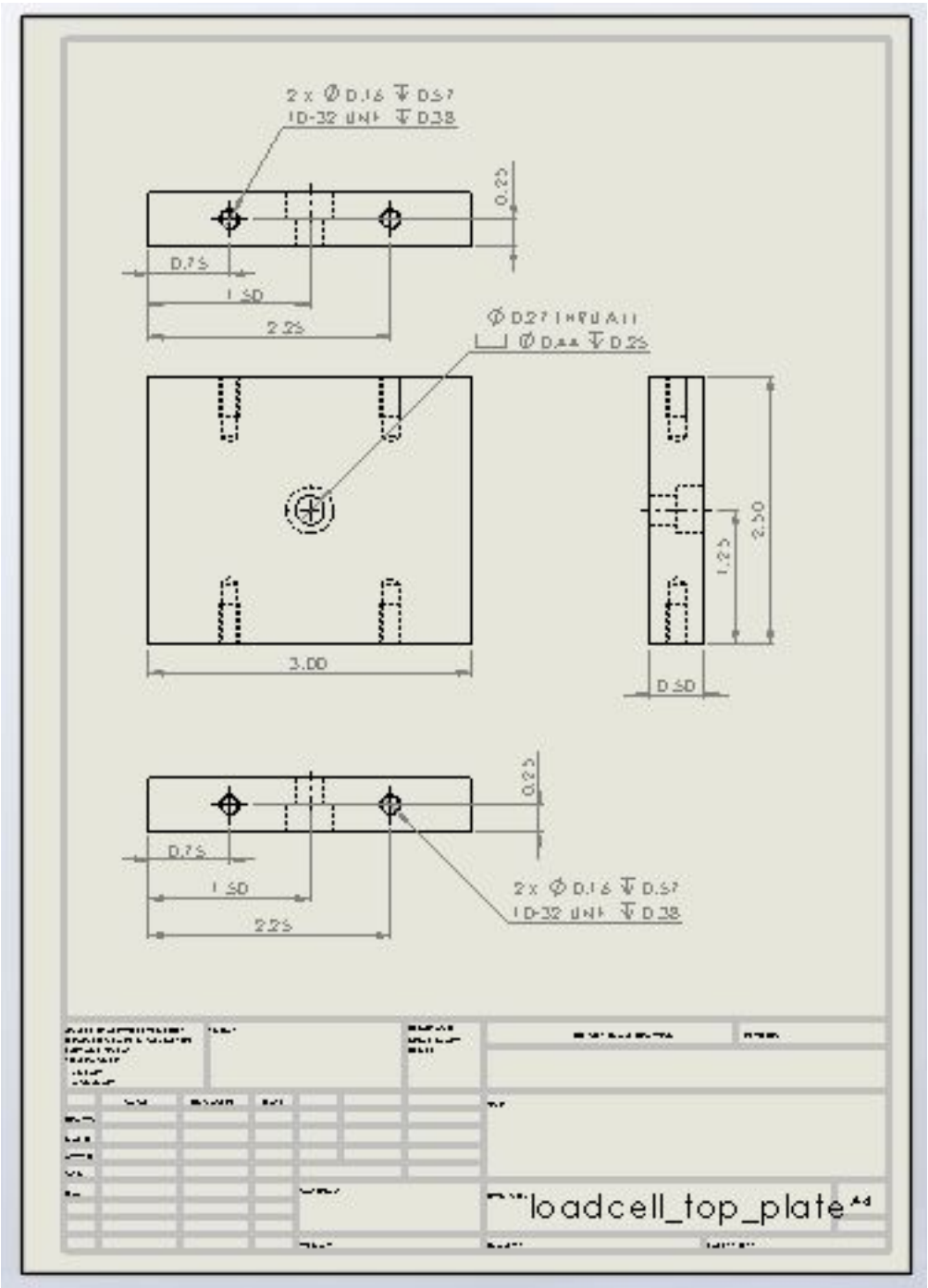

Figure F.7: Dimensioned drawing of loadcell top plate for ligament attachment fixture.

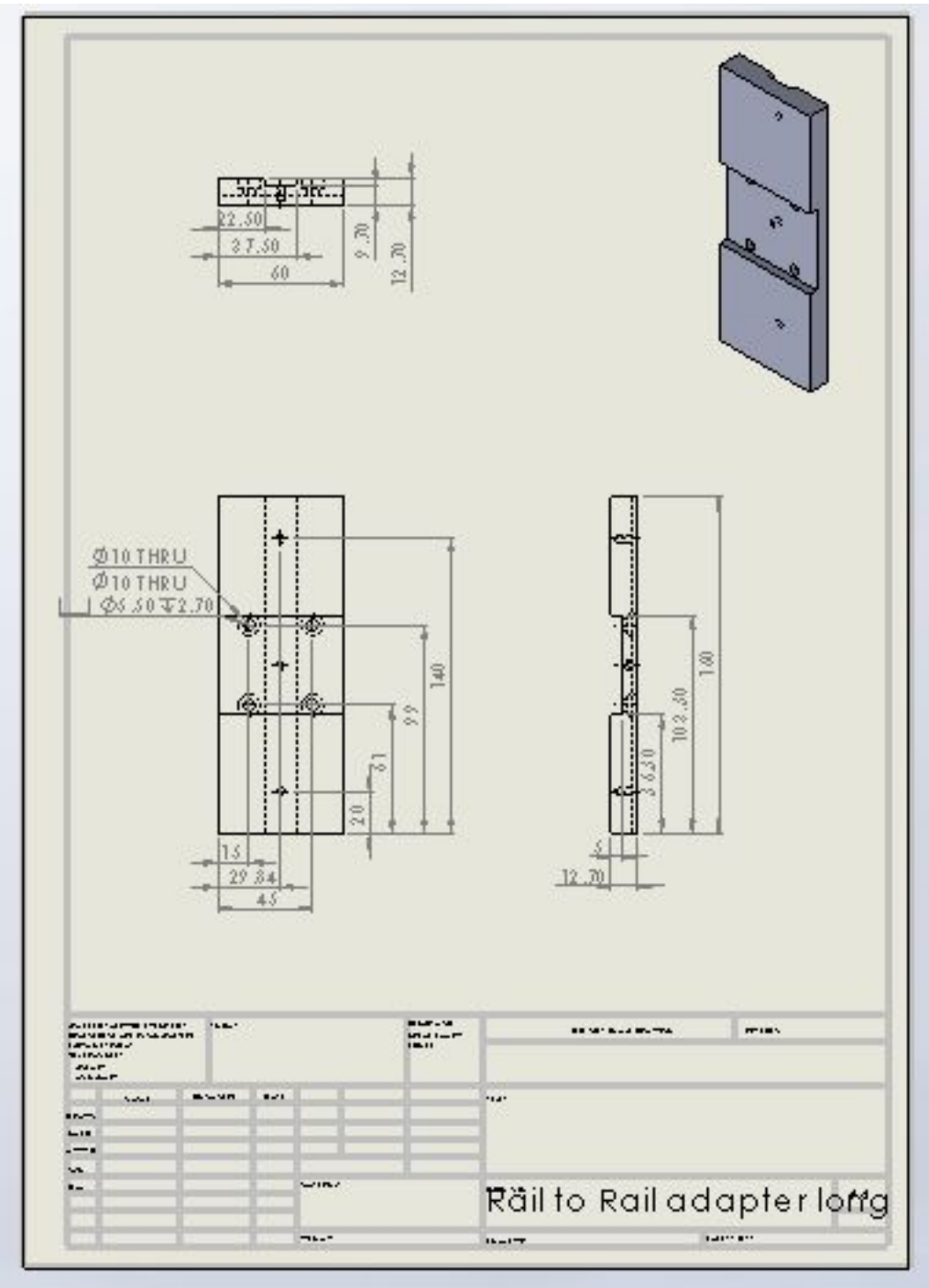

Figure F.8: Dimensioned drawing of rail to rail piece for trapezium attachment fixture.